Evaluation of Phytoplankton Growth in Estuary as Effect of Nutrient Inputs during Rainfall Using Ecological Model

(生態系モデルを用いた降雨時の栄養塩流入後の
内湾における植物プランクトン増殖量の評価)

July, 2019

Doctor of Philosophy (Engineering)

Teuku Mahlil
テウク　マハリル

Toyohashi University of Technology

Abstract

Eutrophication is currently one of most popular water environment issues in the world. This problem has been occurred and could be seen in several countries with high development in infrastructure, industrial, and agricultural. It is associated with rapid population and economic growth where the development has been pressing provision of human needs in form of food and settlement. To accelerate the provisioning process, the used of various biological and chemical substances including nutrients in the form of nitrogen (N) and phosphorus (P) are massively increased. In its application, most of those substances are, directly or indirectly, leached into aquatic environment as diffuse pollution. Particularly in agricultural sector, the high frequency of fertilizer application and increase of non-point nutrient loads from agriculture has been associated to the impairment of surface and ground water qualities. Leaching process of nutrient from agriculture soil into surface water bodies significantly influenced by rainfall. During rainfall, soil nutrients are flushed out by rainfall run-offs into river and transported into estuaries and extending seaward. Enrichment of nutrients loads in waterbodies are resulting in acceleration of phytoplankton growth by the response of nutrient uptake by phytoplankton itself and photosynthesis. Phytoplankton growth could lead to an imbalance of algal production and consumption, which followed by enhanced sedimentation of algal-derived organic matter, stimulation of microbial decomposition and oxygen consumption, depletion of oxygen, and further affecting mass mortalities of marine animals and leave bad impact on aquaculture and local socio-economic conditions. Eutrophication and phytoplankton growth, especially red tide, has become one of the major pollution problems in several estuaries in Japan including Atsumi Bay, Aichi prefecture. For over 40 years, eutrophication accompanies red tide and hypoxia occurred in every summer season as effect of huge nutrients inputs from industrial and agricultural areas around the bay. Several studies have investigated water quality and phytoplankton growth around Atsumi bay areas. However, effect of huge river inputs in estuaries during rainfall still less investigated. In current study, our purpose is to evaluate nutrient dynamics and phytoplankton growth on estuarine waterbodies with focus on huge river inputs effect during rainfall. Here, the pre- and post- rainfall conditions were at normal meteorological conditions, with heavy rainfall and gentle wind induced water bodies, where salinity and concentration alteration mostly occurred at the surface layer. The evaluations methods of this research are based on field measurement and numerical simulation. In

our simulation, we developed depth-averaged two-dimensional ecological model. The model has ability to simulate nutrient dynamics in form of dissolved nutrients, and phytoplankton growth over estuary. Biochemical parameter fitting becomes important part of the simulation in order to figure out dissolved nutrients cycles and phytoplankton growth. The model simulation is including distribution and transformation of dissolved nitrogen (DN), dissolved phosphorus (DP), and primary production of phytoplankton (*Chl a*). From field measurement result, we found that freshwater inputs during rainfall had changed post rainfall salinity stratification in the Umeda river transect of Atsumi bay. Post rainfall, an increase of nutrients and a decline in salinity after rainfall proved that a large amount of freshwater, mixed with nutrients, affected water quality conditions in the estuary. The decrease of dissolved nutrients is from the effects of freshwater dilution and phytoplankton uptake which verified by the increase of *Chl a* and decrease of DN and DP. Moreover, the influence of freshwater was dominant at river mouth station rather than at other the stations. The further the station was from the river mouth, the lower the influence which depicts the large proportion differences between *Chl a*, dissolved nutrients, and particulate nutrients concentrations at river mouth station and at the open sea station. In addition, the surface layer was supplied to more than the bottom layer, because the inputs were more influencing horizontal circulation than vertical circulation. It resulted in a small alteration of nutrients and *Chl a* concentrations compared to the surface layer. In the other hand, our ecological model has provided reasonable results and well correlation with observation data. The evaluation showed, in compare to pre-rainfall condition, increase of dissolved nutrients availability post-rainfall has gained production of phytoplankton in the Bay.

Acknowledgments

In the name of Allah the Most Gracious Most Merciful

First, I would like to thank Allah, the Almighty, for giving me the strength and ability to carry on this study. The completion of this thesis could not have been possible without the participation, support, and assistance of so many people whose names may not all be enumerated. Their contributions are sincerely appreciated and gratefully acknowledged. However, the author would like to express his deep appreciation particularly to the following:

I express my deep gratitude to my supervisor, Professor Takanobu Inoue, for the support and supervision he has provided throughout my study year. He has taught me innumerable knowledge and experience during my study. I have been grateful to be supervised by him who care so much about my work and condition. I would like to thank Professor Shigeru Kato and Associate Professor Kuriko Yokota for taking their time to examine this thesis. I also would like to thank all staff of the Toyohashi University of Technology and Department of Architecture and Civil Engineering to support my study and teaching endeavors.

I must express my very profound gratitude to my parents and family, for the love, endless support and continuous encouragement throughout my years of study and whole life. The accomplishment would not have been likely completed without them.

Finally, great thanks to all my friends, including all Water and Environment Engineering Laboratory of Toyohashi University of Technology's members and all Universitas Pertamina's lecturers and staff. Thank you very much for your friendship, support, and for every kindness and hospitality.

Author,

Teuku Mahlil

Table of Contents

List of Figures

List of Tables

Chapter I

Introduction

1.1 Background of Research

Excessive nutrient or eutrophication is currently one of most popular water environment issues in the world. Due to anthropogenic activities, nutrient loads have been changing water quality of aquatic environment such as rivers, lakes, and estuaries throughout the world (Glibert, 2017). This problem have been occurred and could be seen in several countries with high development in infrastructure, industrial, and agricultural. It is associated with rapid population and economic growth where the development has been pressing provision of human needs in form of food and settlement. In order to accelerate the provisioning process, the used of various biological and chemical substances including nutrients in the form of nitrogen (N) and phosphorus (P) are massively increased. In its application, most of those substances are, directly or indirectly, leached into aquatic environment from point and non-point sources.

Particularly in agricultural sector, the high frequency of fertilizer application and increase of non-point nutrient loads from agriculture has been associated to the impairment of surface and ground water qualities (Sharpley, 2013). Leaching process of nutrients from agriculture soil into surface water bodies significantly influenced by rainfall. During rainfall, accumulated nutrients on surface soil are flushed out by rainfall run-offs into river, and transported into estuaries and extending seaward. Enrichment of nutrient loads in waterbodies are resulting in acceleration of phytoplankton growth by the response of nutrient uptake by phytoplankton itself and photosynthesis. Further effect of the growth, as describe by Cloern (2001), could lead to an imbalance of algal production and consumption, which followed by enhanced sedimentation of algal-derived organic matter, stimulation of microbial decomposition and oxygen consumption, and the depletion of oxygen or also

called hypoxia. In addition, algal growth could affect mass mortalities of marine animals and leave bad impact on aquaculture and local socio-economic conditions.

1.2 General Information

1.2.1 Estuarine Nutrients

Estuaries are semi-enclosed coastal bodies of water where freshwater mixes with seawater (Dyer, 1973). In other words, estuary also describes as a transitional aquatic environment between river and shore, with typical shallow in depth, where freshwater mixed with seawater. As a typical shallow water with strong connection between land and coastal, estuaries have received huge influences by wind, waves, tides, salinities, off-shores current, and especially riverine inputs which makes estuaries rich with biological and chemical sources. Those factors and some morphological factors including the presence of irregular coastlines, islands, shoals and estuarine constructions have led estuaries to very complex hydrodynamic and transport processes (Hu *et al*., 2009).

Water quality of estuaries are influenced by chemical and biological conditions of freshwater inputs. In the watershed, freshwater qualities depend on human activities and values of nutrient released to the environment from point sources and non-point sources. Point sources usually release in small values into channel or river by following standard control of local regulation. On the other hand, non-point sources are more difficult to monitor and to control due to unspecific sources and areas. Agricultural area is one example of the biggest non-point sources in land and watershed areas. Agricultural activities such as the application of fertilizer into agricultural field tends to supply high concentration of nutrients, in form of nitrogen (N) and phosphorus (P), which is resulting in accumulation of nutrients in soil bodies. Then, meteorological parameters, including rainfall and discharges, are supporting on distribution of nutrients to whole ecosystems.

Important roles of rainfall and discharges are held by these parameters to distribute nutrients from watershed to estuaries. During rainfall, run-offs flush out nutrients from soil bodies into river and resulting in water quality changes of river freshwater. From river, the discharges take over the task to transport nutrients into estuaries and seaward. Eventually,

mixing between freshwater and seawater in estuary and excessive inputs of nutrient are affecting on enrichment of nutrients, or called eutrophication, in the water bodies.

1.2.2 Nitrogen Compounds

Nitrogen is a chemical form that exist in form of nitrogen gas and liquid. In liquid form, nitrogen enters the environment in the form of dissolved nitrogen (DN) and particulate nitrogen (PN). Nitrogen have very complicated cycles in environment as shown on Figure 1.1. Major component of nitrogen cycles are in the forms of organic nitrogen (ON), nitrate (NO_3^-), nitrite (NO_2^-) and ammonium (NH_4^+). The primary source of nitrogen is ON which come to environment externally from plants and animal (including animal excretion and death bodies). By influences of bacterial, ON decomposed and mineralized into form of NH_4^+. Furthermore, nitrification process occurs by help of bacterial to oxidize NH_4^+ into the

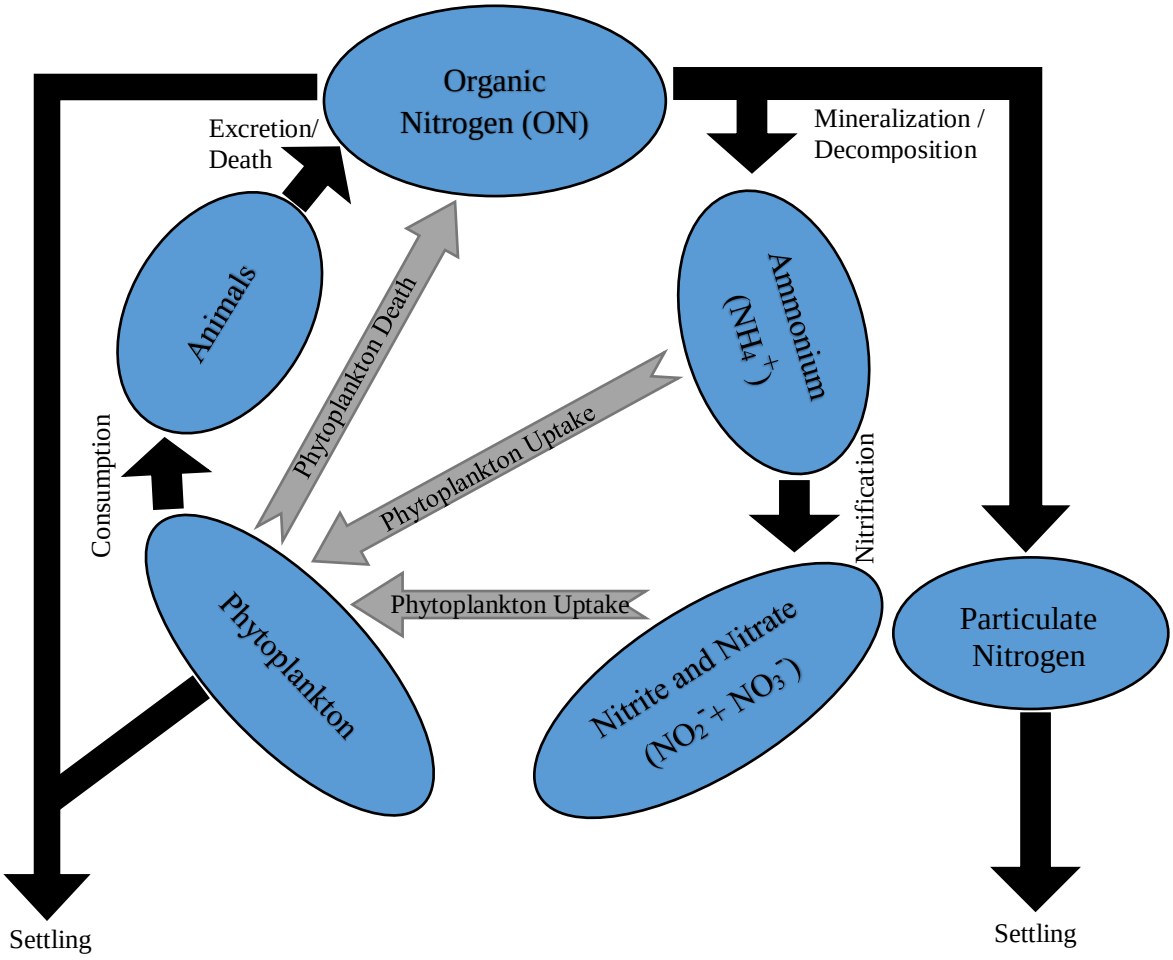

Figure 1.1 Nitrogen Cycle

form of NO_2^- and NO_3^-. NH_4^+, NO_2^-, and NO_3^- are the essential nutrients for algal growth. Those substances uptake by algal during photosynthesis process by influences of light intensity and water temperature.

In addition, some algal have abilities to convert NO_3^- into nitrogen gas form of N_2 by denitrification process, during low DO conditions, and further release from waterbodies to atmosphere. During fixation process, N_2 in atmosphere is consumed by algal and converted into ON form. In this nitrogen cycle, eventually algal is becoming source of nitrogen for animals. Later, all nitrogen from animals is going to be released to environment in the form of ON and the nitrogen cycles restart continuously.

1.2.3 Phosphorus Compounds

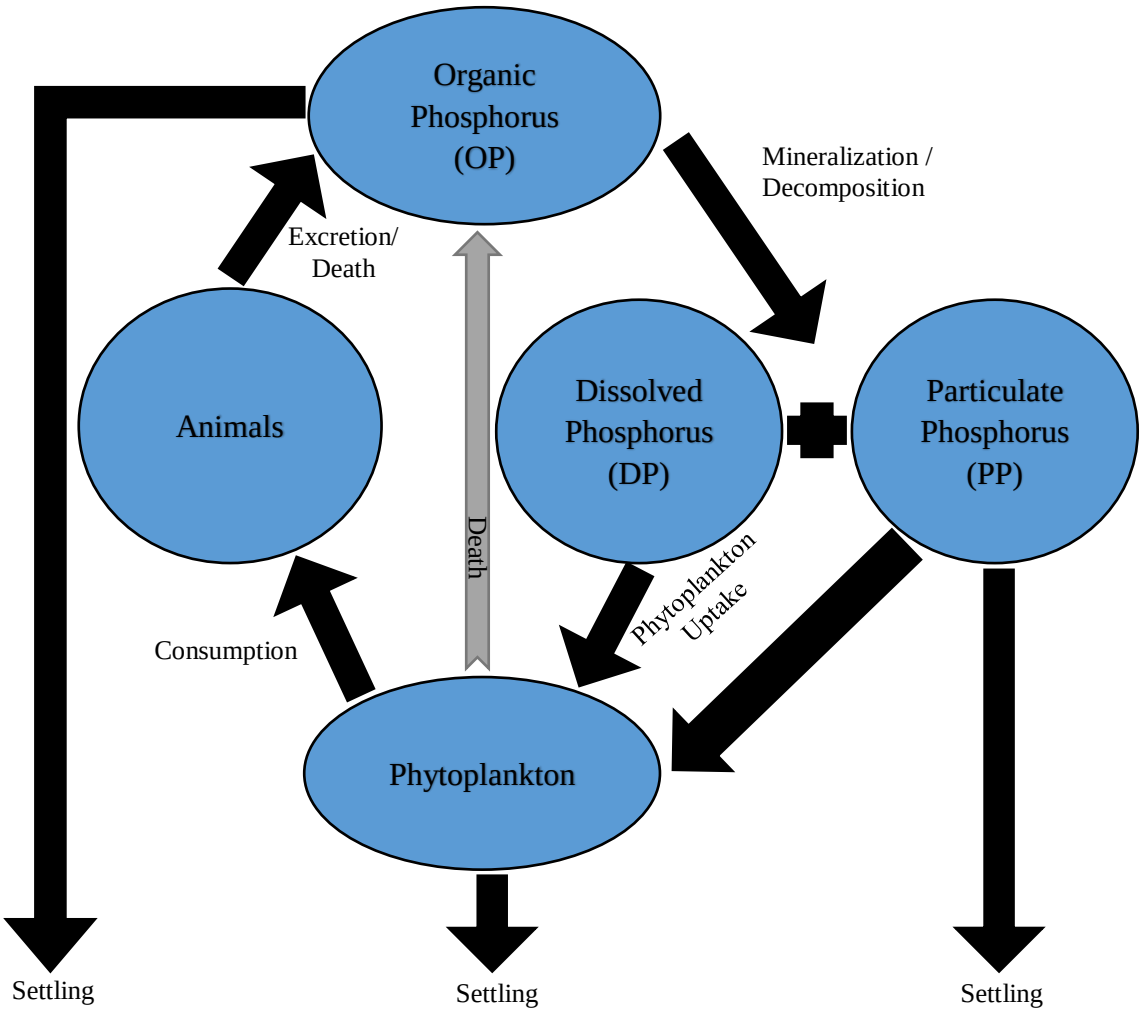

Figure 1.2 Phosphorus Cycle

Phosphorus is also essential nutrients for aquatic organism and vital nutrient for algal growth as well as nitrogen. Phosphorus does not have a gas form, it is existed only in the form of inorganic and organic matter including dissolved phosphorus (DP) and particulate phosphorus (PP). Availability of phosphorus in water bodies is very important for photosynthesis process on algal production. Huge inputs of phosphorus in water bodies could result in eutrophication and give adverse effect on excessive algal growth and hypoxia.

As shown in Figure 1.2, phosphorus cycles in environment are started in the form of organic phosphorus (OP). OP is mineralized and decomposed into dissolved phosphorus (DP) and particulate phosphorus (PP). The dissolved form is up taken by algal for photosynthesis where particulate form is settling down to bottom layer, consumes by animals, and sorb by sediments. Moreover, dissolved phosphate in algal bodies is converted as OP. Then, algal will be consumed by animals where later the excretion waste and death bodies of animals also converted into OP.

1.2.4 Eutrophication

Eutrophication is the enrichment of nutrients, N and P, concentrations in waterbody as response of natural processes or human activities. As natural processes, nutrients enrichment may take more than a decade or century to be eutrophic. On the other hand, artificial process including development of countries, enhancement of industries, and the advanced application of fertilizer in agricultural activities has caused significant anthropogenic impacts including eutrophication in lake, river, and coastal environments. Especially in coastal areas, nutrient enrichment caused by riverine inputs is the most widespread and globally significant anthropogenic impact (Billen and Garnier, 1997). Enrichment of nutrients in estuaries produce huge effects in marine ecosystems such as: increased biomass of marine phytoplankton and epiphytic algae, shifts in phytoplankton species composition, changes in macroalgal production, biomass, reduced of water clarities, dissolved oxygen depletion in the water column, increase probability of death of recreationally and commercially important animal species (Smith *et al*., 1999).

1.2.5 Red Tide

Red tide is phytoplankton overgrowth phenomenon as effect of eutrophication in waterbodies (Figure 1.3). The occurrence of red tide is related to phytoplankton production by influence of nutrients, light intensity, and water temperature. Phytoplankton growth is part of nitrogen and phosphorus cycles where phytoplankton uptakes dissolved nutrients and convert it into organic nutrients. On eutrophic estuaries, availability of high nutrient concentrations led highly growth of phytoplankton in water bodies and affecting water transparencies and depletion of oxygen. Decrease of water transparency gives direct effect

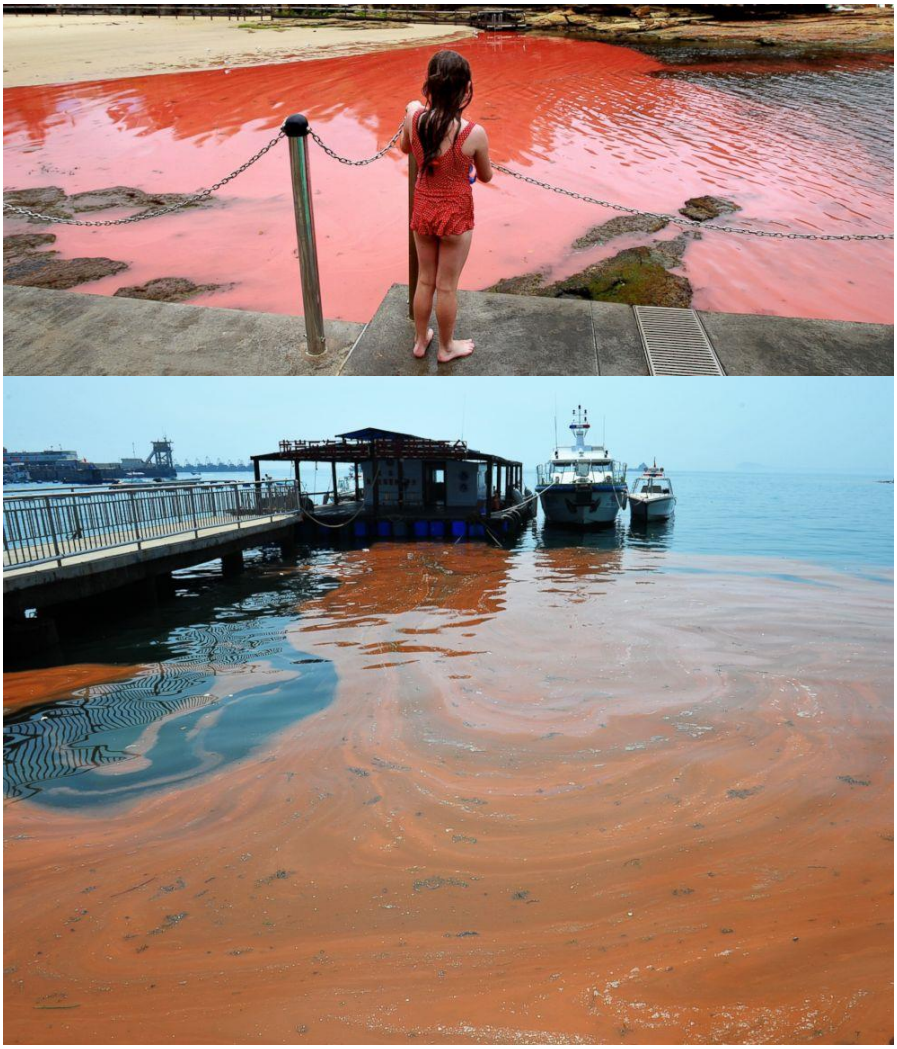

Figure 1.3 Red Tide

Source: http://abcnews.go.com/US/massive-red-tide-off-coast-florida/story?id=24963894

Accessed: 19 August 2017 14.01 JST

in distribution of light intensity in water layer which use by aquatic plans for photosynthesis process. Less photosynthesis process could result in wilt and drop of aquatic plans where it continues to effect aquatic animals that consume those plans. Moreover, depletion oxygen effect also become harmful to aquatic animals. Disruption of aquatic animals' population also gives impact to socio-economic condition of people around estuary who are working in fisheries and tourism sectors. In addition, several species of phytoplankton have ability to produce and release toxin into waterbodies which is harmful for aquatic plants and animals, and for people who are leaving around eutrophic estuaries.

1.3 Ecological Model

An ecological model is a tool to evaluate the physical, chemical, and biological characteristic of water bodies. In this study, the model was developed numerically into depth-integrated two-dimensional model. The model is parted into two segments including hydrodynamic and ecological models. In the first segment, hydrodynamic model uses to evaluate current velocities, water level, salinities, and temperatures. The model is evaluated by concerning various terms including advection, diffusion, Coriolis force, pressure gradient, surface wind stress, bottom stress, and density gradients.

Dynamic results of hydrodynamic model are applied to the second segment or called ecological model. The hydrodynamic results are including current velocities simulate distribution of nutrients and phytoplankton concentration (advection term); salinity and temperature to quantify water density conditions; and temperature also uses in analyzing biochemical reaction of phytoplankton growth. In ecological model, the evaluations are specified to mass balance condition of every concentrations in the model including dissolved nitrogen (DN), dissolved phosphorus (DP), and phytoplankton growth in form of Chlorophyll *a* (*Chl a*).

Development of hydrodynamic and ecological models are following Navier-Stokes equation which commonly used in numerical model development. Model discretization is using explicit first order upwind scheme for advection terms of depth-integrated two-dimensional

model, and explicit second order central scheme for horizontal diffusion terms. Detail of the model is provided at Chapter 2.

1.4 Research Purpose

Eutrophication and phytoplankton growth, especially red tide, has become major pollution problem in several estuaries in Japan such as Tokyo Bay, Ise-Mikawa Bay, and Seto Inland Sea (Nakanishi *et al.*, 1990; Nakane *et al.*, 2006; Suzuki, 2016). Especially for Ise-Mikawa Bay, Aichi Prefecture, Japan, as the widest bay in Central Japan region and surrounding by highly developed cities are continuously dealing with eutrophication and red tides problems. The bay is divided into two bays region which are Ise bay in the western side and Mikawa bay in the eastern side. Some researchers reported that eutrophication accompany by red tide and hypoxia have been occurred in the bay for more than four decades as effect of rapid development around these areas (Matsukawa and Suzuki, 1985; Bodergat, 1997; Suzuki, 2004). Especially at the eastern side of Mikawa Bay or called Atsumi Bay, red tide and hypoxia occurred in every summer season as effect of huge nutrients inputs from industrial and agricultural areas around the bay.

Several studies have investigated water quality and phytoplankton growth around Ise-Mikawa areas (Sakamoto and Tanaka, 1989; Kasih and Kitada, 2004, 2008; Higashi *et al.*, 2012). Especially for water quality changes in Atsumi Bay, the study had been studied by Rasul (2013) and Rasul *et al.* (2013, 2014) with focused on the effects of nutrient enrichment and hypoxia after a typhoon event, with three major river inputs including the Toyo, Umeda, and Shio rivers. In their study, the evaluation was based on extreme meteorological conditions with very heavy rainfall and strong wind induced water bodies, which resulted in salinity dilution and significant changes in nutrient concentrations from the surface to the bottom layer. However, effect of huge river inputs in estuaries during rainfall still less investigated.

In the current study, attention was paid to the effect of the Umeda River inputs on nutrient concentration changes and phytoplankton growth on pre- and post-rainfall water quality conditions in Atsumi Bay, especially around the Umeda transects. Here, the pre- and post-rainfall conditions were observed under normal meteorological conditions with heavy

rainfall and gentle wind-induced waterbodies, where salinity and concentration alteration mostly occurred at the surface layer. The purpose of the current research was to evaluate the influence of nutrient inputs from the Umeda River to Atsumi Bay. Our evaluation of water quality conditions was for the period of peak phytoplankton bloom in the summer of 2010. The evaluations methods of this research are based on field measurement and numerical simulation. In our simulation, we developed an ecological model based on depth-integrated two-dimensional model and three-dimensional sigma-coordinate. Model simulations are including distribution and transformation of dissolved nitrogen (DN), dissolved phosphorus (DP), and primary production of phytoplankton in the form of Chlorophyll *a* (*Chl a*).

1.5 Structure of Thesis

The present thesis is a study about water quality changes in estuary as effect of huge nutrient inputs during rainfall. In this study, we analyze water quality of Atsumi bay during summer 2010 by observation data analysis and numerical simulation. The whole methods and results of current study are presented and discussed in chapter II, III, IV, and V. In addition, general conclusions of our study is presented in chapter VI.

Chapter I is highlights of general information about nutrients in estuaries, eutrophication, red tide, ecological model, and purpose of this research. Chapter II is describing the study area, data collections from observation and other party's secondary data. Data observation and analyses methods, research parameters, and secondary data collection are given in detail at this chapter. Chapter III is illustrating the development of depth-averaged two-dimensional ecological model which begin with governing equation, numerical discretization, and parameter inputs.

Chapter IV is discussing about alteration of water quality of Atsumi Bay as effect of nutrient inputs from Umeda River. This chapter show detail discussion about the important finding about summer 2010 water quality condition of the bay, and the impact of enrichment nutrients on phytoplankton production around the bay. In particular, water quality alteration and phytoplankton biomass (in the form of Chlorophyll *a*) condition around the bay at pre-, during, and post- high precipitation day are clearly explained.

Chapter V is examining phytoplankton growth and nutrient dynamics condition of Atsumi Bay using depth-averaged two-dimensional model. All parameters inputs, model setup, data initialization, boundary setting, physical parameter influences, biochemical reaction, and ecological simulation are explained in this chapter. The discussion about water quality alteration and phytoplankton growth in Atsumi Bay as effect of nutrient inputs from Umeda River is notified clearly and specifically. In the final chapter VI, whole finding and results are summarized and presented as conclusions.

REFERENCES

Billen, G., and J. Garnier. 1997. "The Phison River plume: Coastal eutrophication in response to changes in land use and water management in the watershed." *Aquatic Microbial Ecology* 13: 3–17. doi:10.3354/ame013003.

Bodergat, A-M., Rio, M., Ikeya, N. 1997. "Tide versus eutrophication. Impact on ostracods populations structure of Mikawa Bay (Japan)." *Revue de Micropaléontologie* 40 (1): 3-13. doi:10.1016/S0035-1598(97)90080-5.

Cloern, J.E. 2001. "Our evolving conceptual model of the coastal eutrophication problem." *Marine Ecology Progress Series* 210: 223-253.

Dyer, K. R. 1973. *Estuaries: A physycal introduction.* New York and London: Wiley-Interscience.

Glibert, P. M. 2017. "Eutrophication, harmful algae and biodiversity — Challenging paradigms in a world of complex nutrient changes." *Marine Pollution Bulletin* 124(2): 591-606. doi: 10.1016/j.marpolbul.2017.04.027.

Higashi, H., H. Koshikawa, S. Murakami, K. Kohata, M. Mizuochi, and T. Tsujimoto. 2012. "Effects of land-based pollution control on coastal hypoxia: a numerical case study of integrated coastal area and river basin management in Ise Bay, Japan." *Procedia Environmental Sciences* 13: 232-241.

Hu, K., P. Ding, Z. Wang, and S. Yang. 2009. "A 2D/3D hydrodynamic and sediment transport model for the Yangtze Estuary, China." *Journal of Marine Systems* 77 (1-2): 114-136. doi:10.1016/j.jmarsys.2008.11.014.

Kasih, G. A. A., and T. Kitada. 2004. "Analysis of factors regulating algal bloom in mikawa bay using eutrophication model." *Environmental Engineering Research* 41: 613-624.

Kasih, G. A. A., and T. Kitada. 2008. "Modeling of the role of tideland in eutrophication reduction in Mikawa Bay, Japan." *Proceedings of the Symposium on Global Environment* 16: 41-50.

Matsukawa, Y., and T. Suzuki. 1985. "Box model analysis of hydrography and behaviour of nitrogen and phosphorus in a eutrophic estuary." *Journal of the Oceanographical Society of Japan* 41 (6): 407–426. doi:10.1007/BF02109035.

Nakane, T., K. Nakaka, H. Bouman, and T. Plat. 2006. "Environmental control of short-term variation in the plankton community of inner Tokyo Bay, Japan." *Estuarine, Coastal and Shelf Science* 78 (4): 796-810. doi:doi.org/10.1016/j.ecss.2008.02.023.

Nakanishi, H., M. Ukita, M. Sekine, M. Fukagaw, and S. Murakami. 1990. "Eutrophication Control in Seto Inland Sea." *Marine Coastal Eutrophication* 1239-1256. doi:10.1016/B978-0-444-89990-3.50105-X.

Rasul, E. 2013. *The influence of typhoon on nutrient dynamics and hypoxia in Atsumi bay, Japan.* Toyohashi: Toyohashi University of Technology.

Rasul, E., T. Inoue, S. Aoki, K. Yokota, Y. Matsumoto, Y. Okubo, and Djumanto. 2013. "Influence of tropical cyclone on the water quality of Atsumi Bay." *Journal of Water and Environment Technology* 11 (5): 439-451.

Rasul, E., T. Inoue, S. Aoki, K. Yokota, Y. Matsumoto, and Y. Okubo. 2014. "Nutrient enrichmenr and physical environmental effects caused by typhoons in a semi-enclosed Bay." *Journal of Ecotechnology Research* 17 (3-4): 107-114. doi:10.11190/jer.17.107.

Sakamoto, M., and T. Tanaka. 1989. "Phosphorus dynamics associated with phytoplankton blooms in eutrophic Mikawa Bay, Japan." *Marine Biology* 101 (2): 265-271.

Sharpley, A. N. 2013. "Agriculture, Nutrient Management, and Water Quality." *Encyclopedia of Biodiversity (Second Edition)* 95-110. doi:10.1016/B978-0-12-384719-5.00361-0.

Smith, V.H., G.D. Tilman, and J.C. Nekola. 1999. "Eutrophication: Impacts of Excess Nutrient Inputs on Freshwater, Marine, and Terrestrial Ecosystems." *Environmental Pollution* 100 ((1-3)): 179-196.

Suzuki, C. 2016. "Assessing change of environmental dynamics by legislation in Japan, using red tide occurrence in Ise Bay as an indicator." *Marine Pollution Bulletin* 102 (2): 283-288.

Suzuki, T. 2004. "Large-scale restoration of tidal flats and shallows to suppress the development of oxygen deficient water masses in Mikawa Bay." *Bulletin of Fisheries Research Agency* Supplement 1: 111-121.

Chapter II

Study Area and Data Collection

2.1 Study Area

In central of Japan area, lies one of the biggest bays in Japan which called Ise-Mikawa Bay (Figure 2.1). The bay is in Aichi Prefecture, Japan where several cities such as Nagoya, Toyohashi, Gamagori, other cities located. The Bay is divided into Ise Bay in western side and Mikawa Bay in eastern side (Figure 2.2). Both bays receiving huge influence from Pacific Ocean and watersheds around its surrounding area. Watershed inputs into the bay not only in the form of freshwater discharge, several substances from anthropogenic activities around the watershed also loads to the bay. As example, enrichment nutrients or eutrophication from watershed inputs regularly found in several estuary around the bay which is related to human activities of highly developed cities around the watersheds where most of the cities famed for industrial and agricultural sectors.

This research is conducted in one of the highly developed cities in Aichi Prefecture which calls Toyohashi city. The city is located at eastern part of Mikawa Bay surrounding area where eutrophication and phytoplankton bloom regularly occurred. In this eastern side, people called this bay area as Atsumi Bay. Atsumi Bay is a partially mixed estuary, where river discharge and tidal forces dominantly influence the circulation and stratification of the water bodies. Its topographical condition is shallow and flat with a mean depth of about 10 m. The total area of the bay is approximately 180.5 km^2 (Figure 2.3). There are some ports and famous recreational locations around this area as a vital infrastructure to support socio-economy of people around the Bay, especially people in Toyohashi city. The Toyohashi city and Atsumi Bay areas have a temperate climate with average precipitation was around 1,516 mm/year in 2010. During the summer of 2010, rainfall was recorded 39 times with amounts varying from 0.5 mm/day to 81 mm/day. In addition, several typhoons, along with high precipitation, pass through this the area every year during summer season.

Figure 2.1 Location of Ise-Mikawa Bay in Japan

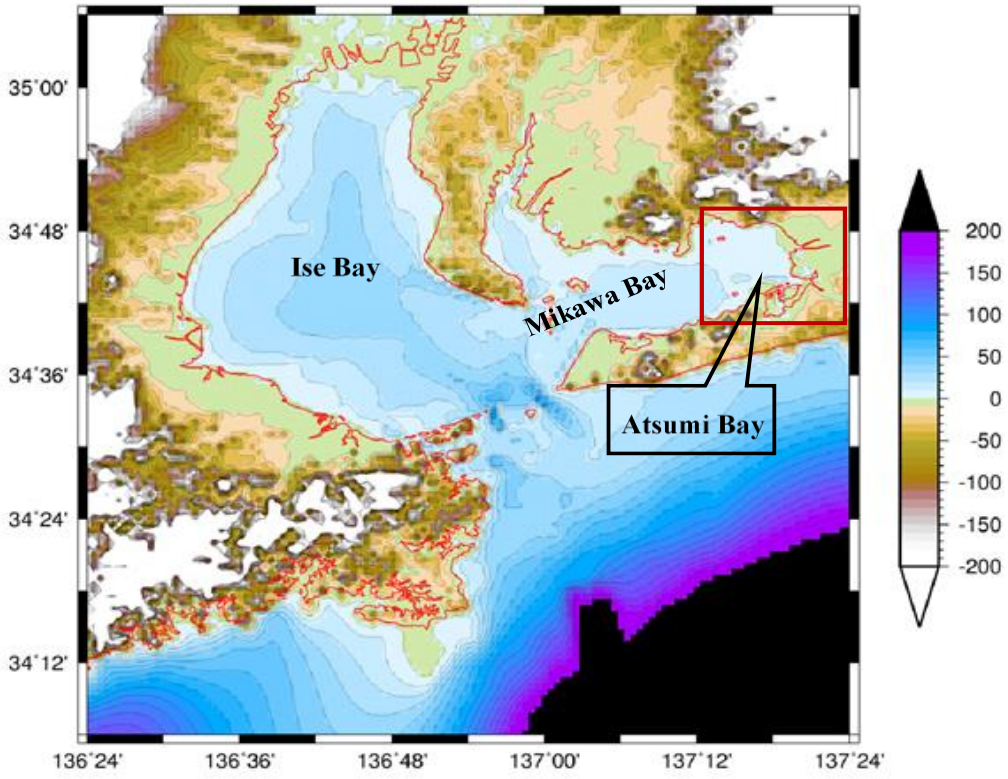

Figure 2.2 Bathymetrical Map of Ise-Mikawa Bay

As in many countries around the globe, agricultural areas in Japan are one of the major non-point sources of nutrients (Yamada and Inoue, 2005). In Japan, especially in Atsumi Bay, red tide and hypoxia have occurred for a significant number of years due to riverine nutrient inputs mainly originating from the surrounding agricultural areas. Several rivers, such as the Toyo, Umeda, and Shio Rivers, are connected and flow into Atsumi Bay. These rivers are the main suppliers of freshwater and nutrients to the bay. The highest input of nutrients into the bay comes from the Umeda River Watershed (Rasul, 2013). The Umeda Watershed covers approximately 134 km^2 and comprises of agricultural area (45.7%), urban area (33.9%), forest area (6.5%), and other areas (13.9%) (Rasul *et al*., 2013). It was reported by Bodergat *et al*. (1997) that Mikawa Bay, including Atsumi Bay, has become highly eutrophic due to the increase of nutrient inputs from livestock farms and municipalities as well as from rapid industrial development since the mid-1960s.

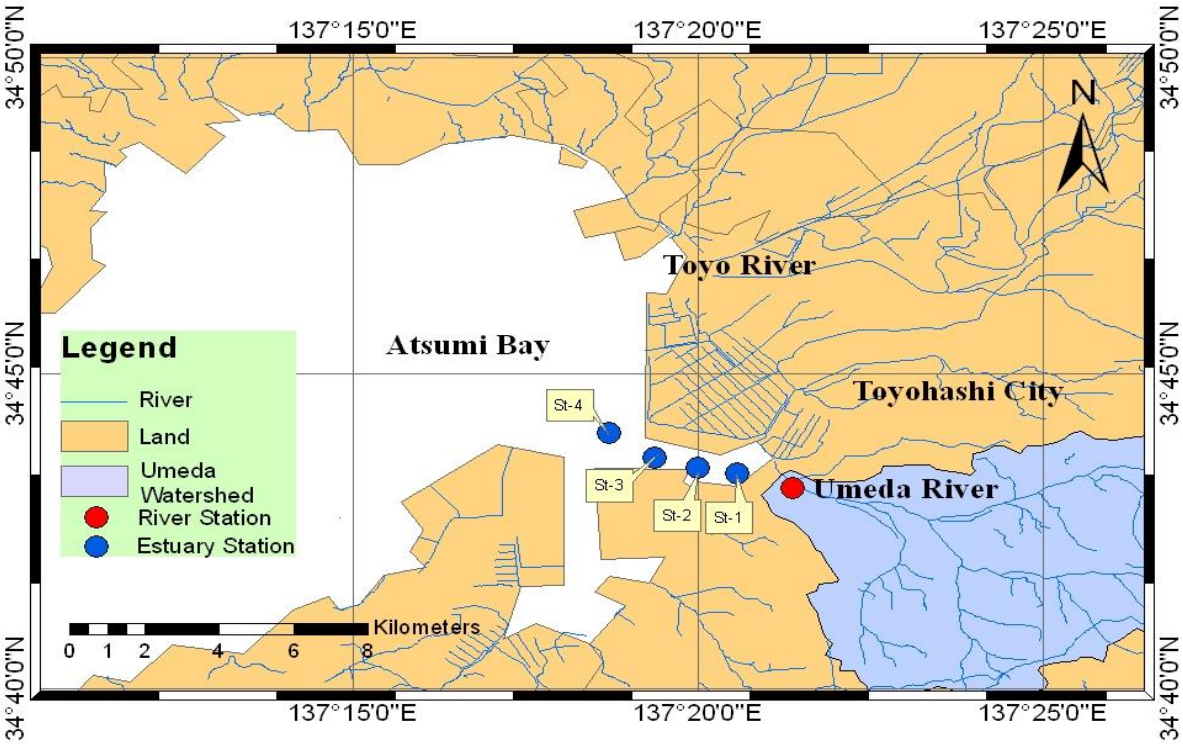

Figure 2.3 Atsumi Bay

2.2 Data Collection

In this study, we used both primary data from field observation and secondary data from other sources. The primary data were observed and analysis by our laboratory member and following guideline of each data analysis method. On the other hand, we used raw secondary data from other sources, such as government, laboratory member, and faculty member, for further evaluation and simulation.

2.2.1 Field Measurement and Analysis Method

2.2.1.1 River Measurement

Samples were collected at the Umeda River Station (Hatakeda Bridge) and four stations along the Atsumi Bay in the summer of 2010 (Figure 2.3). At the Umeda River Station, observations were conducted between July and October 2010 during rainfall and on fine days with a total of 99 samples collected. For each observation, water samples were taken from 8 to 24 times at hourly intervals. Durinh rainfall, samples were collected from when the flood started until the moment the flood subsided. All samples were collected at the surface layer using an auto sampler (6700, Teledyne ISCO, USA) and were then dispensed into 500-mL polypropylene bottles. The sample analysis was conducted at laboratory immediately after sampling.

River samples were used to quantify nutrient load from river to estuary using empirical estimation called L-Q equation model. This model is widely used to quantify river nutrient loads, where the results are used for river boundary inputs on multidimension hydrodynamic and water quality models. The L-Q equation model was constructed using regression model by following the relation between river discharge and nutrient loads (Tsushima *et al.*, 2009). The evaluation of model was evaluated following coefficient of determination (r^2) between observation data and model results. The coefficient of determination values must be approaching ≈ 1 to convince that the results are close to field condition and the *a*, *b* coefficients are adequate to adopt. The mathematical formulation of the L-Q equation model can be seen in equation 2.1.

$$L = aQ^b \quad (2.1)$$

Where: L is the nutrient loads (g s^{-1}), Q is river flow (m^3 s^{-1}), and *a*, *b* are model coefficients.

2.2.1.2 Estuary Measurement

Estuary measurement is conducted to observe salinity, dissolved and particulate nutrients, and *Chl a* condition of Atsumi Bay. The observations were conducted ten times, with intervals of eight to ten days, from July to October 2010 along Umeda River transect. At the estuary stations, 80 samples were collected at 1 m below the surface (surface layer) and 1 m above the bottom (bottom layer), and then dispensed into 500-mL polypropylene bottles with a peristaltic pump. To measure vertical salinity, we used conductivity-temperature-depth and a DO sensor (Rinko Profiler, JFE Advantech Co. Ltd, Kobe, Japan). This instrument measured vertical profiles at 0.1 m depth intervals.

2.2.2 Analysis Method of Water Quality

Nutrient analyses were conducted at the laboratory immediately after sampling. An aliquot of each sample was filtered through a GF/F glass-fiber filter (Whatman International Ltd., Maidstone, UK) for Chlorophyll *a* analysis. The filtrate samples were used for analysis of the dissolved nitrogen (DN) and dissolved phosphorus (DP), while unfiltered samples were used for analysis of total nitrogen (TN) and total phosphorus (TP). The amounts of particulate nitrogen (PN) and particulate phosphorus (PP) were calculated by subtracting total and dissolved nutrients. In order to minimize volatilization and biodegradation, the samples were stored in a dark freezer until analysis was done in the following days.

Nutrient analyses were conducted by adjusting the water characteristics of the sample locations under the measurement procedure of the American Public Health Association (2005). Analysis of the river samples was undertaken using Milli-Q water. In the case of the estuary samples, artificial seawater was created to adjust the density and ion concentration of the water by integrating 28.5 g of NaCl, 6.82 g of $Mg.SO_4.7H_2O$, 5.16 g of $Mg.Cl_2.6H_2O$, and 1.47 g of $CaCl_2.2H_2O$ to 1 L of Milli-Q water. In the analysis of *Chl a*, methanol

extraction was used in accordance with the protocol of Otsuki *et al.* (1987), where the sample residue on the GF/F filters was extracted using 100% methanol.

2.2.3 Secondary Data

2.2.3.1 Meteorological Data

Meteorological data for study location areas were obtained at Toyohashi and Nagoya rain gage station by Automated Meteorological Data Acquisition System (AMeDAS) operated by Japan Meteorological Agency (JMA). The data are openly published through JMA's website www.jma.go.jp that can be accessed by everyone and for unlimited purposes especially academic purpose. In our study, we used several meteorological data of 2010 from Toyohashi rain gage station that includes precipitation (Figure 2.4), wind speed and direction (Figure 2.5), air temperature, and sunshine duration (Figure 2.6). On the other hand, we used solar fluxed radiation and sunshine duration of the same year from the nearest station to Toyohashi city, which is Nagoya rain gage station, to simulate the condition of solar fluxed radiation at Toyohashi city areas. All meteorological data are used for simulation requirements of hydrodynamic and ecological model that detailly explained in Chapter III.

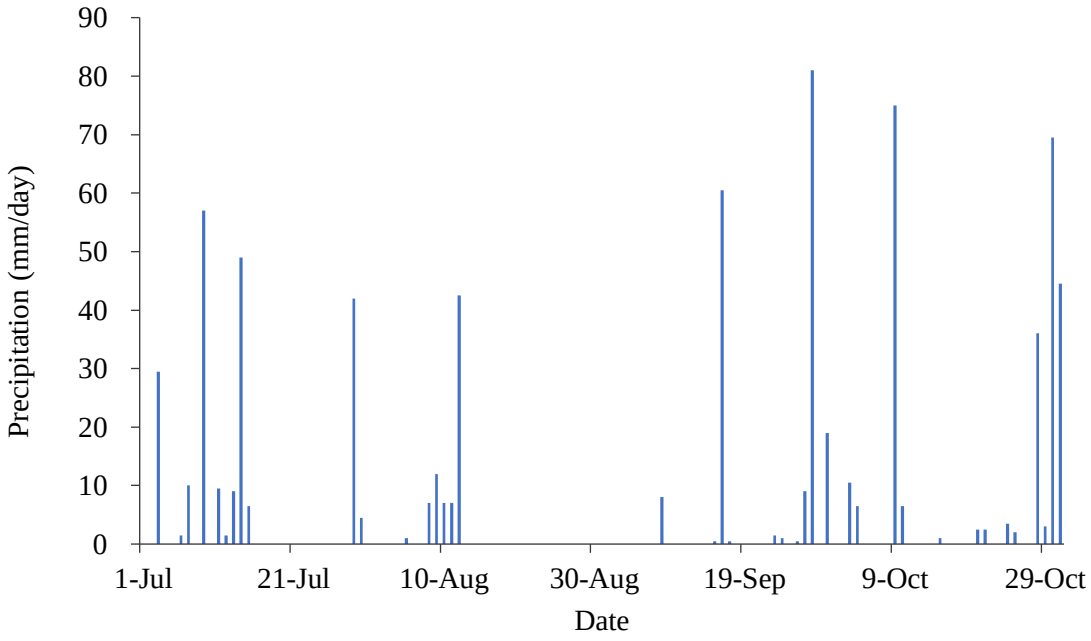

Figure 2.4 Precipitation Data of Toyohashi City on 2010

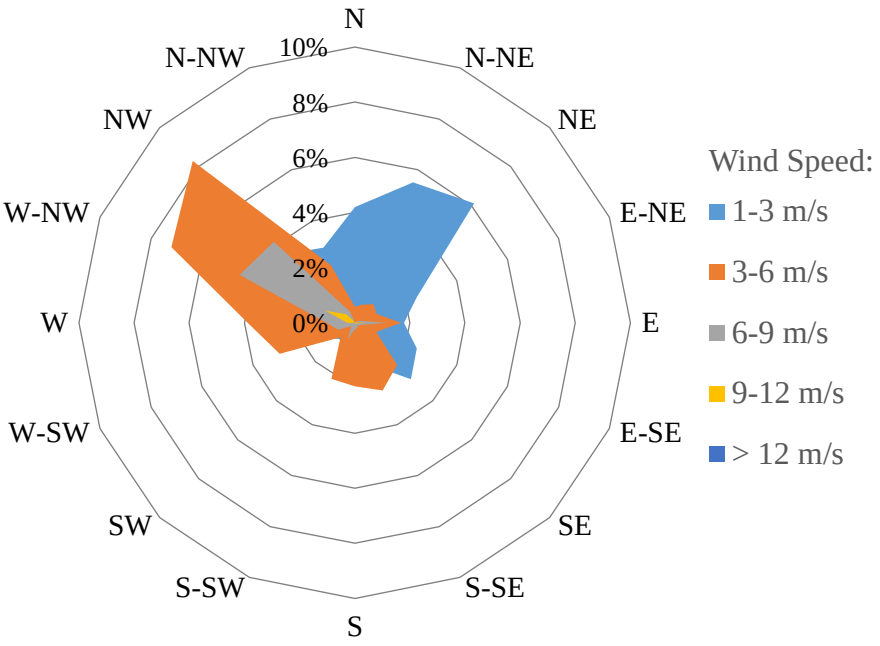

Figure 2.5 Wind Rose of Toyohashi City on 2010

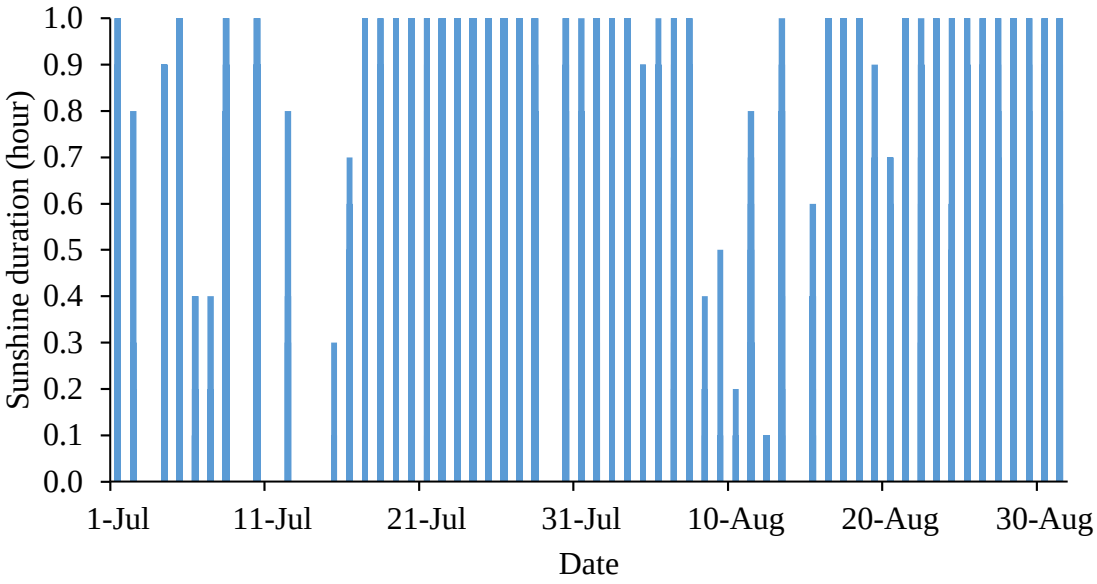

Figure 2.6 Sunshine Duration of Toyohashi City on Summer 2010

2.2.3.2 Discharges and Water Level Data

Umeda River water level data was obtained from measurement of river water level by Yokota *et al.* (2013) and then converted into discharges (Figure 2.7). The discharges and water level data are used in this study to estimate river nutrient loads and as boundary conditions of hydrodynamic and ecological model. Estimation of discharges to nutrient loads in form of DN and DP is explained in more detail on Chapter 3. On the other hand, sea water level also used for the model's boundary conditions. The sea level data was obtained from water level data at Maeshiba Station, which operated by Ministry of Land, Infrastructure and Transport, Japan (Figure 2.8). Mikawa Port Tidal Station is specifically lied Atsumi Bay around Umeda River transects. The station is the inside of our simulation boundary and properly use to predict tidal constituents for basic estimation of tidal water level of Atsumi Bay. The data is in form of water level which observed every one-hour for 30 days duration. The simulation of tidal constituents conducted using harmonic analysis as explained in Chapter 3.

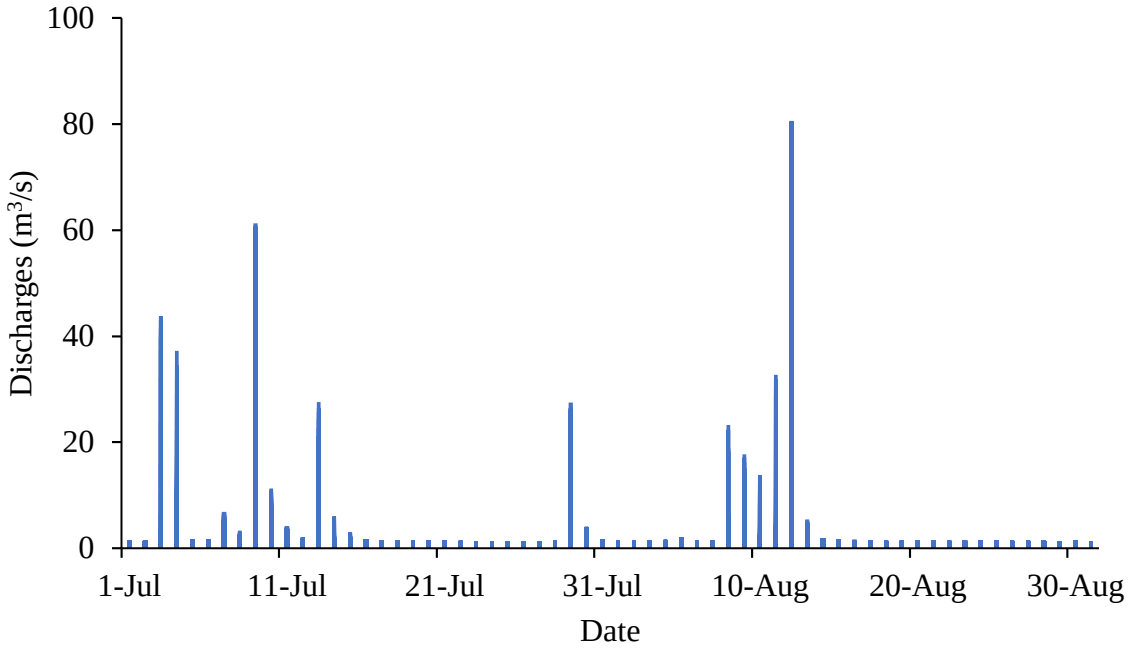

Figure 2.7 Umeda River Discharges on Summer 2010

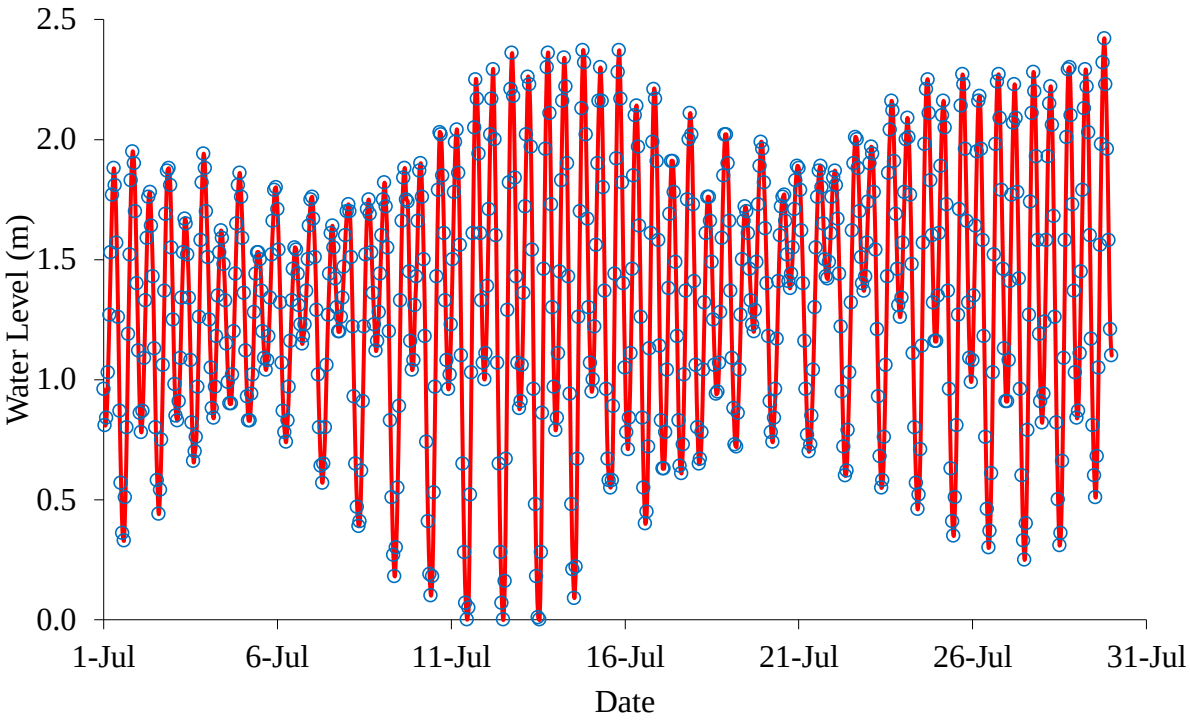

Figure 2.8 Observed Water Level at Mikawa Port Tidal Station

REFERENCES

American Public Health Association/American Water Works Association/Water Environment Federation. 2005. *Standard methods for examination of water and wastewater.* Vol. 21st ed., New York.

Bodergat, A-M., M. Rio, and N. Ikeya. 1997. "Tide versus eutrophication. Impact on ostracods populations structure of Mikawa Bay (Japan)." *Revue de Micropaléontologie* 40 (1): 3-13. doi:10.1016/S0035-1598(97)90080-5.

Otsuki, A., M. M. Watanabe, and K. Sugahara. 1987. "Chlorophyll Pigments in Methanol Extracts from Ten Axenic Cultured Diatoms and Three Green Algae as Determined by Reverse Phase HPLC with Fluorometric Detection." *Journal of Phycology* 23 (3): 404-414.

Rasul, E. 2013. *The influence of typhoon on nutrient dynamics and hypoxia in Atsumi bay, Japan.* Toyohashi: Toyohashi University of Technology.

Rasul, E., Inoue, T., Aoki, S., Yokota, K., Matsumoto, Y., Okubo, Y., Djumanto. 2013. ", Influence of Tropical Cyclone on the Water Quality of Atsumi Bay." *Journal of Water*

and Environment Technology 11: 439-451.

Tsushima, K., T. Koike, Y. Horinouchi, T. Inoue, and T. Yamada. 2009. "Evaluation of Nutrient Loads from a Citrus Orchard in Japan." *Journal of Water and Environment Technology* 7 (2): 267-276.

Yamada, T., and T. Inoue. 2005. "Influence of Phosphorus Runoff from Agricultural Areas on Enclosed Sea Downstream." *Journal of Water and Environment Technology* 3 (2): 157-156.

Yokota, K., Inoue, T., Yokokawa, M., Shimoyama, R. and Okubo, Y. 2013. "Evaluation of nutrient load from Umeda River flowing into the Mikawa Bay." *Environmental Science* 26: 140–149.

Chapter III

Numerical Model Development

3.1 Ecological Model

For decades, researcher have been observing coastal region in order to evaluate hydrodynamic and ecological condition of coastal region. Influence of many meteorological, topographical, and biochemical parameters have made coastal region to be the most complicated waterbodies in comparison to lake and river. Observations have been conducted in many coastal regions over the world. However, sometimes an observation could not evaluate the hydrodynamic and ecological condition of a coastal region continuously due to limitation of times, tools, and resources.

Moreover, since early 20^{th} century many efforts have been made to create numerical models in order to solve those limitations. Various numerical models from one, two, or three dimensions have been developed and upgraded from time to time with purpose to create tools for detail evaluation of coastal hydrodynamic and ecological condition. In current study, an ecological model was developed with purpose not only to evaluate hydrodynamic condition of coastal waterbodies but also to evaluate phytoplankton growth and nutrient dynamic.

Current model was developed based on Navier-Stokes equation for hydrodynamic simulation which commonly used in several models such as Princeton Ocean Model (POM), Bergen Ocean Model (BOM), Delft-3D, Regional Ocean Modeling System (ROMS), and many other models (Mellor and Yamada, 1982; Berntsen *et al*., 2015; Xu *et al.*, 2017; Sikirić *et al.*, 2013). The model is divided into two segments: hydrodynamic and ecological models. Hydrodynamic model is main physical model to evaluate current velocities, water elevation, temperature, and salinity. In this segment, physical influences such as tidal, wind speed, wind direction, river inputs, ocean inflow and outflow are comprehensively estimated as driven forces of coastal hydrodynamic. In ecological model, besides evaluating the physical

parameters, this segments more specifically used to evaluate the distribution and biochemical reaction of phytoplankton growth in the form of phytoplankton biomass (*Chl a*) and the dissolved nutrient dynamics including dissolved nitrogen (DN), dissolved phosphorus (DP).

In shallow waters, such as estuaries and shallow bays like Atsumi Bay, horizontal velocities are more dominant than vertical velocity. It is proved by our observation of salinity distribution along the Bay which dominantly change in surface layer in comparison to bottom layer (detailly explained in the Chapter 4). This condition indicated that the bay circulation mostly influenced by horizontal velocities. Therefore, adopting depth-averaged two-dimensional model to simulate large-scaled circulation in shallow waters is adequate (Ji, 2008).

3.2 Depth-Averaged Two-Dimensional Model

In two-dimensional model, depth-averaged two-dimensional model is commonly adopted for hydrodynamic and ecological models. Basic governing equation of the model is based on three-dimensional model. In assumption that vertical velocity is less dominant than horizontal velocities and constant water density, the *z* coordinates of basic three-dimensional model is neglected and counts as zero flux. Then, horizontal velocities are estimated over total water depth.

$$\frac{\partial \bar{u}}{\partial x} + \frac{\partial \bar{v}}{\partial y} = 0 \tag{3.1}$$

$$\bar{u} = \frac{1}{h+\zeta} \int_h^\zeta u \; dz \tag{3.2}$$

$$\bar{v} = \frac{1}{h+\zeta} \int_h^\zeta v \; dz \tag{3.3}$$

Where: u, v are current velocities in x, y direction (m s^{-1}); $\bar{u}$, $\bar{v}$ are depth-averaged velocities in x and y directions (m s^{-1}); h is water depth (m); and ζ is water level (m).

3.2.1 Depth-Averaged Two-Dimensional Hydrodynamic Model

In hydrodynamic and ecological model, the basic calculation is based on advection and diffusion terms. The advection term is applied to calculate the momentum and mass conservations by influence of water velocities. In this calculation the averaged water velocities in *x* and *y* direction are the main parameters that need to be set and simulate. Diffusion term is applied to calculate the dispersion of velocities or other substances by effect of density gradients and layer stress. In this term, the horizontal kinematic viscosity (N_h, $m^2\ s^{-1}$) must be firstly evaluated using *Smagorinsky equations* as follow:

$$N_h = c\ \Delta x\ \Delta y\ \frac{1}{2}\left|\left(\frac{\partial \bar{u}}{\partial x}\right)^2 + \left(\frac{\partial \bar{v}}{\partial x} + \frac{\partial \bar{u}}{\partial y}\right)^2 + \left(\frac{\partial \bar{v}}{\partial y}\right)^2\right| \qquad (3.4)$$

where: *c* is non-dimensional *horcon* parameter in range of 0.1 - 0.2 (curent model set up uses 0.12); and Δx and Δy is grid size in *x* and *y* directions (m).

In current depth-averaged velocities of *x* and *y* direction, other additional terms are applied including *Coriolis force*, water depth gradient, and shear stress. *Coriolis force* (*f*) is a calculation water circulation motions as effect of earth rotation with respect to an inertial frame. The force influences an aquatic area to rotate following clockwise or counter clockwise which depends on latitude position of study area. The basic equation of *f* is as follow:

$$f = 2\Omega \sin\theta \qquad (3.5)$$

where: *f* is *Coriolis force* (s^{-1}), Ω is angular rotation of earth with value 7.2921×10^{-5} (rad s^{-1}), and θ is latitude of location (°).

Water depth gradient is calculation of hydrostatic force in water bodies or sometimes called water pressure. The pressure comes from influence of dynamic condition of total water depth due to tidal and water elevation change. Shear stress are type of frictional stress that occurs in surface and bottom layer. The explanation of shear stress is given in sub-chapter 3.5.

a) Motion equation in *x* direction:

$$\underbrace{\frac{\partial \bar{u}\, D}{\partial t} + \frac{\partial \bar{u}^2\, D}{\partial x} + \frac{\partial \bar{u}\, \bar{v}\, D}{\partial y}}_{\textit{Advection term}} = \underbrace{f\, \bar{v}\, D}_{\textit{Coriolis force term}} - \underbrace{g\, D \frac{\partial \zeta}{\partial x}}_{\textit{Water depth gradient term}} +$$

$$\underbrace{\frac{\partial}{\partial x}\left(D\, N_h \frac{\partial \bar{u}}{\partial x}\right) + \frac{\partial}{\partial y}\left(D\, N_h \frac{\partial \bar{u}}{\partial y}\right)}_{\textit{Diffusion term}} + \underbrace{D\, \frac{1}{\zeta \rho}\{\tau_{sx} - \tau_{bx}\}}_{\textit{Shear stress term}} \quad (3.6)$$

b) Motion equation in *y* direction:

$$\frac{\partial \bar{v} D}{\partial t} + \frac{\partial \bar{v} \bar{u} D}{\partial x} + \frac{\partial \bar{v}^2 D}{\partial y} = -f \bar{u} D - g D \frac{\partial \zeta}{\partial y} +$$

$$\frac{\partial}{\partial x}\left(D\, N_h \frac{\partial \bar{v}}{\partial x}\right) + \frac{\partial}{\partial y}\left(D\, N_h \frac{\partial \bar{v}}{\partial y}\right) + D\, \frac{1}{\zeta \rho}\{\tau_{sy} - \tau_{by}\} \quad (3.7)$$

c) Water surface elevation equation:

$$\frac{\partial \zeta}{\partial t} + \frac{\partial D \bar{u}}{\partial x} + \frac{\partial D \bar{v}}{\partial y} = 0 \quad (3.8)$$

d) Temperature dynamic equation:

$$\frac{\partial T D}{\partial t} + \frac{\partial T \bar{u} D}{\partial x} + \frac{\partial T \bar{v} D}{\partial y} = \frac{\partial}{\partial x}\left(D\, N_m \frac{\partial T}{\partial x}\right) + \frac{\partial}{\partial y}\left(D\, N_m \frac{\partial T}{\partial y}\right) \quad (3.9)$$

e) Salinity dynamic equation:

$$\frac{\partial S D}{\partial t} + \frac{\partial S \bar{u} D}{\partial x} + \frac{\partial S \bar{v} D}{\partial y} = \frac{\partial}{\partial x}\left(D\, N_m \frac{\partial S}{\partial x}\right) + \frac{\partial}{\partial y}\left(D\, N_m \frac{\partial S}{\partial y}\right) \quad (3.10)$$

Where: D is total water depth (m); ζ is water level (m); S is salinity (psu); T is temperature (°C); and N_m is viscosity coefficient ($m^2\ s^{-1}$).

3.2.2 Depth-Averaged Two-Dimensional Ecological Model

Ecological model is estimated based on result of hydrodynamic model including horizontal depth-average velocities ($\bar{u}$, $\bar{v}$) and water level (ζ) in form of total water depth ($D = h + \zeta$). There are three main terms for the model simulation, which are advection term for calculation of substances transport, diffusion term for calculation of substances dispersion, and biochemical reaction terms for kinetic calculation of biological and chemical reaction of the substances. Detail explanation about biochemical reaction are given in sub-chapter 3.6.

a) Dissolved nitrogen dynamic equation:

$$\frac{\partial DN\ D}{\partial t} + \frac{\partial DN\ \bar{u}D}{\partial x} + \frac{\partial DN\ \bar{v}D}{\partial y} = \frac{\partial}{\partial x}\left(D\ N_h \frac{\partial DN}{\partial x}\right) + \frac{\partial}{\partial y}\left(D\ N_h \frac{\partial DN}{\partial y}\right) + (phyt \cdot uptake)\ D \quad (3.11)$$

b) Dissolved phosphorus dynamic equation:

$$\frac{\partial DP\ D}{\partial t} + \frac{\partial DP\ \bar{u}D}{\partial x} + \frac{\partial DP\ \bar{v}D}{\partial y} = \frac{\partial}{\partial x}\left(D\ N_m \frac{\partial DP}{\partial x}\right) + \frac{\partial}{\partial y}\left(D\ N_m \frac{\partial DP}{\partial y}\right) + (phyt \cdot uptake)\ D \quad (3.12)$$

c) Phytoplankton dynamic equation:

$$\frac{\partial Chl\ a\ D}{\partial t} + \frac{\partial Chl\ a\ \bar{u}D}{\partial x} + \frac{\partial Chl\ a\ \bar{v}D}{\partial y} = \frac{\partial}{\partial x}\left(N_m \frac{\partial Chl\ a}{\partial x}\right) + \frac{\partial}{\partial y}\left(N_m \frac{\partial Chl\ a}{\partial y}\right) + \left(net \cdot phyt_{growth}\right)D \quad (3.13)$$

Where: *DN* is dissolved nitrogen concentration (mg L^{-1}); *DP* is dissolved phosphorus concentration (mg L^{-1}); *Chl a* is chlorophyll *a* concentration (µg L^{-1}); *phyt·uptake* is biochemical reaction of phytoplankton uptake nutrients (mg L^{-1} s^{-1}); and $net \cdot phyt_{growth}$ is biochemical reaction of net phytoplankton production (µg L^{-1} s^{-1}).

3.3 Water Density

Water density is an important parameter for three dimensional hydrodynamic, water quality, sediment transport, and other numerical models. Different density gradient in upper and lower model layer may influence pressure gradient and vertical mixing, and also creating stratification of water bodies. Therefore, accuracy of water density calculation is significantly influenced on the accuracy of model results. In estuary, mixing between freshwater and saltwater change water density gradient and generates stratification in waterbodies. It causes by mixing between different temperature and salinity level in which the main function of density ($\rho = f(T,S)$). Generally, water density is evaluated using UNESCO (1981) algorythm as follow:

$$\rho = \rho_0 + 6.793952 \times 10^{-2}\, T - 9.095920 \times 10^{-3}\, T^2 + 1.001685 \times 10^{-4}\, T^3 - 1.120083 \times 10^{-6}\, T^4 + 6.536332 \times 10^{-9}\, T^5 + (0.824493 - 4.0899 \times 10^{-3}\, T + 7.6438 \times 10^{-5}\, T^2 - 8.2467 \times 10^{-7}\, T^3)\, S + (-5.72466 \times 10^{-3} + 1.0227 \times 10^{-4}\, T - 1.6546 \times 10^{-6}\, T^2)\, S^{3/2} + 4.8314 \times 10^{-4}\, S^2 \quad (3.14)$$

Where: ρ is water density (kg m^{-3}), ρ_0 is water density reference at temperature 4 °C which equal to 999.842594 kg m^{-3}.

3.4 Initial Conditions

In numerical modelling, the starting point of the process is by initiating initial conditions for all dependent variables, such as velocities, water level, depth, salinity, temperature, and concentrations, at each grid point within the domain (Martin and McCutcheon, 1999). Usually, velocities and water level elevation are set to be zero to express calm condition before external forces influence the domain. In case of salinity, temperature, nutrients, and chlorophyll *a* concentration, the values are necessary to specify as starting values for mass conservation dynamic. These initial values are determined to create smooth calculation at the beginning of simulation and as the starting values for further simulations.

3.5 Boundary Conditions

Boundary conditions are the driving forces that cause flow and water quality changes within the domain (Martin and McCutcheon, 1999). Boundary conditions were set up artificially by following geometrical and morphological conditions of study area and availability of data. Geometrical and morphological conditions are important in setting up the reference point of domain. By this reference point, a researcher could easily decide a suitable boundary condition for model such as close or open boundaries. Close boundaries typically set as zero inflow and outflow values at all sides which indicates no external forces such as tidal or river inputs through the domain. Oppositely, open boundaries are set by considering all external inputs. It is commonly used for estuaries simulations due to many critical forces influencing dynamic condition of estuaries.

Meteorological and topographical factors are included as boundary condition as external factors. These factors are including wind speed and direction, tides, free short radiation of ocean outflow and inflow, river or reservoir discharges, temperature inputs, salinity inputs, typical concentrations inputs, solar radiation, etc. The factors are coming from various directions and various layer where each factor has its own influences on the model set up. Detailed about type of forces produce by those factors are explained in the following subchapters.

3.5.1 Shear Stress

In hydrodynamic simulation, wind shear stress and bottom shear stress are important parameters to develop and influence water circulation and particle transport in estuaries. In the surface, wind stress is triggered by effect of wind induce. Tsanis *et al.* (2007) illustrates that the primary causes of water circulation were wind shear stress and heat across the air-water interface. In order to specify wind shear stress, parameters including wind speed, wind direction, air density, and drag coefficient are used in the calculation.

$$\left(\tau_{sx}, \tau_{sy}\right) = \rho_a C_d \sqrt{W_x^2 + W_y^2}\left(W_x, W_y\right) \tag{3.15}$$

$$C_d = (0.8 + 0.065W) \text{ x } 10^{-3} \quad (3.16)$$

Where τ_{sx},τ_{sy} are are wind shear stress in x and y direction; ρ_a is air density (kg m^{-3}); *Cd* is wind drag coefficient; and *Wx* , *Wy* are wind speed in x and y direction (m s^{-1}).

On the other hand, roughness of bottom layer condition is caused frictional stress that influence bottom layer velocities and circulations. The bottom shear stress calculation is like quadratic law on wind shear stress equation. However, the differences are at the bottom condition where all parameters come from waterbodies, and no air-water interface at this layer. Therefore, bottom shear stress is estimated by multiplication of several important parameters including water density, bottom friction coefficient, and water velocities.

$$(\tau_{bx}, \tau_{by}) = \rho C_f \sqrt{\bar{u}^2 + \bar{v}^2}\ (\bar{u}, \bar{v}) \quad (3.17)$$

Where τ_{bx}, τ_{by} is bottom shear stress in *x* and *y* directions; ρ is water density (kg m^{-3}); and C_f is bottom friction.

3.5.2 Free Radiation of Open Boundaries

In open boundaries, inflow and outflow dominantly influence water circulation inside model's boundary. These in and out flows are depending on the characteristic of estuaries boundary such as rivers and tidal forces. In numerical model, estimation of in and out flows of boundary condition is very important in order to produce well and reasonable model results. Miller and Thorpe (as cited by Tsanis *et al.*, 2007) suggested the application of free radiation equation for numerical boundary condition. Free radiation condition is calculated by considering several factors of numerical boundary conditions including current velocities, water surface elevation, topographical depth, and gravitation. Here, the current velocities type are using the depth-averaged velocities which applies in every grid point along the open boundary. The equation of free radiation condition is greatly influeced by the fucntion of gravitational acceleration and tidal harmony which have direct effect on the change of water depth and current velocities.

The free radiation equation of open boundaries is written as follow:

$$h\,(\bar{u},\bar{v}) = \zeta\sqrt{g\,h} \tag{3.18}$$

Where: *h* is bottom depth (m); and g is gravity (m s^{-2}).

3.5.3 Tidal Amplitude

Tides are the alternate rising and falling of water levels resulting from the gravitational attraction between the earth, sun, and moon (Ji, 2008). Tides plays significant role in hydrodynamic and particle transport where the interactions between tides, topograhic characteristic, and other forces in influencing water circulation and surface water level. Tides also hold an important role on specifying volume of estuaries where main in and out flows through estuary controls by tides. Here, the tides affecting the in and out flows as mentioned in subchapter 3.5.2 is set up in the numerical model as free radiation condition at open boundaries.

Tides is dinamicly changing water level condition from lowest to highest level, or called ebb and flood tides, during short or long period of time. The variation of tide level is called as tidal amplitude. Tidal amplitude depends on tidal periods, or time interfal between lowest and highest tides, of one location. Tidal amplitudes are divided into three main components including *semi diurnal component*, *diurnal component*, and *long-period* (Emery and Thomson, 1997; Triatmodjo, 1999). These components are various between one and other locations, therefore, observation at specified study location is needed. At least fifteen or thirty days tidal observations are needed to determine tidal amplitudes of one location. From observation data, tidal amplitudes and phase shift are specified using harmonic analysis method and further used to estimate tidal elevation as shown on the following equation:

$$\zeta = \sum_{i=1}^{n} a_i \cos\left(\frac{2\pi t}{T_i} + \varphi_i\right) \tag{3.19}$$

Where: *a* is tidal amplitude (m); t is time (h); *T* is tidal period (h); and φ is the phase shift.

Tabel 3.1 Tidal amplitude tabel of Mikawa Port Tidal Station, Atsumi Bay

No	Constituents	Symbol	Description	Period (hour)	φ_i	a_i (m)
1	Main lunar	M_2	semi diurnal	12.42	214.537	0.615
2	Main solar	S_2		12.00	166.194	0.289
3	Lunar, due to Earth-Moon distance	N_2		12.66	265.623	0.115
4	Soli-lunar, due to the change of declination	K_2		11.97	37.821	0.102
5	Soli-lunar	K_1	diurnal	23.93	28.144	0.272
6	Main lunar	O_1		25.82	12.585	0.196
7	Main solar	P_1		24.07	321.191	0.086
8	Main lunar	M_4	quarterly	6.21	73.865	0.004
9	Soli-lunar	MS_4		6.10	331.177	0.006

3.6 Biochemical Reaction

Biochemical reaction terms in this study are used to evaluate biochemical inputs and loss of phytoplankton and nutrients concentrations. The evaluations are adjusted base on characteristic of substances. On phytoplankton dynamic simulation, *Chl a* is set as function of phytoplankton, and its biochemical reaction is emphasized by concerning factors of phytoplankton production that include availability of nutrients in water bodies, light intensity and water temperature. In addition, concentration loss by metabolism, predation, and sinking also must become consideration for the simulation. On the other hand, biochemical reaction of nutrient dynamics is estimated on the loss of nutrient values as result of phytoplankton uptake for growing. The biochemical reaction parameters on this study were defined by *trial* and *error* to get the optimum approach between observation and simulation conditions. All biochemical reaction parameters are given in Table 3.2.

3.6.1 Phytoplankton Production

The mathematical expression of phytoplankton production is function of nutrient uptakes by phytoplankton, light intensity, and temperature. Ji (2008) describes that phytoplankton growth occurs when all these functions are favorable and will continue to bloom until one or more of the functions are no longer available. This production was counted as very important sources of phytoplankton dynamic in ecological model. Furthermore, the dynamic process of this model also estimating the reduction and rates sinking of phytoplankton by subtracting phytoplankton production with basal metabolism, phytoplankton dead rates and settling velocity to receive the net phytoplankton production values.

$$net \cdot phyt_{growth} = \left(P_{growth} - BM - PR - P_{set}\right) Chl\ a \left(\frac{1}{86{,}400}\right) \quad (3.20)$$

$$P_{growth} = P_{max} \cdot f_1(DN, DP) \cdot f_2(I) \cdot f_3(T) \quad (3.21)$$

Where: P_{growth} is phytoplankton production (day^{-1}), P_{max} is maximum phytoplankton growth per day (day^{-1}), $f_1(DN,DP)$ is nutrient uptakes, $f_2(I)$ is light intensity, and $f_3(T)$ is temperature.

Nutrient uptake $f_1(DN,DP)$ estimation is following Michaelis-Menten formulation by taking the minimum value of DN and DP uptake. Function of KDN and KDP on the following equation is representing half-saturation constant of DN and DP. Function of light intensity $f_2(I)$ is analyzed as values of solar radiation penetration through water level. Here, light intensity is estimated at depth-averaged condition with specified layer depth set for surface condition evaluation. Function of temperature $f_3(T)$ is calculated based on hydrodynamic model result of water temperature.

$$f_1(DN, DP) = min\left\{\frac{DN}{KDN+DN}, \frac{DP}{KDP+DP}\right\} \quad (3.22)$$

$$f_2(I) = \frac{I}{I_{opt}} exp\left(1 - \frac{I}{I_{opt}}\right) \quad (3.23)$$

$$I = \frac{1}{D}\int_0^D I_s e^{-K_e z}\, dz \quad (3.24)$$

Where: I is light intensity (W m^{-2}), I_{opt} is optimum light intensity for phytoplankton growth (W m^{-2}), I_S is solar radiation above the surface (W m^{-2}), z is specified layer depth (m), K_e is light extinction coefficient (m^{-1}).

If TM1 ≤ T ≤ TM2 then

$$f_3(T) = e^{-KTG1(T-TM1)^2} \tag{3.25}$$

If T > TM2 then

$$f_3(T) = e^{-KTG2(T-TM2)^2} \tag{3.26}$$

Where: *TM1* & *TM2* is lower and end of optimal temperature range for phytoplankton growth (℃), *KTG1* is effect of temperature bellow TM1, and KTG2 is effect of temperature bellow TM2.

The reduction and sinking rates of phytoplankton were estimated based on phytoplankton loss by the function of metabolism, predation or death, and sinking as shown in the following equations:

$$BM = BMR\, e^{KTB(T-TR)} \tag{3.27}$$

$$PR = PRR\, e^{KTB(T-TR)} \tag{3.28}$$

$$P_{set} = \frac{\omega_{pyth}}{D} \tag{3.29}$$

Where: *TR* is temperature reference of basal metabolism (°C), *BMR* is basal metabolism rate at *TR* (day^{-1}), *KTB* is effect of temperature on metabolism, *PRR* is predation rate at *TR*, and ω_{pyth} is settling velocity of phytoplankton (m day^{-1}).

3.6.2 Phytoplankton Uptake

In this study, biochemical term of DN and DP evaluation are only concerned on concentration loss by phytoplankton uptake. *Phyt·uptake* used as biochemical reaction of

DN and DP to represent nutrient uptake by phytoplankton. The estimation is based on conversion of DN and DP into *Chl a* where stoichiometry ratio of *Chl a:N* and *Chl a:P* ($\alpha_{Chl\ a:N:P}$) multiply to P_{growth} and *Chl a* concentrations. Values of *Chl a* : N : P mass stoichiometry of Atsumi Bay were adopted from study of Rasul (2013) as 1:16.6:2.3.

$$phyt \cdot uptake = \alpha_{Chl\ a:N:P}\ P_{growth}\ Chl\ a\ \left(\frac{1}{86{,}400}\right) \tag{3.30}$$

Here, $\alpha_{Chl\ a\ :\ N}$, $\alpha_{Chl\ a\ :\ P}$ are mass stoichiometry ratio of N and P.

Table 3.2 Biochemical reaction parameters

Parameters	Descriptions	Values	Unit
P_{max}	maximum phytoplankton growth per day	2.4	(day^{-1})
KDN	half-saturation constant of DN	0.01	
KDP	half-saturation constant of DP	0.001	
I_{opt}	optimum light intensity for phytoplankton growth	200.0	($W\ m^{-2}$)
KTG1	effect of temperature bellow *TM1*	0.004	
KTG2	effect of temperature above *TM2*	0.006	
T_{opt}	optimal temperature range for phytoplankton growth	20.0	(°C)
TR	temperature reference of basal metabolism	20.0	(°C)
BMR	basal metabolism rate at *TR*	0.06	
PRR	Predation rate at *TR*	0.05	
KTB	effect of temperature on metabolism	0.07	
ω_{pyth}	settling velocity of phytoplankton	0.3	($m\ day^{-1}$)
FMN	fraction of basal metabolism of N	1.0	
FMP	fraction of basal metabolism of P	1.0	
FRN	fraction of predation of N	0.1	
FRP	fraction of predation of P	0.5	

3.7 Solar radiation

Solar radiation is total amount of solar energy received on earth surface through energy distribution from the sun. Solar radiation is one of important parameter for plants photosynthesis and phytoplankton production. In current ecological model, biochemical term of phytoplankton production is including function of light intensity. This function is assessed by using net solar radiation from observation station where it only available at some designated places. If the solar radiation data of study area are not available, then adopting coefficient from sunshine duration and solar radiation conversion of the nearest observation station are much recommended. The reason of adopting these coefficients are following the assumption that meteorological conditions between two short distance areas have numerous similarities.

The method is by recalculating solar radiation of observation station using conversion of sunshine duration to solar radiation. The conversion could be conducted by following Angstrom equation (Angstrom, 1924; Rahimi *et al.*, 2012). Armstrong equation is contained coefficients *a* and *b* which obtained by model fitting. The results of this recalculation are then validated by comparing the results and observation data. The results are accepted if coefficient of determination reach values between 0.9 until 1. Furthermore, the best fitting values of coefficient *i* and *j* are used to estimate solar radiation of selected study area by following the same method to convert sunshine duration of selected location into solar radiation. The Angstrom equation is expressed as follow:

$$\frac{H}{H_0} = i + j\left(\frac{S}{S_0}\right) \tag{3.31}$$

$$H_0 = \frac{24}{\pi} G_{sc} d_r [\omega_s \, sin(\varphi) \, sin(\delta) + cos(\varphi) \, cos(\delta) \, sin(\omega_s)] \tag{3.32}$$

$$d_r = 1 + 0.033 \, cos\left(\frac{2\pi}{365} Jul\right) \tag{3.33}$$

$$\delta = 0.409 \; sin\left(\frac{2\pi}{365} Jul + 1.39\right) \tag{3.34}$$

Where: H is hourly solar radiation (MJ m^{-2}), H_0 is extraterrestrial radiation (MJ m^{-2}), S is sunshine duration (h), S_0 is maximum sunshine duration (h), G_{sc} is Solar constant (1,367 W m^{-2}), d_r is inverse relative instant factor for the earth-sun, ω_s is sunset hour angle (rad), φ is latitude (rad), δ is solar declination (rad), Jul is Julian day, and i, j are the Angstrom model coefficients.

3.8 Numerical Method

Numerical method is one of the method to solve fluid dynamic problems by using mathematical analysis such as *finite difference method* (FDM), *finite volume method* (FVM), and *finite element method* (FEM). It is generally used for hydrodynamic and water quality simulations where many numbers and points calculated repeatedly. Numerical method have function to solve many complicated mathematical calculation by quick and eficient ways. This method also widely use to depict the natural phenomenon and conditions of such area with purpose to study its characteristic or to further plan the best management practice of the designated area.

Basicly, results of numerical method are approximation of the real conditions in the field study. Number of data, accuracy in inputting data and defining supporting parameter, and writing precise formula are needed in order to get good numerical simulation results. Sometimes, some mistakes in inputing data, parameter or formula could produce unacceptable results which have huge discrepancy to real condition as can be seen from observation data. In order to avoid these problems, fidelity and accuracy of the researcher are very important in the numerical calculations.

In this research, finite different method was chosen for the simulation. There are many kinds of schemes use in FDM, in general these schemes are divided into explicit and implicit scheme. In explicit scheme, the calculation is use to get unknown variable of future time step $t+\Delta t$ by using values of previous time step. In implicit scheme, an unknown variable at time step $t+\Delta t$ depends not only on the values of variables at previous time step, but also on variables in other locations at time step $t+\Delta t$ (Tsanis *et al.*, 2007). The differetinal forms of time and space can be written as follow:

$$\frac{\partial u}{\partial t} \approx \frac{u_{i,j}^{n+1} - u_{i,j}^{n}}{\Delta t} \tag{3.35}$$

In calculation of space different form, explicit scheme is used in this simulation because of its simplicity, accuracy, and efficiens in time calculations. Many formulations occationally use in explicit scheme where the most common forms are upwind scheme, backwind schemes, and center different scheme.

a) Upwind scheme

$$\frac{\partial u}{\partial x} \approx \frac{u_{i+1,j} - u_{i,j}}{\Delta x} \tag{3.36}$$

b) Backwind scheme

$$\frac{\partial u}{\partial x} \approx \frac{u_{i,j} - u_{i-1,j}}{\Delta x} \tag{3.37}$$

c) Central different scheme

$$\frac{\partial u}{\partial x} \approx \frac{u_{i+1,j} - u_{i-1,j}}{2\Delta x} \tag{3.38}$$

Where: u is function of velocity (m s^{-1}), Δx and Δy is spatial increment of mesh in x and y directions (m), Δt is time interval (s), n is time point, and i, j are coordinate point at x and y directions.

There are also other modified forms of explicit schemes time different such as *Leapfrog* scheme, *Lax-Wendroff* scheme, etc. In this model, *Leapfrog* scheme time different and *upwind* scheme space different were used. In addition, stability of explicit scheme is very important to reach in order to get stable simulation condition and to have good results from the simulation. Therefore, to reach all these requirement, Courant *et al.* (1928) suggested a control value to maintain stabilty of explicit FDM method that commonly called as Courant number. This number is calculated by function of time deference, gravitaty acceleration, maximum water depth of study area, and grid size of model. The Courant number must be set less equal 1 or $Cr \leq 1$ to avoid error during simulation.

$$C_r = \Delta t \sqrt{gH_{max}} \sqrt{\frac{1}{\Delta x^2} + \frac{1}{\Delta y^2}} \tag{3.39}$$

Where: C_r is courant number, Δt is time interval (s), g is gravity acceleration (m s^{-2}), H_{max} is maximum water depth (m), and Δx, Δy are model's grid size in x and y directions (m).

In addition, spatial discretization is set as staggered grid system in this model to its stability for spatial calculations (Figure 3.1). In this system, all variables are defined in different location where: depth, pressure, or substances set in the center of grid cell and velocities are set in center grid cell faces. Following aplication of staggered grid system, advection scheme, and diffusion scheme, all of the hydrodynamic and ecological model are discretized by following 1st order upwind scheme for advection and 2nd order central scheme for diffusion terms as shown in the following equations:

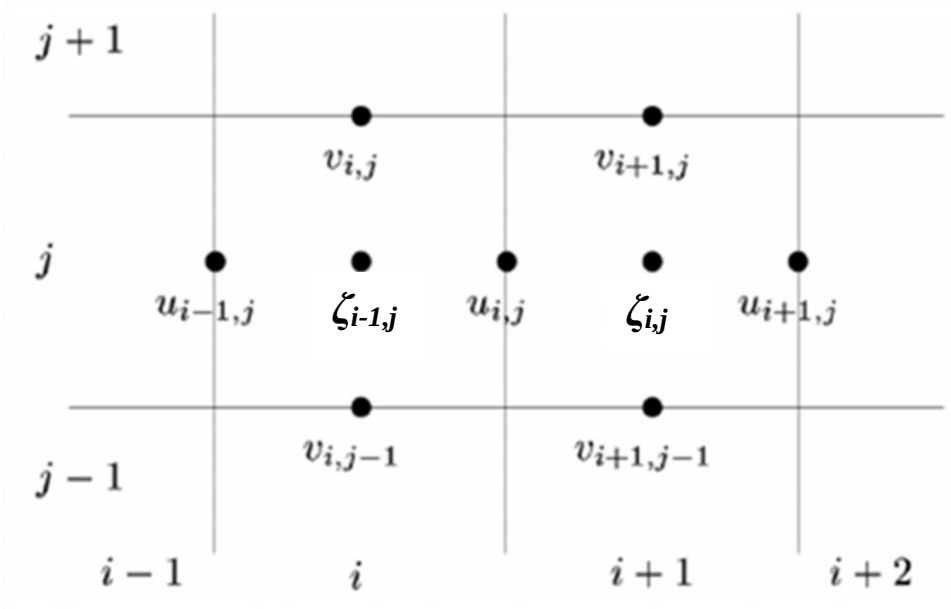

Figure 3.1 Staggered Grid System

a) Discretized motion equation in *x* direction:

$$\frac{u_{i,j}^{n+1}-u_{i,j}^{n}}{\Delta t}=-u_{i,j}D\,\frac{u_{i+1,j}^{n}-u_{i,j}^{n}}{\Delta x}-\bar{v}D\,\frac{u_{i,j+1}^{n}-u_{i,j}^{n}}{\Delta y}-f\bar{v}+$$

$$D_h\,D\,\frac{u_{i+1,j}^{n}-2u_{i,j}^{n}+u_{i-1,j}^{n}}{\Delta x^2}+D_h\,D\,\frac{u_{i,j+1}^{n}-2u_{i,j}^{n}+u_{i,j-1}^{n}}{\Delta y^2}-D\,\frac{g}{\Delta x}\left[\zeta_{i+1,j}-\zeta_{i,j}\right]+D\,\frac{\{\tau_{sx}-\tau_{bx}\}}{\rho_w\zeta^{(1/3)}} \tag{3.40}$$

b) Discretized motion equation in *y* direction:

$$\frac{v_{i,j}^{n+1}-v_{i,j}^{n}}{\Delta t}=-\bar{u}D\,\frac{v_{i+1,j}^{n}-v_{i,j}^{n}}{\Delta x}-v_{i,j}D\,\frac{v_{i,j+1}^{n}-v_{i,j}^{n}}{\Delta y}+f\bar{u}+$$

$$D_hD\,\frac{v_{i+1,j}^{n}-2v_{i,j}^{n}+v_{i-1,j}^{n}}{\Delta x^2}+D_hD\,\frac{v_{i,j+1}^{n}-2v_{i,j}^{n}+v_{i,j-1}^{n}}{\Delta y^2}-D\,\frac{g}{\Delta x}\left[\zeta_{i,j+1}-\zeta_{i,j}\right]+D\,\frac{\{\tau_{sy}-\tau_{by}\}}{\rho_w\zeta^{(1/3)}} \tag{3.41}$$

c) Discretized water surface elevation equation:

$$\frac{\zeta_{i,j}^{n+1}-\zeta_{i,j}^{n}}{\Delta t}=-\frac{(d+\zeta^{n})_{i+\frac{1}{2},j}\,u_{i+\frac{1}{2},j}^{n}-(d+\zeta^{n})_{i-\frac{1}{2},j}\,u_{i-\frac{1}{2},j}^{n}}{\Delta x}$$
$$-\frac{(d+\zeta^{n})_{i,j+\frac{1}{2}}\,v_{i,j+\frac{1}{2}}^{n}-(d+\zeta^{n})_{i,j-\frac{1}{2}}\,v_{i,j-\frac{1}{2}}^{n}}{\Delta y} \tag{3.42}$$

d) Discretized temperature dynamic equation:

$$\frac{T_{i,j}^{n+1}-T_{i,j}^{n}}{\Delta t}=-D_{i,j}\bar{u}\,\frac{T_{i+1,j}^{n}-T_{i,j}^{n}}{\Delta x}-D_{i,j}\bar{v}\,\frac{T_{i,j+1}^{n}-T_{i,j}^{n}}{\Delta y}+$$
$$N_HD_{i,j}\,\frac{T_{i+1,j}^{n}-2T_{i,j}^{n}+T_{i-1,j}^{n}}{\Delta x^2}+N_HD_{i,j}\,\frac{T_{i,j+1}^{n}-2T_{i,j}^{n}+T_{i,j-1}^{n}}{\Delta y^2} \tag{3.43}$$

e) Discretized salinity dynamic equation:

$$\frac{S_{i,j}^{n+1}-S_{i,j}^{n}}{\Delta t}=-D_{i,j}\bar{u}\,\frac{S_{i+1,j}^{n}-S_{i,j}^{n}}{\Delta x}-D_{i,j}\bar{v}\,\frac{S_{i,j+1}^{n}-S_{i,j}^{n}}{\Delta y}+$$
$$N_H\,D_{i,j}\,\frac{S_{i+1,j}^{n}-2S_{i,j}^{n}+S_{i-1,j}^{n}}{\Delta x^2}+N_H\,D_{i,j}\,\frac{S_{i,j+1}^{n}-2S_{i,j}^{n}+S_{i,j-1}^{n}}{\Delta y^2} \tag{3.44}$$

f) Discretized dissolved phosphorus dynamic equation:

$$\frac{DP_{i,j}^{n+1} - DP_{i,j}^{n}}{\Delta t} = -D_{i,j}\bar{u}\frac{DP_{i+1,j}^{n} - DP_{i,j}^{n}}{\Delta x} - D_{i,j}\bar{v}\frac{DP_{i,j+1}^{n} - DP_{i,j}^{n}}{\Delta y} +$$
$$N_H\, D_{i,j}\frac{DP_{i+1,j}^{n} - 2DP_{i,j}^{n} + DP_{i-1,j}^{n}}{\Delta x^2} + N_H\, D_{i,j}\frac{DP_{i,j+1}^{n} - 2DP_{i,j}^{n} + DP_{i,j-1}^{n}}{\Delta y^2} - (phyth \cdot uptake)\, D_{i,j} \tag{3.45}$$

g) Discretized dissolved nitrogen dynamic equation:

$$\frac{DN_{i,j}^{n+1} - DN_{i,j}^{n}}{\Delta t} = -D_{i,j}\bar{u}\frac{DN_{i+1,j}^{n} - DN_{i,j}^{n}}{\Delta x} - D_{i,j}\bar{v}\frac{DN_{i,j+1}^{n} - DN_{i,j}^{n}}{\Delta y} +$$
$$N_H\, D_{i,j}\frac{DN_{i+1,j}^{n} - 2DN_{i,j}^{n} + DN_{i-1,j}^{n}}{\Delta x^2} + N_H\, D_{i,j}\frac{DN_{i,j+1}^{n} - 2DN_{i,j}^{n} + DN_{i,j-1}^{n}}{\Delta y^2} - (phyth \cdot uptake)\, D_{i,j} \tag{3.46}$$

h) Discretized phytoplankton growth dynamic equation:

$$\frac{Chla_{i,j}^{n+1} - Chla_{i,j}^{n}}{\Delta t} = -D_{i,j}\bar{u}\frac{Chla_{i+1,j}^{n} - Chla_{i,j}^{n}}{\Delta x} - D_{i,j}\bar{v}\frac{Chla_{i,j+1}^{n} - Chla_{i,j}^{n}}{\Delta y} +$$
$$N_H\, D_{i,j}\frac{Chla_{i+1,j}^{n} - 2Chla_{i,j}^{n} + Chla_{i-1,j}^{n}}{\Delta x^2} + N_H\, D_{i,j}\frac{Chla_{i,j+1}^{n} - 2Chla_{i,j}^{n} + Chla_{i,j-1}^{n}}{\Delta y^2} - \left(net \cdot phyth_{growth}\right) D_{i,j} \tag{3.47}$$

REFERENCES

Angstrom, A. 1924. "Solar and terrestrial radiation. Report to the international commission for solar research on actinometric investigations of solar and atmospheric radiation." *Quarterly Journal of Royal Meteorological Society* 50: 121-125. doi:10.1002/qj.49705021008.

Berntsen, J., Ø. Thiemb, and H. Avlesenb. 2015. "Internal pressure gradient errors in σ-coordinate ocean models in high resolution fjord studies." *Ocean Modelling* 92: 42-55. doi:10.1016/j.ocemod.2015.05.009.

Courant, R., K. Friedrichs, and H. Lewy. 1928. "Über die partiellen Differenzengleichungen der mathematischen Physik." *Mathematische Annalen* 100 (1): 32 - 74.

Emery, W. J., and R. E. Thomson. 1997. *Data Analysis Methods in Physical Oceanography.*

Amsterdam: Elsevier Science BV.

Ji, Z-G. 2008. *Hydrodynamics and Water Quality: Modeling Rivers, Lakes, and Estuaries.* Hoboken, New Jersey: John Wiley & Sons, Inc. doi:10.1002/9780470241066.

Martin, L. J., McCutcheon, S. C. 1999. *Hydrodynamic and Transport for Water Quality Modeling.* Boca Raton, Florida: CRC Press, Inc.

Mellor, G. L., and T. Yamada. 1982. "*Development of a turbulence closure model for geophysical fluid problems*." *Reviews of Geophysics* 20 (4): 851–875.

Rahimi, I., B. Bakhtiari, K. Qaderi, and M. Aghababaie. 2012. "*Calibration of Angstrom Equation for Estimating Solar Radiation using Meta-Heuristic Harmony Search Algorithm (Case study: Mashhad-East of Iran)*." *Energy Procedia* 18: 644-651. doi:10.1016/j.egypro.2012.05.078.

Rasul, E. 2013. *The influence of typhoon on nutrient dynamics and hypoxia in Atsumi bay, Japan.* Toyohashi: Toyohashi University of Technology.

Sikirić, M. D., A. Roland, I. Janeković, I. Tomažić, and M. Kuzmić. 2013. "Coupling of the Regional Ocean Modeling System (ROMS) and Wind Wave Model." *Ocean Modelling* 72: 59 - 73. doi:10.1016/j.ocemod.2013.08.002.

Triatmodjo, Bambang. 1999. *Teknik Pantai.* Yogyakarta: Beta Offset.

Tsanis, I. K, Wu, J., Shen, H., Valeo, C. 2007. *Environmental Hydraulics: Hydrodynamic of Pollutant Modelling of Lakes and Coastal Water.* Amsterdam: Elsevier.

UNESCO. 1981. *Tenth Report of the Joint Panel On Oceanographic Tables and Standards UNESCO Technical Papers in Marine Sciences.* Vol. No. 36. Paris: UNESCO.

Xu, C., J, Zhang, X. Bi, Z. Xu, Y. He, and K. Y-H. Gin. 2017. "Developing an integrated 3D-hydrodynamic and emerging contaminant model for assessing water quality in a Yangtze Estuary Reservoir." *Chemosphere* 188: 218 - 230. doi:10.1016/j.chemosphere.2017.08.121.

Chapter IV

Effect of Nutrient Inputs on Water Quality Change and Phytoplankton Growth

4.1 Introduction

Enrichment of nutrient or eutrophication around Umeda watershed and Atsumi bay have been occurred for years. The eutrophication is generally reached high values during the growing season, from spring to summer. It is coincided with increasing of fertilizer application in agricultural fields around the Umeda watershed. The application of fertilizer which contains nitrogen (N) and phosphorus (P) has diffused huge concentrations of nutrients to the surface soil layer continuously. It is further resulting in accumulation of N and P in the soil body, and eventually becomes one of the source nutrients of nearby waterbodies through leaching, erosion, and run-off (Ngoc, *et al.*, 2016). Moreover, there are significant relationships between rainfall and the distribution of nutrients from watershed to estuary.

Rainfall is an important phenomenon for changing water quality and the hydrographic characteristic of riverine and estuarine environments. Xia, *et al.* (2016) explained that rainfall acts as a nutrient driver and source which is expected to have significant consequences for river nutrient dynamics. During rainfall, precipitation drives run-off on flushing nutrients from the land around the watershed into the river which is a channel to deliver through the estuary and seaward. This input is later accumulated and enriching nutrient concentration in water body. Eventually, nutrient enrichment in an estuary leads to harmful algal blooming, or sometimes called red tide (Wang, *et al.*, 2015), and subsequently the depletion of oxygen which is also known as hypoxia. The occurrence of hypoxia is a response of algal blooming and the decomposition of organic matter that consumes the availability of oxygen in waterbodies (Caballero-Alfonso, *et al.*, 2015).

4.2 Water Quality Condition during Summer 2010

4.2.1 Water Quality Condition at River Station

Rainfall is one of the driving factors in increasing nutrient release to river and marine environments. High precipitation intensity drives run-off in flushing nutrient and soil from watershed to river, and also elevates river water levels and discharges whilst also delivering high inputs to estuary. Riverine inputs is one of the main circulation and nutrient inputs in an estuary, especially in Atsumi Bay, and indeed phytoplankton growth in the estuary was closely related to the amount of nutrient inputs from river.

Our study location in Atsumi bay has been experiencing eutrophication for the last four decades as an effect of the rapid development occurring around these areas which has contributed to the release of nutrients into the bay. In order to analyse the effects of nutrient concentration changes and phytoplankton growth on pre- and post- rainfall in Atsumi Bay, we need to briefly talk about the Umeda river conditions during rainfall and how much the concentrations, in the forms of nitrogen (N) and phosphorus (P), were delivered. During the study periods, three typhoons and thirty-nine occurrences of rainfall were recorded around the Umeda watershed and Atsumi Bay with amounts ranging between 0.5 mm to 81 mm. Figure 4.2 shows that dissolved nutrients were higher than particulate nutrients on fine days, and oppositely the concentrations of particulate nutrients became higher at rainfall event. The reason for the particulate nutrients increase was the high intensity precipitation which significantly effected in elevating run-offs, discharge levels and particularly soil erosion which became the main sources of particulate nutrients released to the river.

In this study, our focus is on the 1st August conditions when phytoplankton growth in Atsumi Bay reached the highest peak in the summer of 2010 where concentration of *Chl a* attained to 97.9 µg/L. The 1st August, post-rainfall, was related with heavy rainfall on 29th July which flushed out huge amounts of freshwater and nutrients to the estuary. On 29th July, heavy rain in which the total precipitation was 42 mm, occurred (Figure 4.3). During rainfall, there are significant relationships between the discharges and the nutrients found in the Umeda River. Two discharge peaks occurred during a flood event which was followed by the alteration of

particulate and dissolved nutrient concentrations. Generally, particulate nutrients were more dominant than dissolved nutrients as a result of particulate release from the soil. In particular, with PN and PP, the concentrations decreased at the first peak, was then stable between the two peaks, and later levelled out after the second peak. On the other hand, DP and DP concentration shows a different condition where it decreased after a flood occurred, and the concentration was relatively stable during the flood event. Decrease of DN and DP were

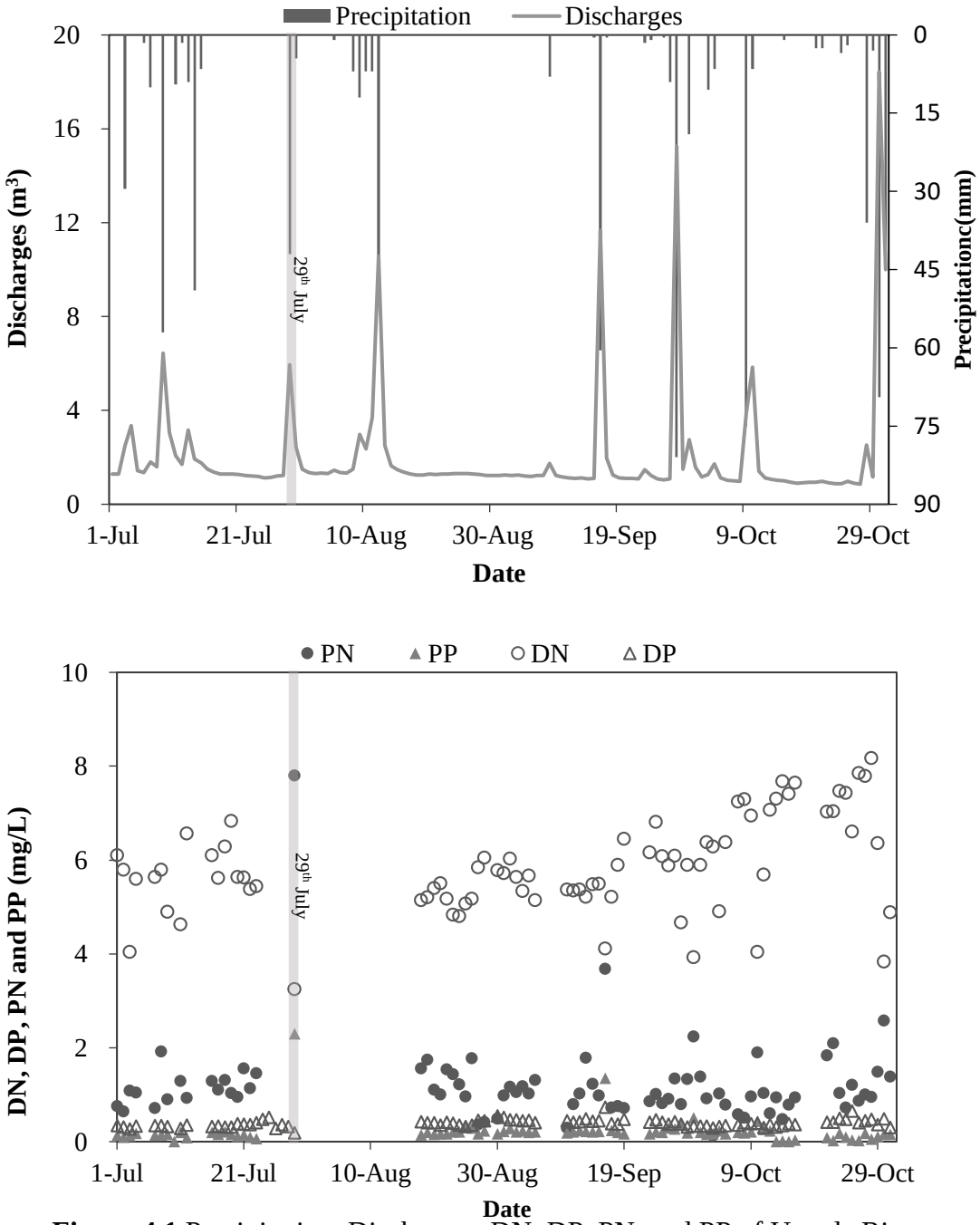

Figure 4.1 Precipitation, Discharges, DN, DP, PN, and PP of Umeda River Conditions on Summer 2010

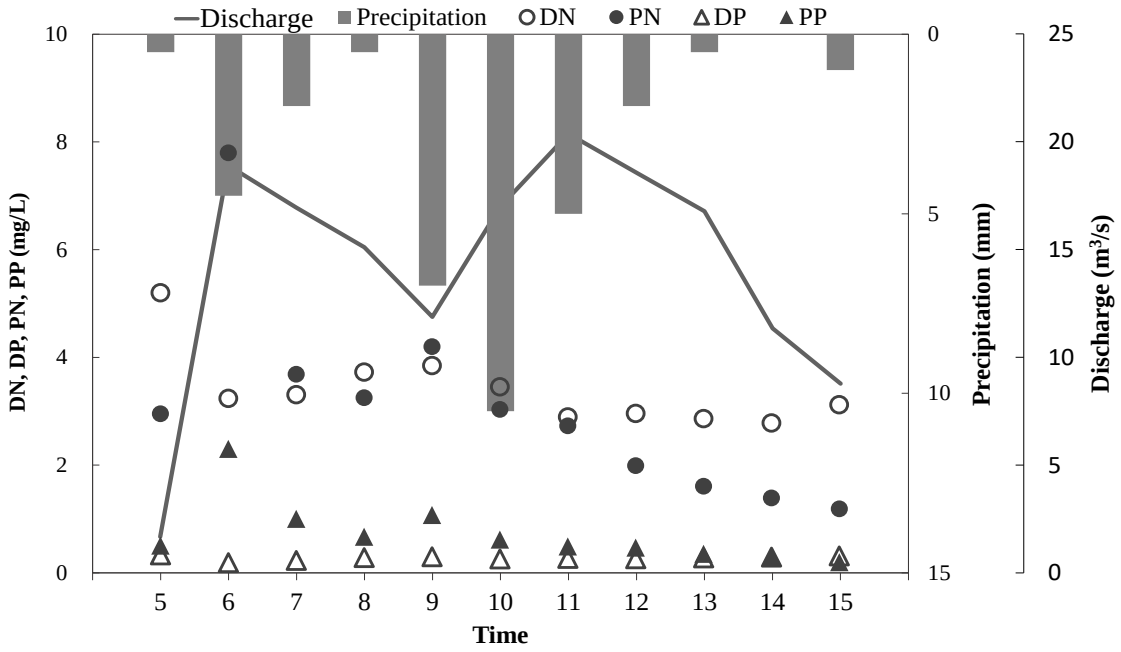

Figure 4.2 Precipitation, Discharges and Nutrients on 29th July during Rainfall at Umeda River

assumed as effects of dilution by freshwater. During the observation, the discharge weighted average of DN, DP, PN, and PP were 3.23 mg/L, 0.26 mg/L, 3.35 mg/L, and 0.79 mg/L, respectively. Eventually, these inputs were later to be the source of the change in water quality in Atsumi bay at 1st August post-rainfall.

4.2.2 Water Quality Conditions at Estuary Stations

During our study in the summer of 2010, we found that the total amount of particulate and dissolved nutrients in Atsumi bay exceeded the Japanese water quality standard. According to the Japanese Ministry of Environment, the permitted amount of TN and TP for Atsumi bay are 0.6 mg/L and 0.05 mg/L, respectively. We also found typical changes of eutrophic water in Atsumi bay as an effect of the riverine freshwater inputs. In relation with rainfall, an increase of water discharges after rainfall transported freshwater, which mixed with nutrients and suspended solid, through the estuary and extended seaward. In addition, excessive nutrient inputs and a proper water temperature, around 22 °C–30 °C, had also stimulated algal blooming in the bay. Moreover, meteorological conditions became important factors on the water quality dynamics of the estuary.

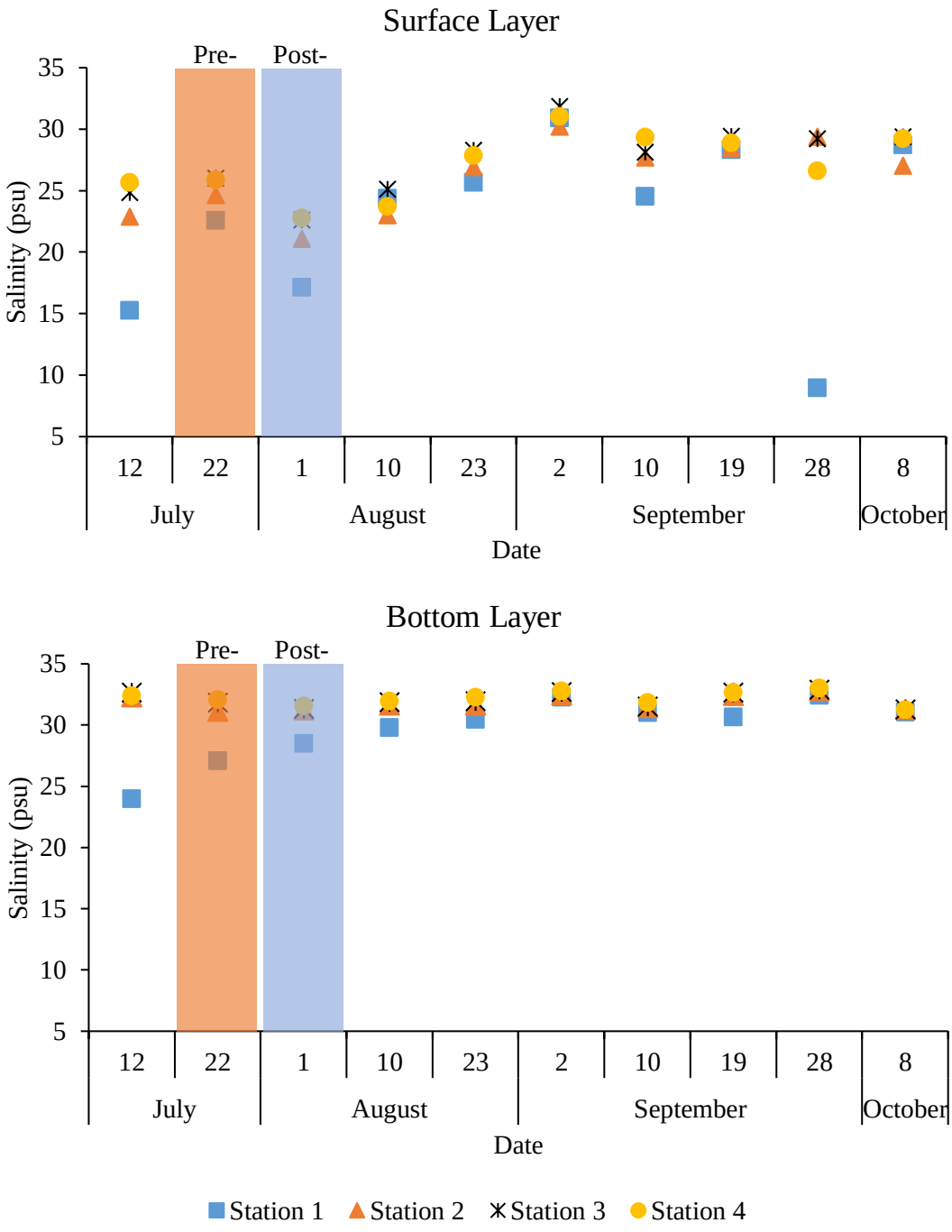

Figure 4.3 Observed Estuarine Salinity during Summer 2010

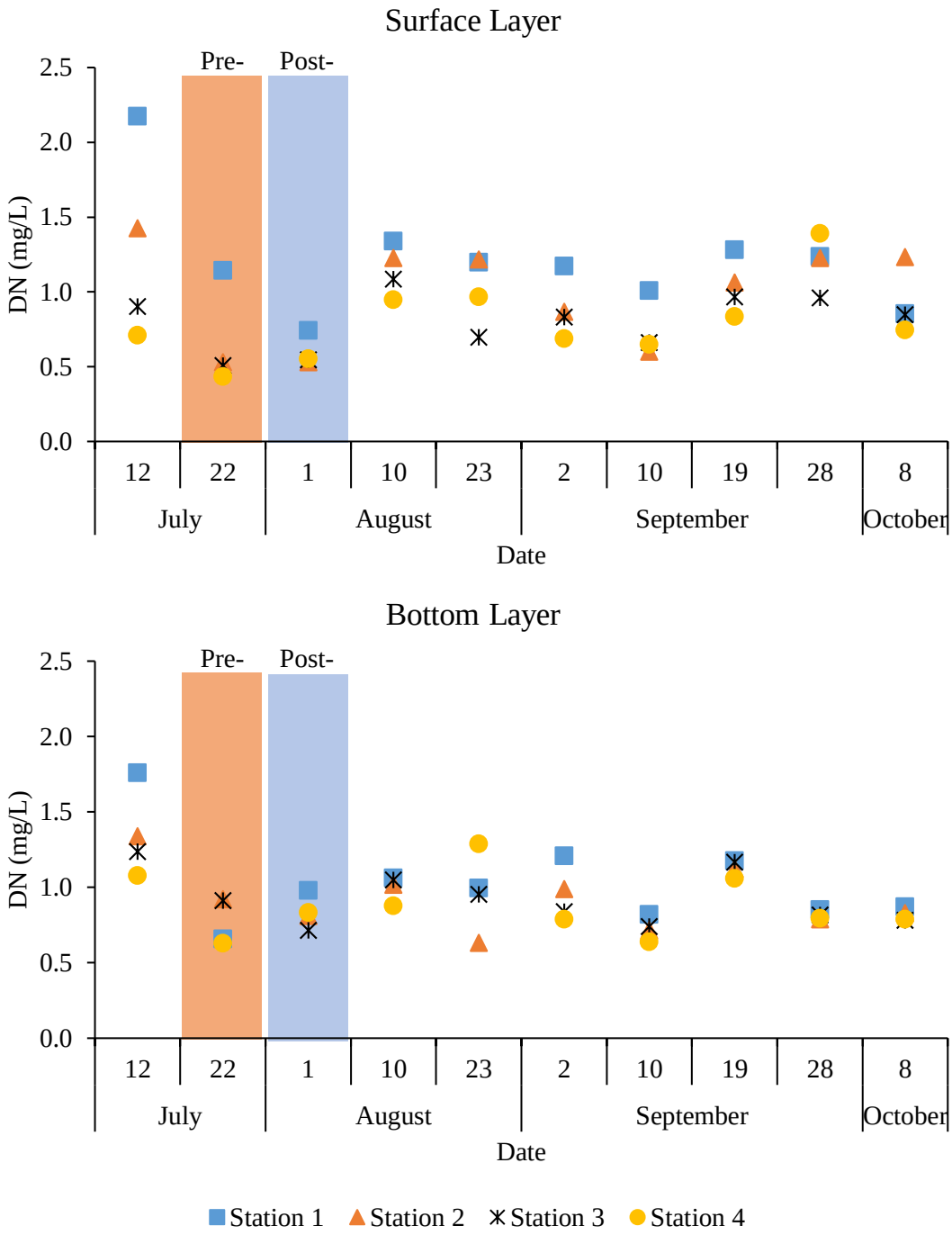

Figure 4.4 Observed Estuarine DN during Summer 2010

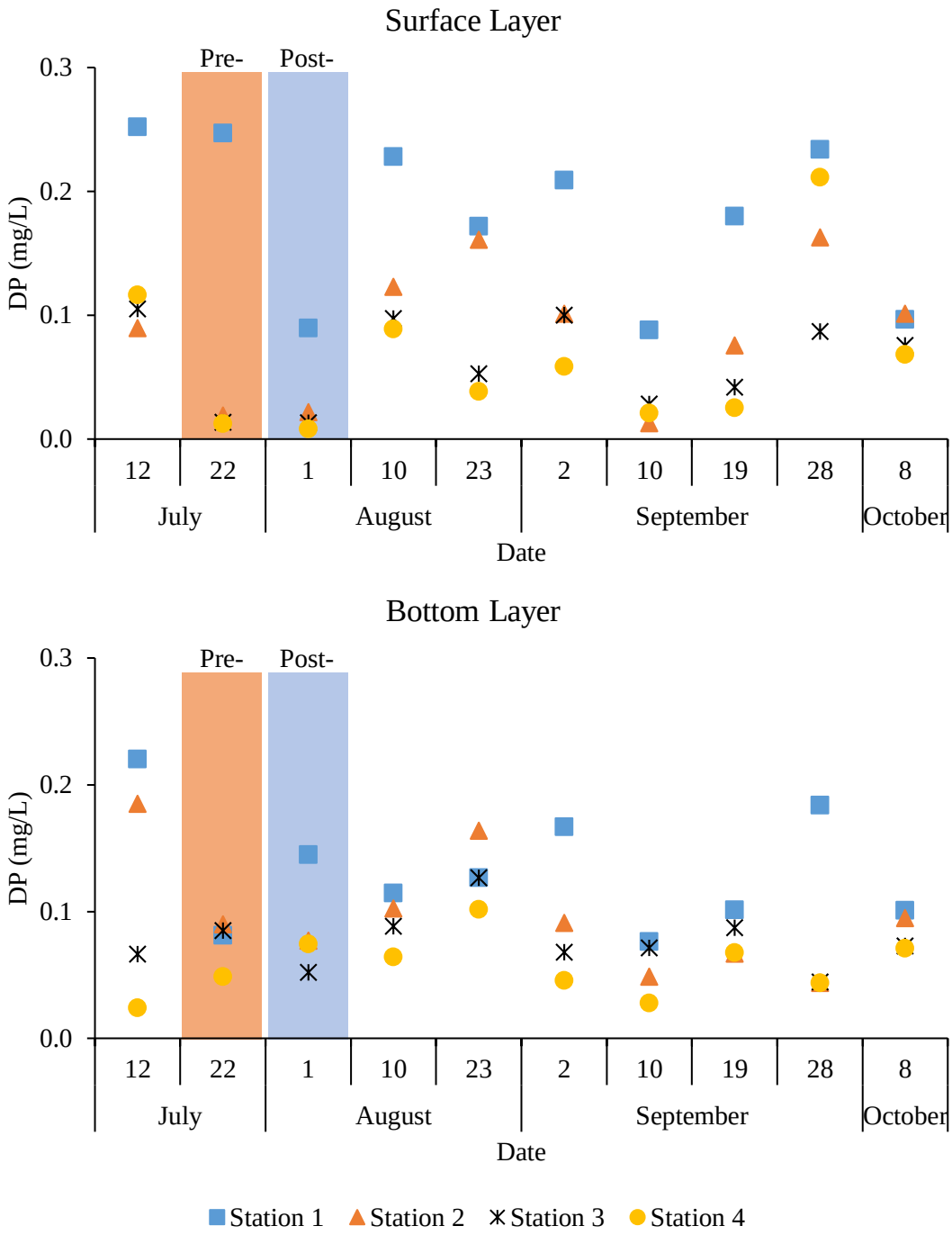

Figure 4.5 Observed Estuarine DP during Summer 2010

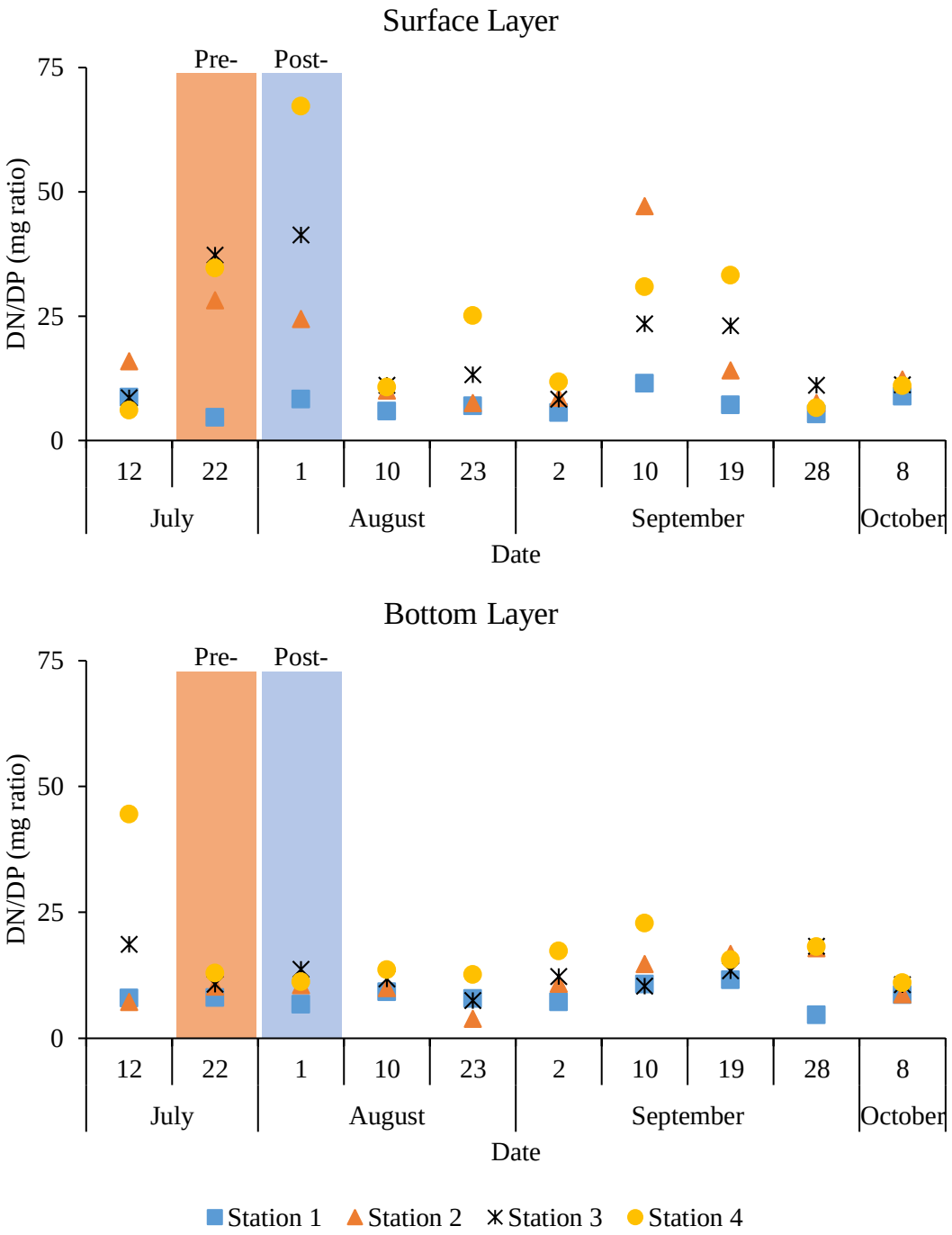

Figure 4.6 Observed Estuarine DN/DP Ratio during Summer 2010

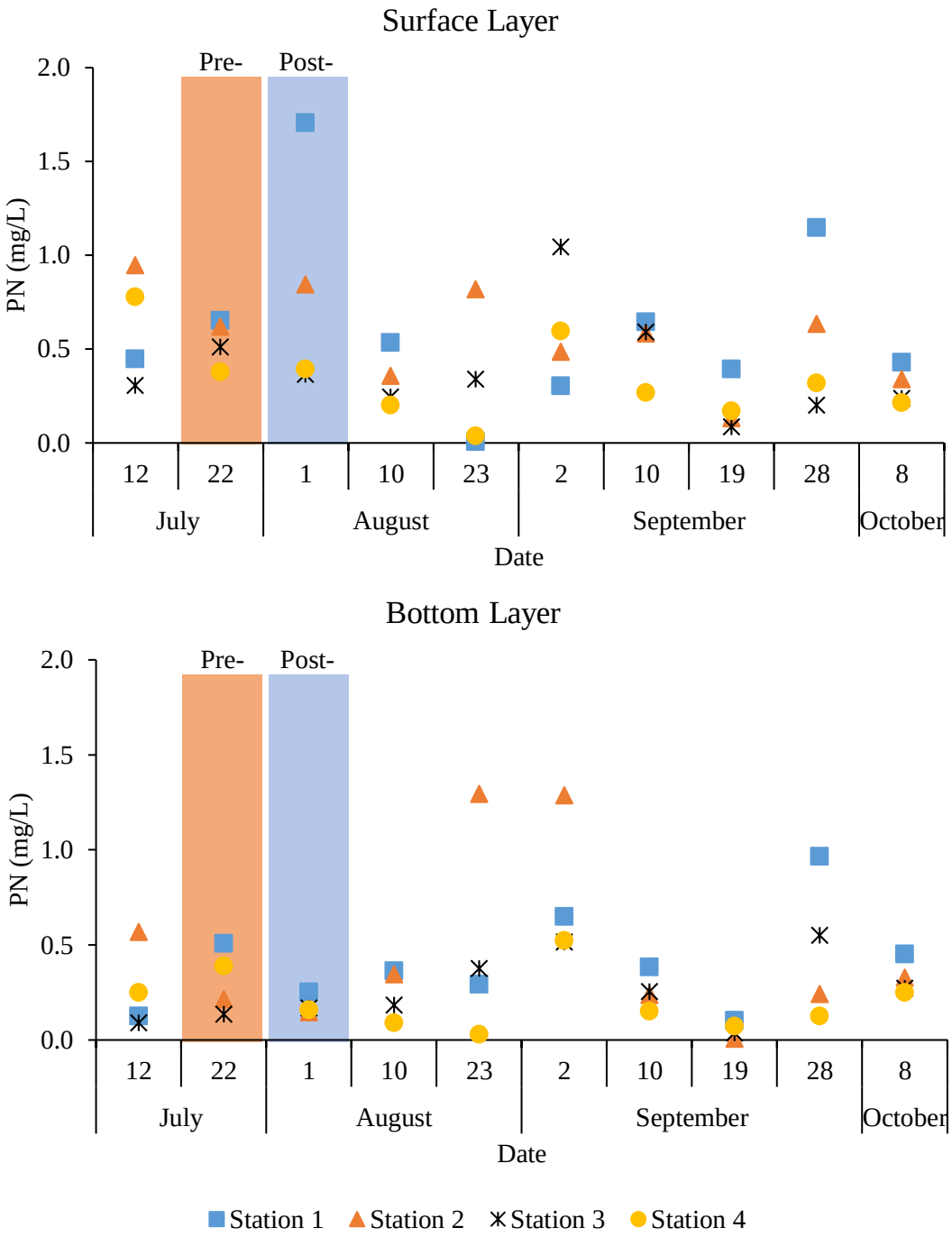

Figure 4.7 Observed Estuarine PN during Summer 2010

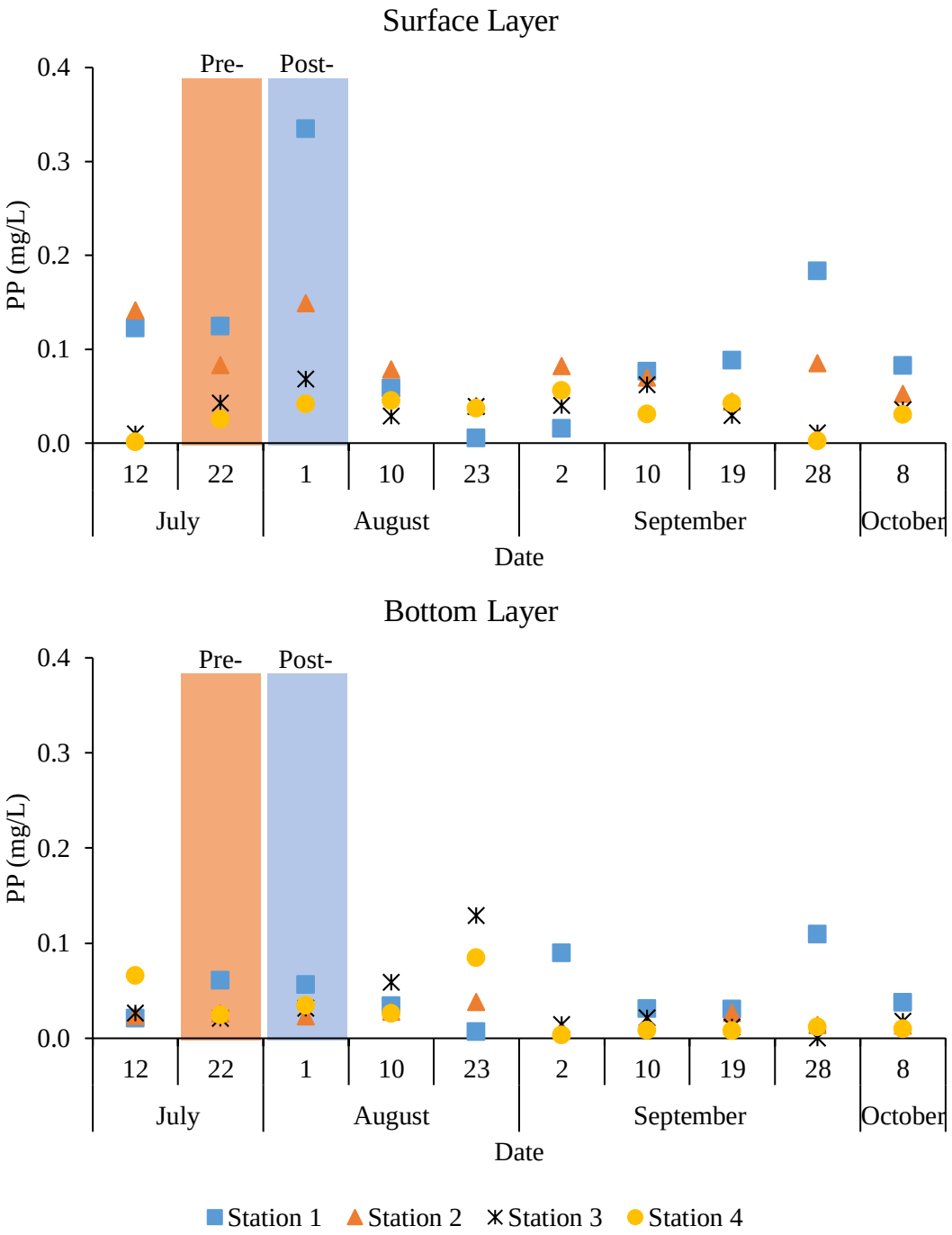

Figure 4.8 Observed Estuarine PP during Summer 2010

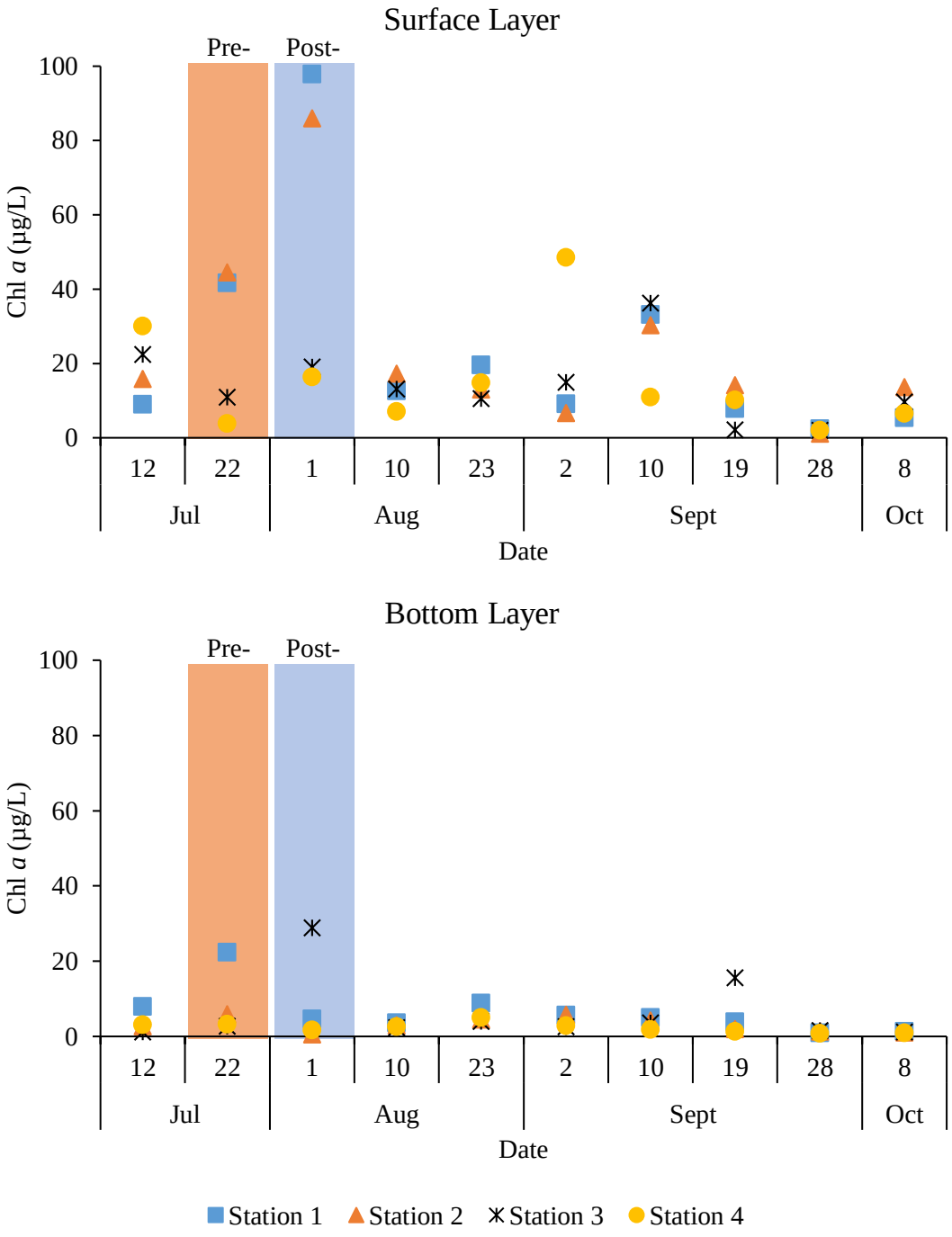

Figure 4.9 Observed Estuarine *Chl a* during Summer 2010

The time series graphs in figures 4.3 to 4.9 depict the water quality changes at four observation stations along Atsumi Bay during the study period. On several days, such as 12th July, 1st August, and 28th September, indicate a depression of salinity at the surface layer due to mixing between freshwater and seawater (Figure 4.3). The salinity levels at the bottom layer tended to be stable and have a higher salinity level than the surface layer which denotes the river inputs dominantly forcing surface layer circulations.

The dominant water quality changes occurred on 1st August and 28th September (Figures 4.4 to 4.9). Both days went through a large rain event with total precipitations of 42 mm and 81 mm, respectively. The difference between the days were: 1st August was post-rainfall conditions or exactly three days after rainfall, and the 28th September was during rainfall. Both days experienced a declining of salinity and an increasing of particulate nitrogen as a result of river inputs (Figure 4.7). However, the escalation of *Chl a* and the depletion of dissolved nutrients only occurred post-rainfall, 1st August (Figure 4.4, 4.5, and 4.9). The casualty came from the phytoplankton dynamic which needed to uptake dissolved nutrients for growing, as explained by Chen *et al.* (2015) in that nutrients, especially dissolved nutrients, and their assimilation or conversion are needed by phytoplankton for growth.

DN/DP ratio at all estuary stations were also clearly clarified the limitation of N, except at the bottom layer concentration of station 1 (Figure 4.6). Richards *et al.* (1965) explained that the Redfield ratio of N and P is in at a rate of 16:1 molar ratio or 7.2 mass ratio. The ratio determined that the limitation of N occurred when the Redfield ratio was below 7.2 mass ratio, and the limitation of P was vice versa.

4.3 Post-Rainfall Water Quality Condition

4.3.1 Freshwater Influence Salinity Alteration on Pre and Post-Rainfall

The high number of freshwater discharges during rainfall constitutes as one of the important factors in controlling and changing of estuarine salinity (Habib *et al.*, 2008). These inputs were not only possessing a significant role in influencing the salinity of water bodies, but also affected the stratification and circulation of coastal water (Whitney, 2010). Bárcena *et*

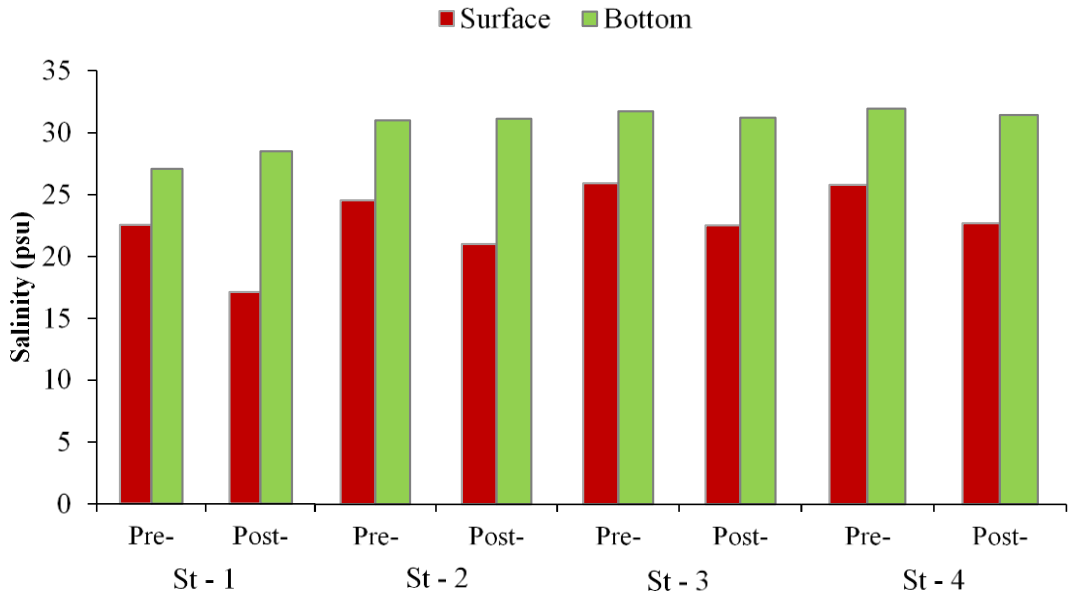

Figure 4.10 Estuarine Salinity Condition between Pre- and Post-Rainfall

al. (2016) in their study also described that huge freshwater inputs during rainfall becomes the main force for estuarine circulations and that at the same time the estuary was constantly mixed. After heavy rainfall on 29th July, high freshwater inputs had stratified salinity around the Umeda River transect.

As explained before, the river inputs mostly influenced surface circulation which resulted in dominant alterations of surface salinity gradient rather than at bottom layer. As depicted in figure 4.10, surface salinity on 22nd July (pre-rainfall) at stations 1, 2, 3, and 4 were around 22.6 psu, 24.6 psu, 26.0 psu, and 25.9 psu, respectively. The surface salinity gradually decreased between 3.3 – 5.5 psu on 1st August (post-rainfall) where the salinity at stations 1, 2, 3, and 4 were around 17.1 psu, 21.1 psu, 22.6 psu, and 22.8 psu, respectively. This condition suggested that high freshwater inputs during heavy rainfall influenced surface estuarine circulation and mixing which resulted in a depletion of surface salinity.

Conversely, bottom salinity around the estuary at post-rainfall tended to increase at the river mouth station and tended to be stable at the seaward stations. Post-rainfall, the bottom salinity at station 1 was increased to 28.5 psu. On the other hand, the bottom salinity at the remaining stations 2, 3, and 4 were prone to be stable with alterations around 0.1-0.5 psu.

Eventually, the declining of the salinity on the surface layer and the stable condition of the bottom layer indicates that the river inputs were dominantly influencing the horizontal circulation of the estuary rather than the vertical circulation.

Moreover, observation data concluded that the density difference of freshwater and seawater becomes an important factor in overlying the high denser salinity layer by lower salinity layer. It is strengthened by Ji (2008) statement that there is a tendency for low dense freshwater to flow over surface estuarine layer when the surface layer circulation has a lower salinity than the bottom layer. In addition, freshwater mostly influenced the nearest area to the river mouth as shown in the data where salinity at stations close to the ocean tends to be higher than at other stations. In addition, the decrease of surface salinity by high freshwater inputs has a correlation with the decrease of DN and DP as an effect of dilution by freshwater at the surface layer. This correlation will be discussed at the next section.

4.3.2 Chlorophyll *a* and Nutrient Alterations on Pre and Post-Rainfall

Water quality changes post-rainfall significantly occurred at the surface layer rather than the bottom layer due to dominant horizontal circulation from freshwater inputs into the estuary. At the surface layer condition, we found that river mouth station 1 was experiencing the highest rate of *Chl a* growth compared to the other estuarine stations. At station 1, surface *Chl a* at post-rainfall elevated to be two times higher than at the pre-rainfall condition. The concentration was 41.7 µg/L at pre-rainfall which further elevated to 97.9 µg/L at post-rainfall (Figure 4.11).

Other estuarine stations were experiencing a similar tendency to station 1. Pre-rainfall, *Chl a* concentration at stations 2, 3, and 4 were around 44.6 µg/L, 10.9 µg/L, and 3.8 µg/L, respectively, which later increased to be 86.0 µg/L, 19.1 µg/L, and 16.3 µg/L post-rainfall. This growth was also assisted by the influence of the summer water temperature, light intensity, and nutrient concentrations. Ji (2008) described that phytoplankton blooms may occur during a favourable condition of nutrients, sunlight, and water temperature, until one or more of these factors are no longer available.

In situ observation found that the average temperature at the estuarine station was around 29 °C–32 °. Based on Huertas et al. (2011), several marine phytoplankton can grow in warm water temperatures of around 22 °C–35 °C. Regarding nutrient uptake, post-rainfall conditions show an increase of *Chl a* and decrease of DN and DP which assumed had positive correlation with nutrient uptake by phytoplankton, beside dilution by freshwater. According to figure 3, inputs of dissolved nutrients from the river during rainfall represented the existence of huge levels of dissolved nutrient inputs into the estuary. However, the post-rainfall data shows the decline of surface DN and DP at estuarine station 1 and a steady state of these concentrations at the remaining stations 2, 3, and 4 (Figures 4.12 and 4.13).

Pre-rainfall, DN concentrations at stations 1, 2, 3, and 4 were 1.14 mg/L, 0.53 mg/L, 0.51 mg/L, and 0.43 mg/L, respectively. At the same event, DP concentrations were 0.25 mg/L at station 1, 0.02 mg/L at station 2, and 0.01 mg/L at the other stations. Post-rainfall, depletion of DN and DP occurred at station 1 where the concentrations were 0.74 mg/L and 0.09 mg/L, respectively, or one third and two third times lower pre-rainfall, respectively. Furthermore, both DN and DP at the other stations remained stable between pre and post-rainfall.

The decline of DN and DP gave a negative correlation between river inputs and estuarine concentrations. The decrease of DN and DP were related into two conditions including:

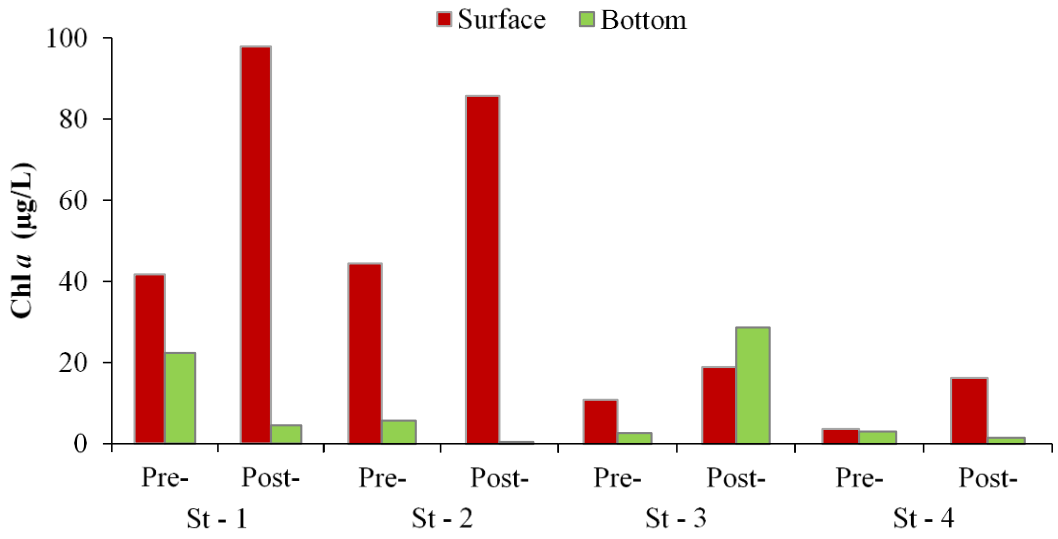

Figure 4.11 Estuarine *Chl a* Condition between Pre- and Post-Rainfall

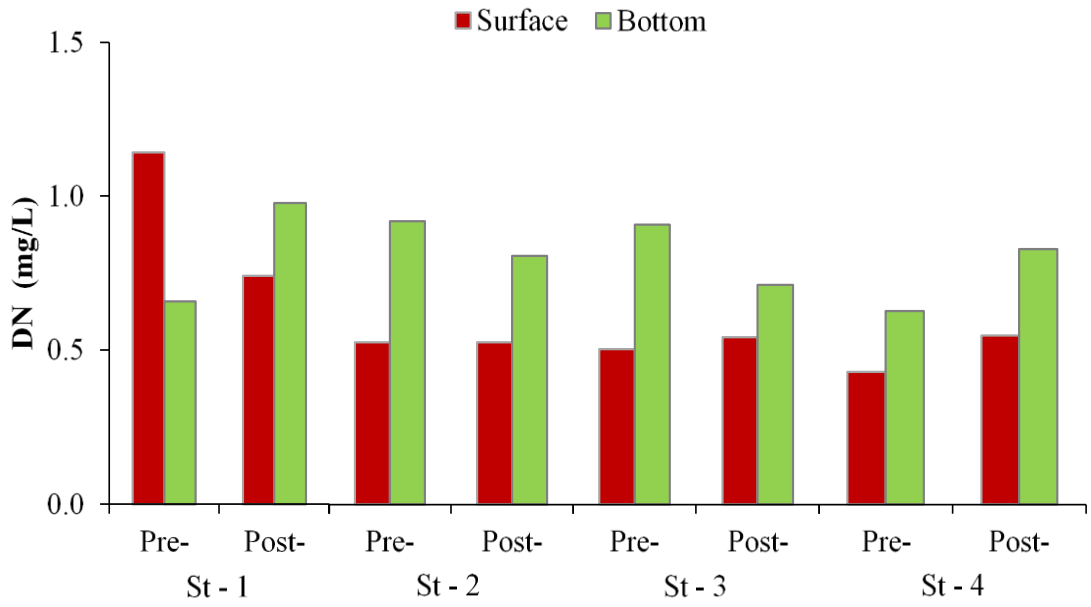

Figure 4.12 Estuarine DN Condition between Pre- and Post-Rainfall

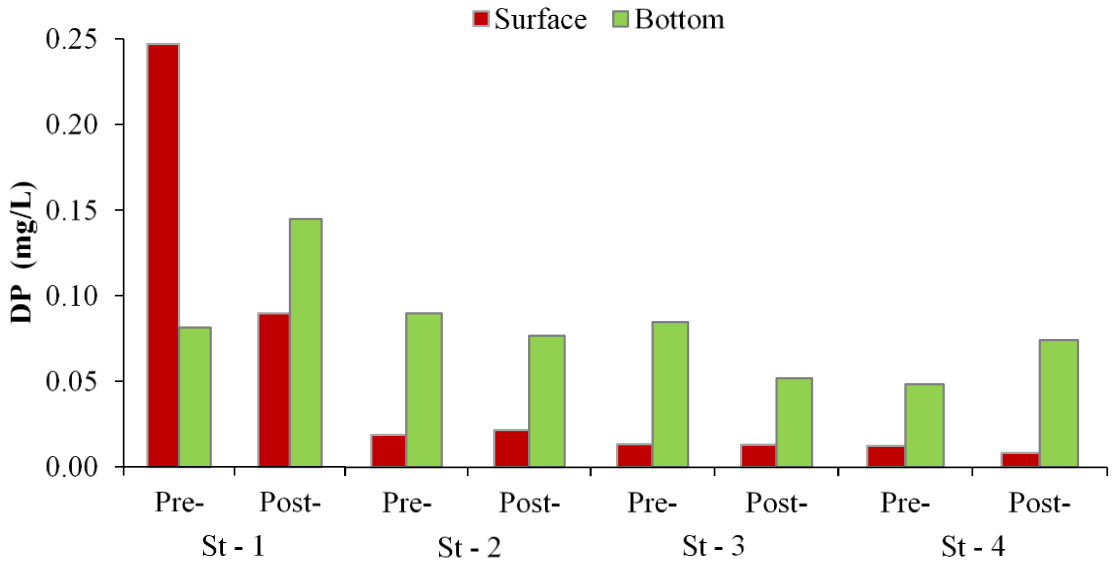

Figure 4.13 Estuarine DP Condition between Pre- and Post-Rainfall

dilution effect which has a correlation with the decline of salinity as an effect of freshwater inputs, and phytoplankton uptake which correlated with the increase of *Chl a*, especially at the surface layer. Relation between salinity and DN, and salinity and DP on figure 4.14 shows good correlation which is strengthened by the coefficients of correlation 0.86 and 0.98, respectively. These correlations define that freshwater inputs had occupied the surface layer of water bodies which resulted in the declining of salinity and assisted the dilution of DN and DP.

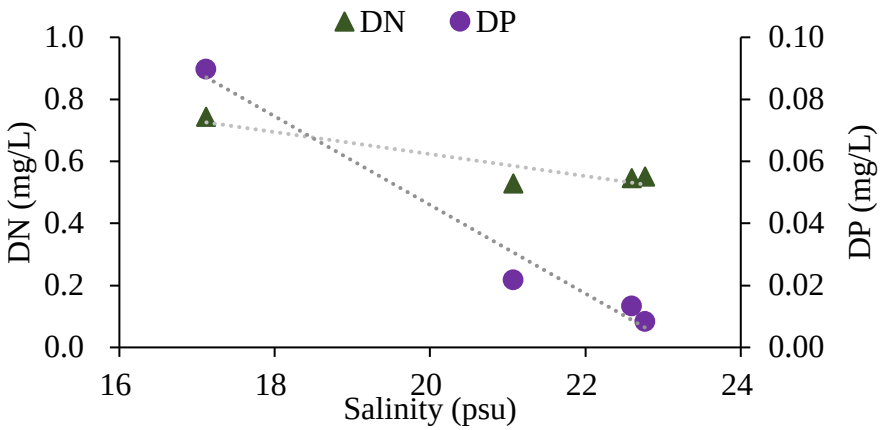

Figure 4.14 Surface Salinity and Dissolved Nutrients (DN and DP) Relation

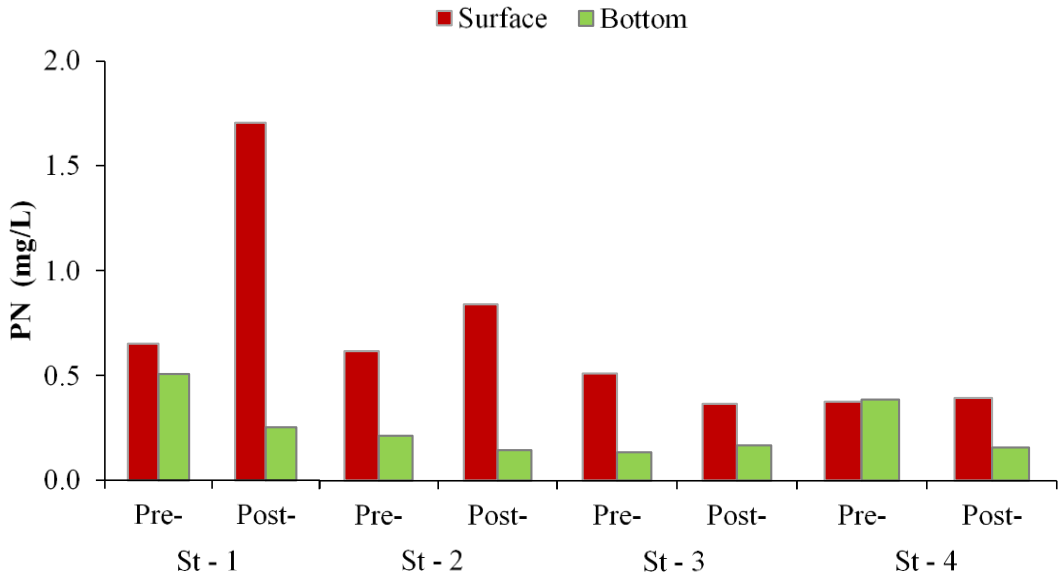

Figure 4.15 Estuarine PN Condition between pre- and post-rainfall

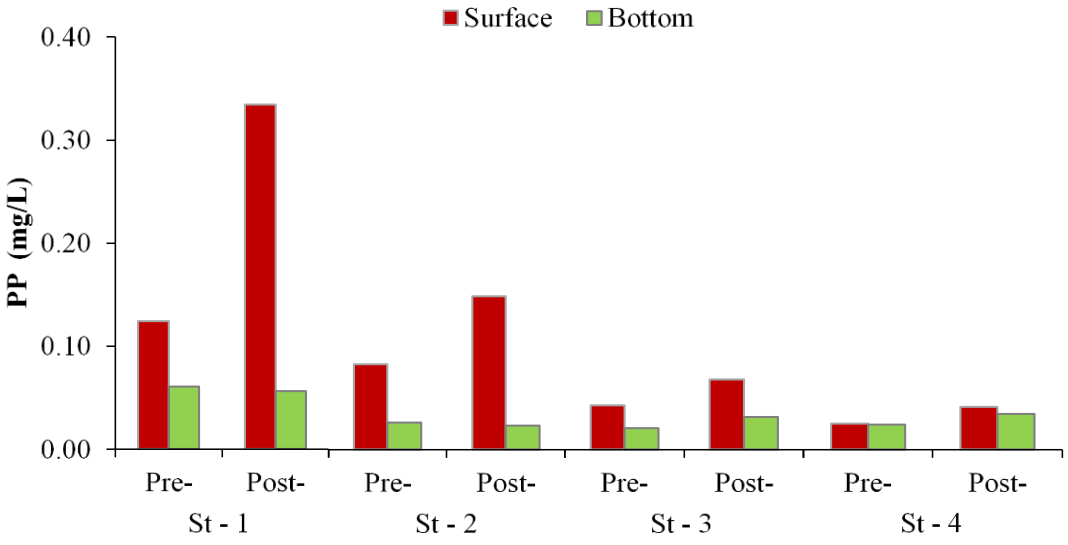

Figure 4.16 Estuarine PP Condition between pre- and post-rainfall

In addition, the decrease of DN and DP also has a relationship to phytoplankton growth which consumes dissolved nutrients in major amounts. Eventually, post-rainfall DN and DP concentrations were the rest after dilution by freshwater and uptake by phytoplankton. The duration between 29th July (during rainfall) and the 1st August was an appropriate time for *Chl a* to grow by uptaking dissolved nutrients. In addition, Rasul *et al.* (2013) on their study at the Toyo river transect of Atsumi bay found similar conditions and corroborated that nutrient uptake by phytoplankton resulted in the decrease of surface dissolved nutrients.

Beside the decrease of dissolved nutrients, the escalation of *Chl a* post-rainfall was also followed by particulate nutrients PN and PP. Figures 4.15 and 4.16 show the increase of particulate nutrients which appeared significantly at the station nearest the river mouth. The highest concentration of PN and PP was recorded at station 1 where both concentrations elevated 2.6 times higher than pre-rainfall. Similar results were found at station 2 with an increase of PN and PP at about 1.4 and 1.9 times, respectively, than pre-rainfall. On the other hand, the PN and PP at station 3 had small declination and it was assumed to have sunk to the bottom layer. Moreover, the PN and PP at station 4, which lies in the open sea, were relatively more stable than at the other stations. Inclination of PN and PP have similar trend with *Chl a*, where a positive correlation was found between *Chl a* and PN, and *Chl a* and PP with the coefficients of determination being 0.78 and 0.77, respectively (Figure 4.17). These significant and positive values indicated that a concentration of *Chl a* was contained in the particulate bodies. By this fact, we presumed that sources of PN and PP post-rainfall were not only coming from river inputs but also from other sources, especially phytoplankton.

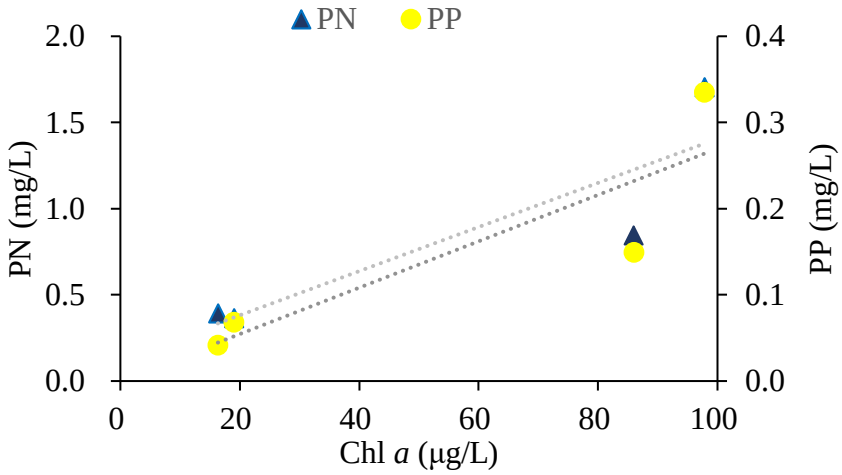

Figure 4.17 *Chl a* and Particulate Nutrients (PN and PP) Relation

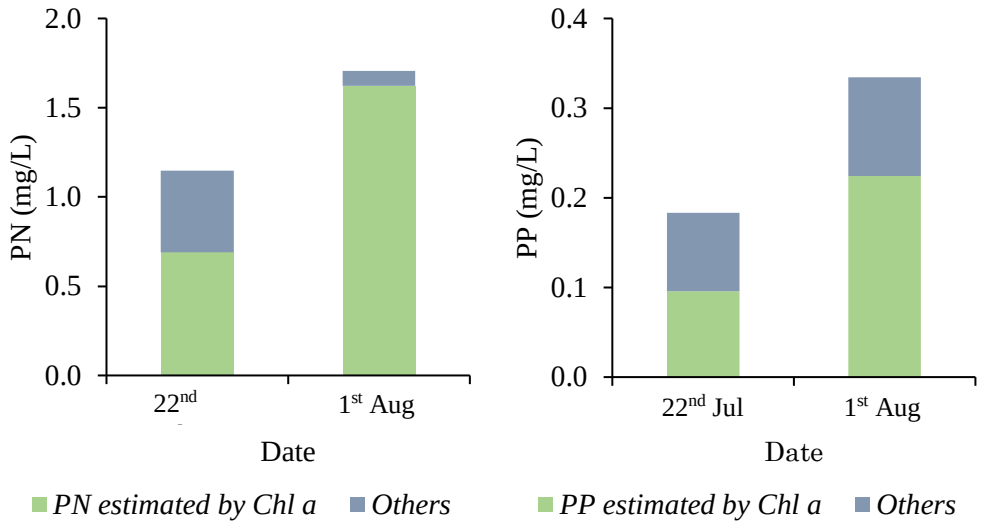

Figure 4.18 Phytoplankton Biomass on PN and PP

In order to confirm and strengthen this assumption, we used *Chl a* : N : P mass stoichiometry to verify *Chl a* concentration in particulate nutrients bodies. By referring to Rasul (2013) estimation of Atsumi Bay's *Chl a*: N: P mass stoichiometry as 1:16.6:2.3, multiplication of N: *Chl a* and P: *Chl a* with *Chl a* concentration has given correlation between PN, PP, and *Chl a* as depicted in figure 4.18. The figure describes a relation between PN, PP, and *Chl a* on 22nd July (pre-rainfall) and 1st August (post-rainfall) whether PN and PP were coming from phytoplankton growth in the estuary or from other sources.

Pre- rainfall, phytoplankton biomass on PN and PP show smaller values of *Chl a* influencing PN and PP, where about half of PN and PP concentrations possibly came from the river and other sources. On the other hand, data on the 1st August described that high *Chl a* was not only related to the particulate nutrients input from river but also as a result of estuarine phytoplankton growth. The graph indicated that phytoplankton biomass on PN and PP were higher at post-rainfall as well as the *Chl a*. This condition concluded that the source of PN and PP at post-rainfall dominantly came from phytoplankton growth beside other sources.

4.4 Conclusion

In our study, freshwater inputs during rainfall had changed post-rainfall salinity stratification in the Umeda river transect of Atsumi bay. Post-rainfall, an increase of nutrients and a

decline in salinity after rainfall proved that a large amount of freshwater, mixed with nutrients, affected water quality conditions in the estuary. The decrease of dissolved nutrients is from the effects of freshwater dilution and phytoplankton uptake which verified by the increase of *Chl a*, PN, PP, and decrease of DN and DP.

Moreover, the influence of freshwater was dominant at river mouth station 1 rather than at other the stations. The further the station was from the river mouth, the lower the influence which depicts the large proportion differences between the *Chl a*, dissolved nutrients, and particulate nutrients concentrations at river mouth station 1 and the open sea station 4. In addition, the surface layer was supplied to more than the bottom layer, because the inputs were more influencing horizontal circulation than vertical circulation. It resulted in a small alteration of nutrients and *Chl a* concentration compared to the surface layer.

REFERENCES

Bárcena, J. F., J. García-Alba, A. García, and C. Álvarez. 2016. "Analysis of Stratification Patterns in River-Influenced Mesotidal and Macrotidal Estuaries Using 3D Hydrodynamic Modelling and K-means Clustering." *Estuarine, Coastal and Shelf Science* 181: 1-13.

Caballero-Alfonso, A. M., Cartensen, J., Conley, D. J. 2015. "Biogeochemical and Environmental Drivers of Coastal Hypoxia." *Marine Systems* 141: 190-199.

Chen, M., M. Fan, R. Liu, X. Wang, X Yuan, and H. Zhu. 2015. "The Dynamics of Temperature and Light on Growth of Phytoplankton." *Journal of Theoretical Biology* 8 - 19.

Habib, E., Larson, B. F., Nuttle, W. K., Rivera-Monroy, V. H., Nelson, B. R., Meselhe, E. A., Twiley, R. R. 2008. "Effect of rainfall spatial variability and sampling on salinity prediction in an estuarine system." *Journal of Hydrology* 350: 56-67.

Huertas, E., Rouco, M., Lopez-Rodas, V., Costas, E. 2011. "Warming will affect phytoplankton differently: evidence through a mechanistic approach." *Proceeding of the royal society B* 1-10.

Ji, Z-G. 2008. *Hydrodynamics and Water Quality: Modeling Rivers, Lakes, and Estuaries.* Hoboken, New Jersey: John Wiley & Sons, Inc. doi:10.1002/9780470241066.

Ngoc, M. N., Inoue, T., Yokota, K. 2016. "Ultrasonic treatment for quantificatiion of bioavailable phosphorus in soil and suspended sediments." *Water Science Technology: Water Supply* 1-12. doi:10.2166/ws.2016.100.

Rasul, E. 2013. *The influence of typhoon on nutrient dynamics and hypoxia in Atsumi bay, Japan.* Toyohashi: Toyohashi University of Technology.

Rasul, E., Inoue, T., Aoki, S., Yokota, K., Matsumoto, Y., Okubo, Y., Djumanto. 2013. ", Influence of Tropical Cyclone on the Water Quality of Atsumi Bay." *Journal of Water and Environment Technology* 11: 439-451.

Richards, F. A., J. D. Cline, W. W. Broenkow, and L. P. Atkinson. 1965. "Some Consequences of the Decomposition of Organic Matter in Lake Nitinat, an Anoxic Fjord." *Limnology and Oceanography* 10: R185.

Wang, J., Yan, W., Chen, N., Li, X., Liu, L. 2015. "Modeled long-term changes of DIN:DIP ratio in the Chiangjiang River in relation to Chl-α and DO concentrations in adjacent estuary." *Estuarine, Coastal and Shelf Science* 166: 163-160.

Whitney, M. M,. 2010. "A study on river discharge and salinity variability in the Middle Atlantic Bight and Long Island Sound." *Continental Shelf Research* 30: 305-318.

Xia. Y., ,Tia. C., Sheb. D., Yana. X. 2016. "Linking river nutrient concentrations to land use and rainfall in a paddy agriculture–urban area gradient watershed in southeast China." *Journal of Science of The Total Environment* 566-567: 1094–1105. doi:10.1016/j.scitotenv.2016.05.134.

Chapter V

Simulation of Phytoplankton Growth as Eutrophication Effect in Estuary

5.1 Introduction

Excessive nutrient levels, or eutrophication, are currently one of the most concerning water environment issues in the world. Nutrient loads due to anthropogenic activities have been changing the water quality of aquatic environments such as rivers, lakes, and estuaries throughout the world (Glibert, 2017). This problem can be seen in several countries with high development in infrastructure, industrial, and agricultural sectors. It is associated with rapid population and economic growth where development increases pressure to provide for human needs in the form of food and shelter. To accelerate the provisioning process, there is a massive increase in the use of various biological and chemical substances, including nutrients in the form of nitrogen (N) and phosphorus (P). After their application, most of these substances are directly or indirectly leached into the aquatic environment from point and non-point sources.

In the agricultural sector in particular, the high frequency of fertilizer application and increase of non-point-source nutrient loads has been associated with the impairment of surface and groundwater quality (Sharpley, 2013). The leaching of nutrients from agricultural soil into surface waterbodies is strongly influenced by rainfall. During rain events, the nutrients accumulated in surface soil are flushed out by runoff to rivers and then transported into estuaries and seaward. The enrichment of nutrient loads in waterbodies results in acceleration of phytoplankton growth through responses to nutrient uptake by phytoplankton itself and by photosynthesis. A further effect of this growth is the possible imbalance between algal production and consumption, followed by enhanced sedimentation of algal-derived organic matter, stimulation of microbial decomposition and oxygen

consumption, and the depletion of oxygen, known as hypoxia (Cloern, 2001).In addition, heavy algal growth can affect mass mortalities of marine animals and have negative impacts on aquaculture and local socio-economic conditions.

Eutrophication and phytoplankton growth, especially red tides, have become major pollution problems in several estuaries in Japan such as Tokyo Bay, Ise-Mikawa Bay, and the Seto Inland Sea (Nakanishi *et al*., 1990; Nakane *et al*., 2006; Suzuki, 2016). Ise-Mikawa Bay, Aichi Prefecture, Japan, is the widest bay in Central Japan. The bay is divided into two bay regions: Ise Bay on the western side and Mikawa Bay on the eastern side. Eutrophication accompanied by red tides and hypoxia has been reported in the bay for more than four decades as a result of rapid development in this area (Matsukawa and Suzuki, 1985; Bodergat *et al.*, 1997; Suzuki, 2004). In Atsumi Bay on the eastern side of Mikawa Bay in particular, red tides and hypoxia have occurred every summer as a result of large nutrient inputs from industrial and agricultural areas around the bay.

Several studies have investigated water quality and phytoplankton growth in areas around Ise-Mikawa Bay (Sakamoto and Tanaka, 1989; Kasih and Kitada, 2004, 2008). In this chapter, our purpose was to evaluate nutrient dynamics and phytoplankton growth in estuarine waterbodies with a focus on the effect of large river inputs during rain events. Our evaluation methods are based on field measurements and a depth-averaged ecological model of the distribution and transformation of dissolved nitrogen (DN), dissolved phosphorus (DP), and primary production of phytoplankton (*Chl a*) in an estuary over a short period time. The detail method of field observation and ecological model are discussed in previous Chapter 2 and 3, respectively.

5.2 Numerical Model Setup

In this study, model is developed using explicit finite difference method as model mentioned in Chapter 3. Time difference calculation is set using Leapfrog scheme with Δt set as 3 second. Following Δt value, stability checked has conducted by referring to Courant number which must be less than 1. Model's courant number with Δt equal to 3 second is 0.48 which acceptable under maximum value of 1. Even though Δt can be increased until 6 second to

reach value approaching 1, application Δt as 3 second is better to maintain the smoother simulation.

The spatial condition is set as staggered grid system with grid size is 100 m x 100 m in each cell. The model was set with an open boundary and an area of about 5 km × 9 km around the transect of stations extending from the Umeda River into Atsumi Bay. The grid generated for the model area was set at 4500 grid cells with a grid size of 100 m × 100 m. The boundaries consisted of open ocean boundaries on the western and northern sides, and two river boundaries: the Umeda River on the eastern side and the Shio River on the southern.

The water elevation was set at the north and west boundaries and was estimated using nine tidal constituents, including the principal lunar semi-diurnal (M2), principal solar semi-diurnal (S2), larger lunar elliptic semi-diurnal (N2), luni-solar semi-diurnal (K2), luni-solar declinational diurnal (K1), luni-lunar declinational diurnal (O1), solar declinational diurnal (P1), shallow water principal of principal lunar (M4), and shallow water quarter diurnal (MS4). These constituents were determined using harmonic analysis method which evaluated a 30-day period of water elevation data at the Mikawa Port Tidal Station in Atsumi Bay. The harmonic analysis is discussed in subchapter 3.5.3. Temperature and salinity data were also set within these boundaries on the basis of in situ observations around Atsumi Bay. The water temperature at the river boundary was estimated by conversion of air temperature data.

On the eastern boundary, river boundaries were set as source of freshwater discharges and nutrient loads. River discharge data was obtained from in situ observation at Umeda River. Nutrient loads defined using the L-Q equation by following the relationship between discharge level and nutrient concentrations. The lateral surface boundary is influenced by wind force, air temperature, and solar radiation. For the surface boundary wind speed, wind direction, air temperature, and sunshine duration, we used secondary data which is obtained by the Japan Meteorological Agency at Toyohashi observation station. Solar radiation was determined by converting sunshine duration data to solar radiation using the Angstrom equation (Angstrom, 1924). Both L-Q and Angstrom equations are discussed in subchapter 2.2.1 and 3.7, respectively.

5.3 Physical Parameter

In hydrodynamic and ecological simulation, several physical parameters must be considered such as tidal, discharges and nutrient loads, and solar radiation. Firstly, tidal action is used as water inflow and outflow parameter at ocean boundaries where nine tidal constituents used in this model were obtained from the nearest observation station inside Atsumi Bay simulation boundary or exactly at Mikawa Port Tidal Station (Figure 5.1). Tidal constituents were estimated using *discrete fourier transform* (DFT) methods based on 30 days water level observation data in every one-hour duration. This analytical method

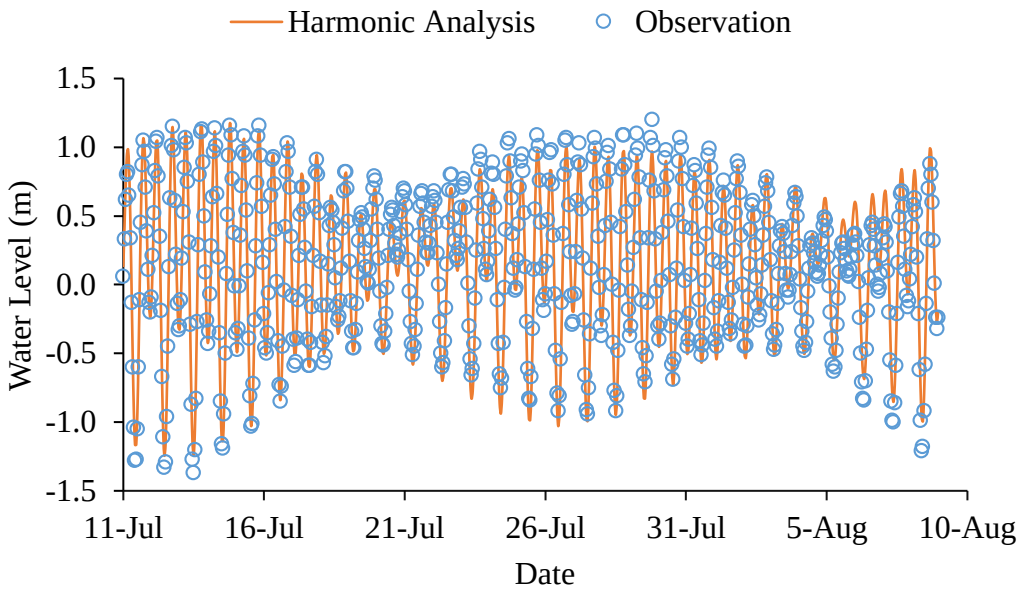

Figure 5.1 Tidal Harmonic and Water Elevation Simulation at Mikawa Port Tidal Station

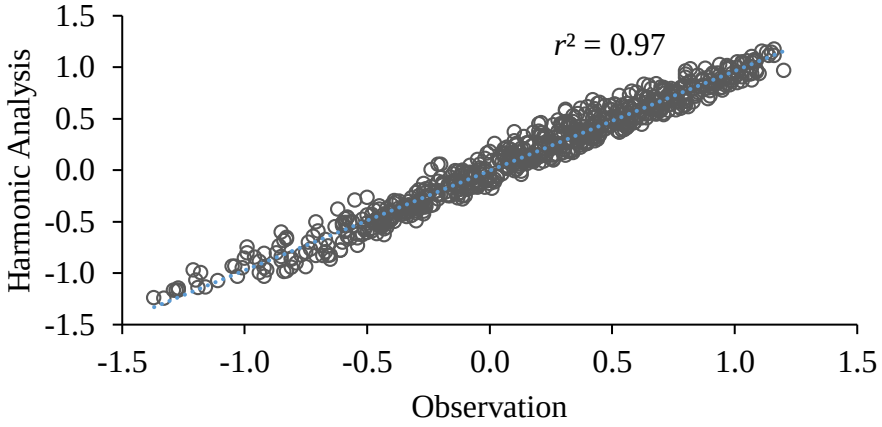

Figure 5.2 Observed and Harmonic Analysis Correlation

resulting phase of nine tidal constituents as shown in Table 3.1 chapter 3. The results had been validated by comparing between the results and observation data where the validation shows good relation between results and observation data where coefficient of determination (r^2) was 0.97 (Figure 5.2).

Second, the freshwater discharges and nutrient inputs that acted as river boundary inputs were obtained using the L-Q equation by following the relationship between river discharge and DN and DP in the Umeda River (Figure 5.3). The relationships were linear, yielding coefficients *a* and *b* in the linear regression (Load = aQ^b) used to define nutrient loads at the river boundary. As depicted in Figures 5.4 and 5.5, the L-Q equation agreed well with observation results where coefficient of determination (r^2) of DN and DP are above 0.9 and close to 1. It strengthened that coefficients *a* and *b* can give appropriate results and able to use in the ecological model as nutrient inputs at the river boundary. Fluctuation of discharges condition, as effect of precipitation, influence values of DN and DP inputs at the river boundary condition where during high discharges the DN and DP concentration is increasing compare to normal discharges.

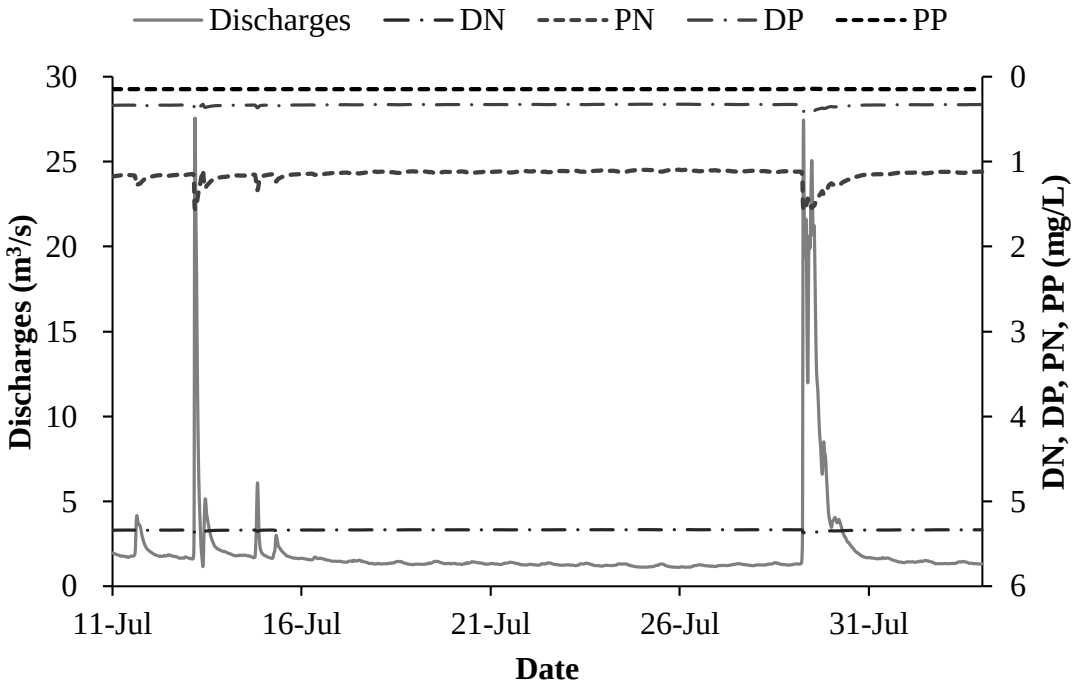

Figure 5.3 Discharges and Nutrients Concentrations at Umeda River

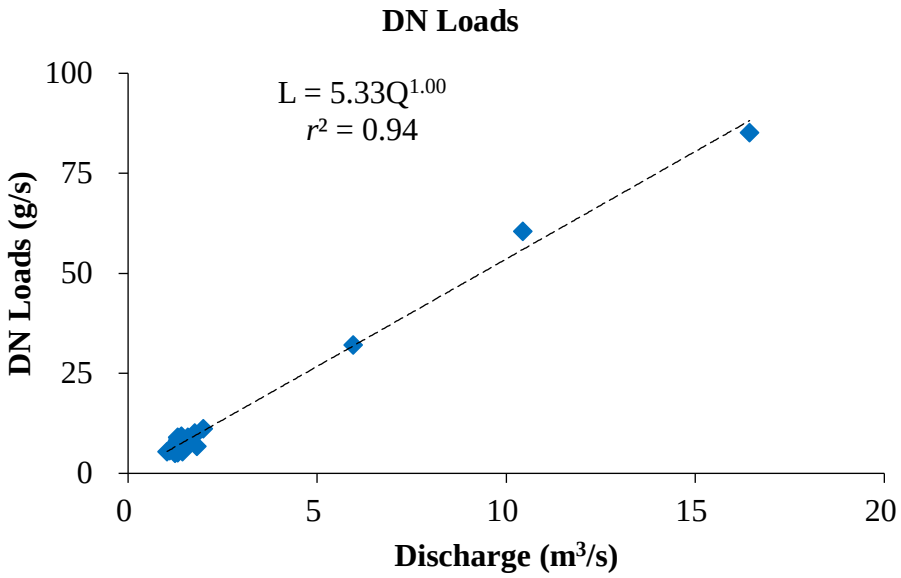

Figure 5.4 Relationship between Discharge and DN Loads

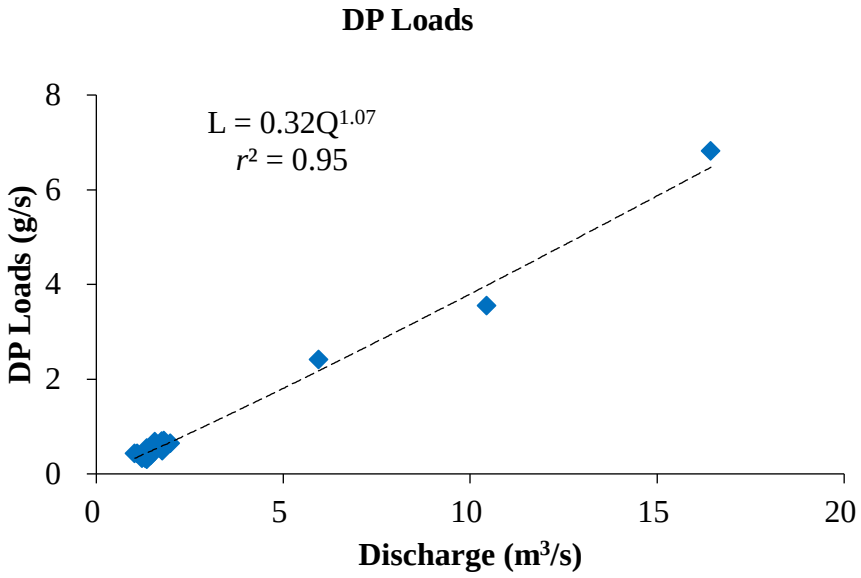

Figure 5.5 Relationship between Discharge and DP Loads

Thirdly, another important factor is solar radiation, which is specifically used in estimating the available irradiance for phytoplankton growth. At Toyohashi Station, only data for sunshine duration were available. Therefore, we determined the solar radiation at Toyohashi City by converting the sunshine duration data into hourly solar radiation using the Angstrom equation (Angstrom, 1924). Coefficients *j* and *k* of Armstrong equation were estimated using solar radiation and sunshine duration data at Nagoya city station. Data of Nagoya city were

chosen because Nagoya city station is the nearest station to Toyohashi city that observed both sola r radiation and sunshine duration data. The simulation is started by estimating maximum extraterrestrial solar radiation where several parameter including solar constant, inverse relative instant factor for the earth-sun, sunset hour angle, and solar declination must be calculated separately before it can be applied to solar radiation simulation.

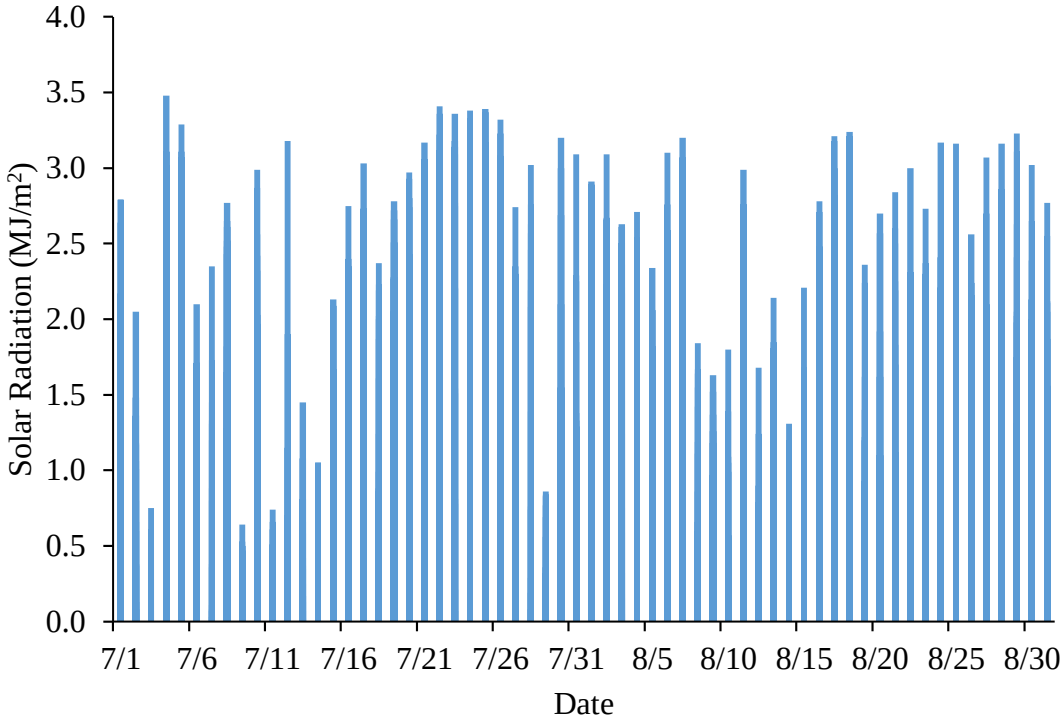

Figure 5.6 Observed Solar Radiation of Nagoya Station

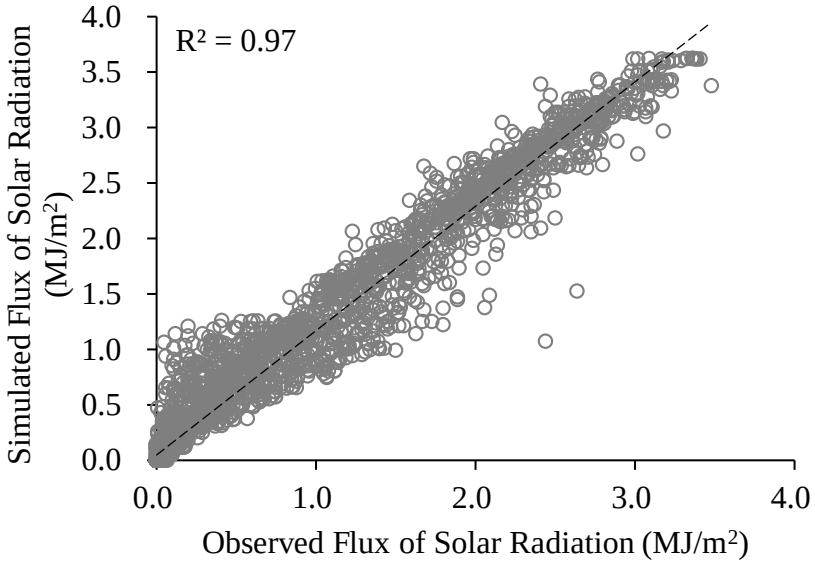

Figure 5.7 Validation of Angstrom Equation for Solar Radiation

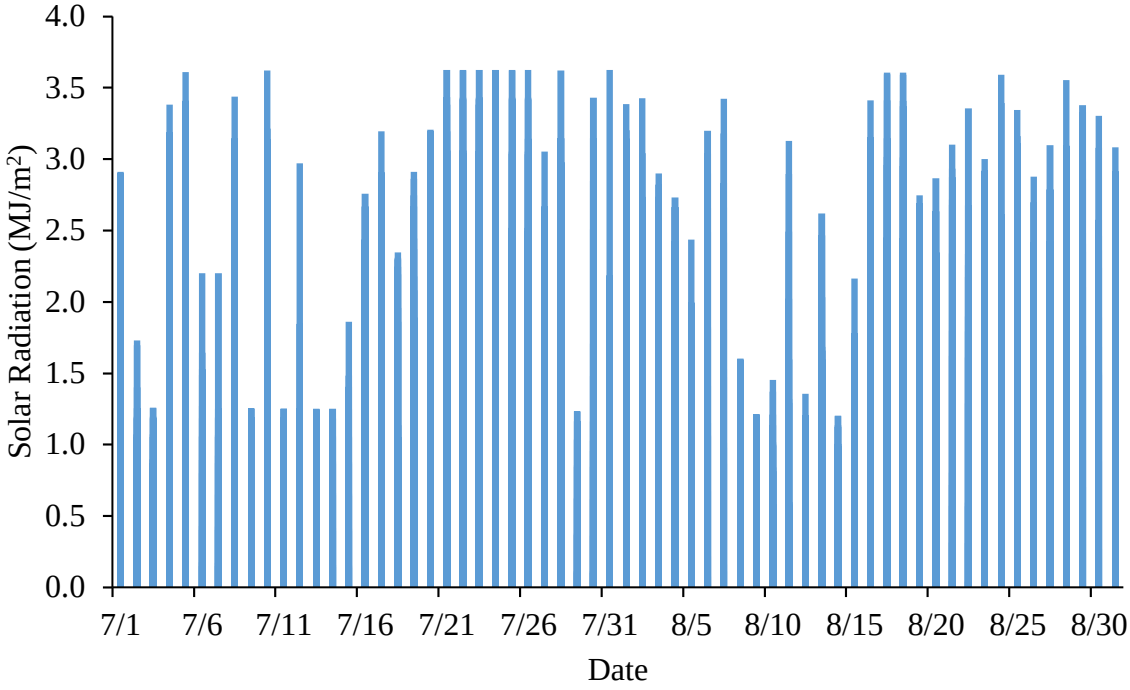

Figure 5.8 Simulated Solar Radiation of Toyohashi City

In simulation, total four months Nagoya city solar radiation and sunshine duration data of July to November 2010 with one-hour range had been simulated (Figure 5.6). The simulation of Nagoya City solar radiation resulted in values for coefficients *j* and *k* of 0.255 and 0.258, respectively, and showed good correlation with observed data (r^2 = 0.97, Figure 5.7). We used these coefficients to simulate Toyohashi City solar radiation using that city's sunshine duration data. Eventually, the calculated Toyohashi City solar radiation was used as an input parameter for phytoplankton growth in the ecological model. We used these coefficients to simulate Toyohashi City solar radiation using that city's sunshine duration data. Eventually, the calculated Toyohashi City solar radiation was used as an input parameter for phytoplankton growth in the ecological model (Figure 5.8).

5.4 Depth-Averaged Two-Dimensional Model

5.4.1 Hydrodynamic Model Results

Current model was set up to evaluate hydrodynamic and water quality condition of Atsumi Bay with simulation small area of 5 km × 9 km. Open boundary condition in particular at north and west sides are influenced by tidal level which highly controlled water circulation

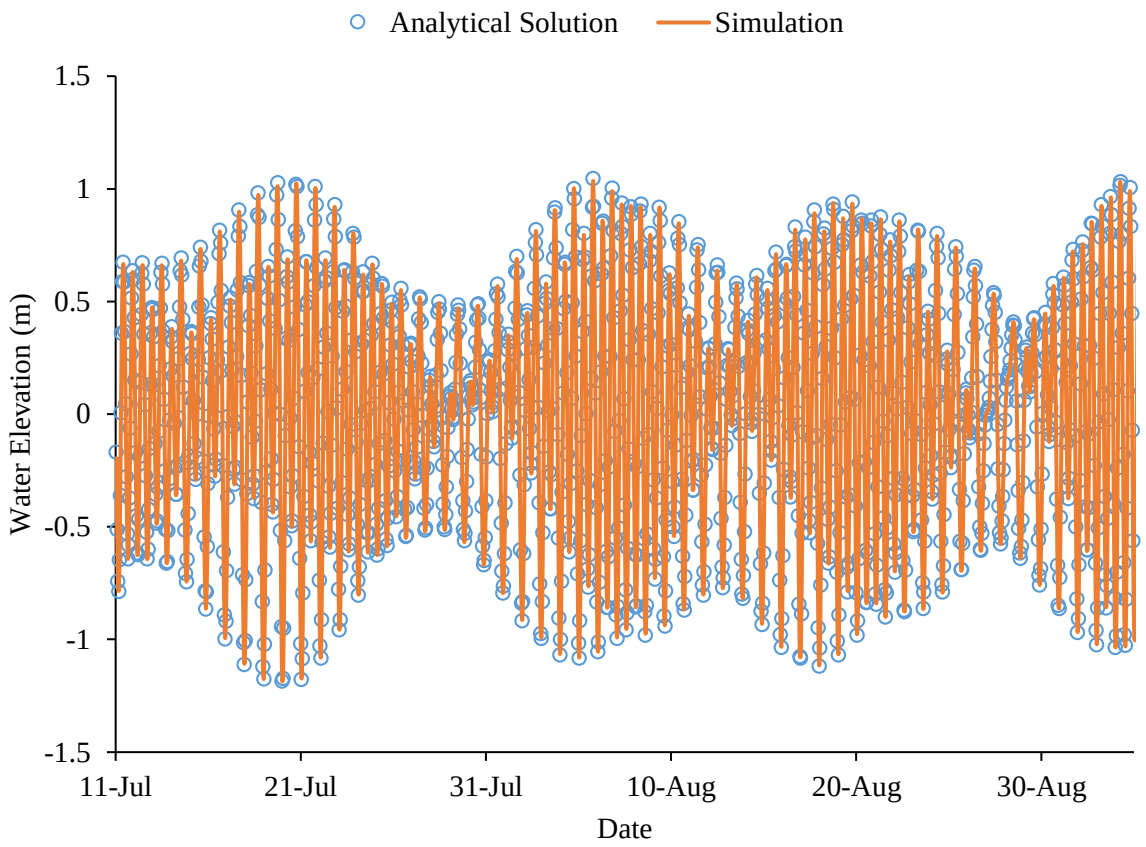

Figure 5.9 Analytical Solution and Simulation Result of Water Level (ζ)

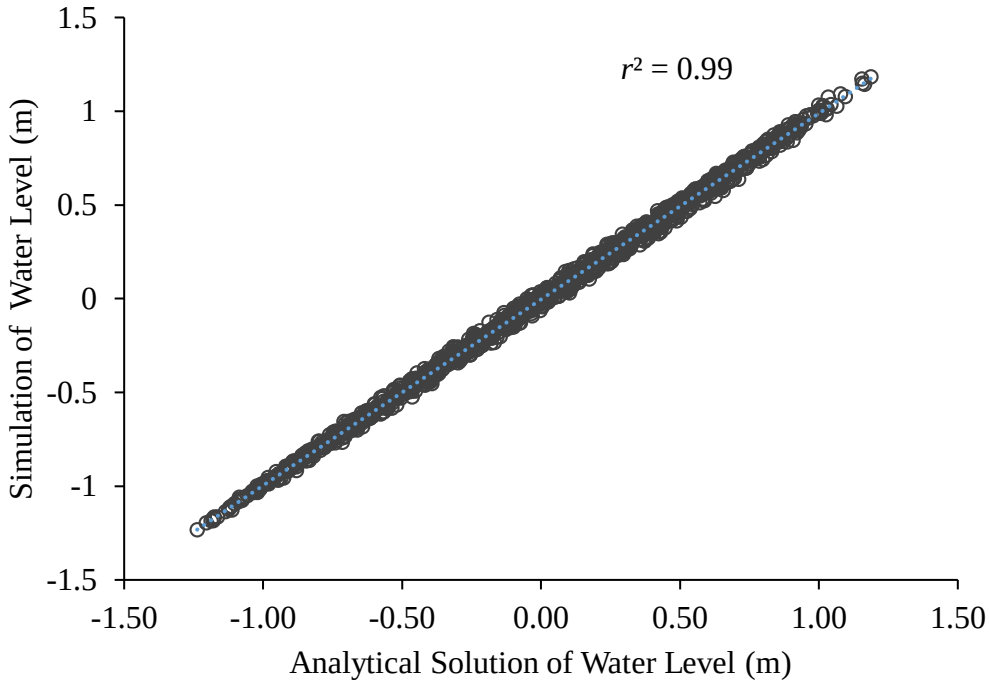

Figure 5.10 Analytical Solution and Simulation Correlation

of the study. Our input of tidal level at these boundaries were based on observation data at Mikawa Port Tidal Station inside simulation domain. During some rainy day with high discharge, the effect of river inputs become significant in river mouth area especially at ebb tide period where discharges dominantly flush to estuary. However, effect of tidal inputs still generally plays as important role on hydrodynamic condition of the estuary.

To evaluate the model ability, we used water level data as the evaluation term. The tidal level, which is an analytical solution of tidal harmonic analysis, was used as input at open boundaries for the evaluation. The analytical solution of observation data at Mikawa Port Tidal Station is clearly represent actual field condition (Figure 5.2). In the evaluation of the model, tidal input must influence all the simulation domain with less error with very small water level different. The hydrodynamic model shows very well ability to produce accurate result with good agreement between analytical solution and simulation result of water level (r^2) as shown in Figures 5.9 and 5.10.

5.4.2 Ecological Model Results

In this study, we collected water quality data between July and October 2010. The peak phytoplankton biomass (*Chl a*) occurred in early August. We therefore focus our discussion on the water quality and phytoplankton growth in July and August 2010. We used the depth-averaged 2D ecological model to simulate the water quality from the Umeda River estuary through a small section of Atsumi Bay. We then compared the simulated results for DN, DP, and *Chl a* to in-situ data to evaluate the model performance.

Generally, the model produced reasonable results and showed trends that followed the observed data as shown in figure 5.8 to 5.9. The phytoplankton (*Chl a*) were mostly growing around the river mouth station compared to the rest of the estuary during summer 2010. The *Chl a* concentration at station 1, the nearest station to the river mouth, increased slightly faster than at stations 2, 3 and 4. This was evident post-rainfall (after 29 July to 1 August) when *Chl a* concentration at the river mouth were higher than at the other stations. Post-rainfall, the data at station 1 show a stable trend followed by a decreasing trend. The other two stations showed patterns that were similar. Phytoplankton growth still occurred in some

parts of the estuary, as explained further in the next section, where water-quality changes pre- and post-rainfall are discussed.

In the model, the amount of river freshwater mixed with DN and DP entering an estuary is an important factor that influences estuarine water quality. Increases in discharge are very dependent on the intensity and duration of precipitation. Between 12 July and 4 August, the daily average discharge ranged from 1.11 m^3 s^{-1} to 5.95 m^3 s^{-1}. The L-Q model (Figures 5.3and 5.4) yielded relationships between discharge and DN load ($L = 5.33Q^{1.00}$) and between discharge and DP load ($L = 0.32Q^{1.07}$) with values for the coefficient b almost equal to 1. According to Inoue and Ebise (1991), values for coefficient *b* in the L-Q model for dissolved matter, including DN and DP, are generally close to 1. The indication is that the concentrations are almost constant and independent of the discharges.

The results of the ecological model show that there are nutrients constantly entering the estuary on both clear and rainy days. On 29 July in particular there was precipitation for more than 14 hours that increased the river discharge and flushed nutrients into the river (Figure 5.11). At the same time, the nutrient loads to the estuary and conditions in the estuary were only slightly altered, as shown from simulation results (Figure 5.8 and 5.9). This reinforces the observation that nutrient enrichment in estuaries is influenced not only by river inputs but also through other biochemical reactions of phytoplankton growth.

Both the simulation and observations showed that station 1 as the nearest station to the river mouth had the highest DN and DP concentrations compared to stations 2, 3 and 4 (Figure 5.8 and 5.9). Concentrations of DN and DP were generally higher around river-mouth station 1 than at the other stations, which were more than two kilometers from the river mouth. In the simulation, DN and DP concentrations fluctuated following the effects of circulation, phytoplankton uptake and water dilution. Phytoplankton uptake of nutrients was highly correlated with phytoplankton growth, which was evident in *Chl a* concentrations at all stations. The model simulation showed that on average 30–40% of dissolved nutrients, especially DN, was taken up by phytoplankton to support production.

The simulated *Chl a* concentrations at all stations followed the same relative trends as the observation data. Changes in *Chl a* concentrations were also influenced by the available

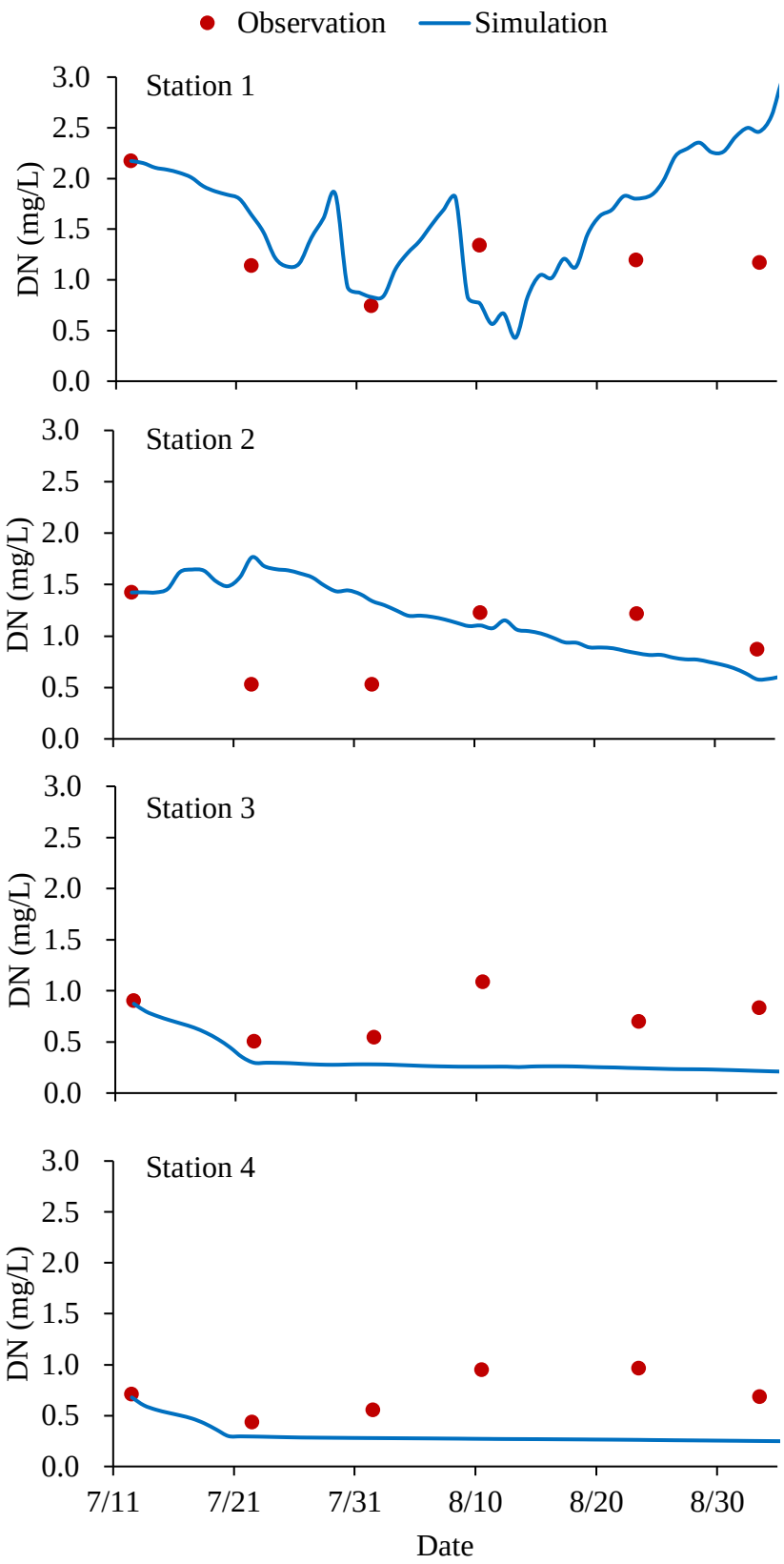

Figure 5.11 DN Concentration during Summer 2010

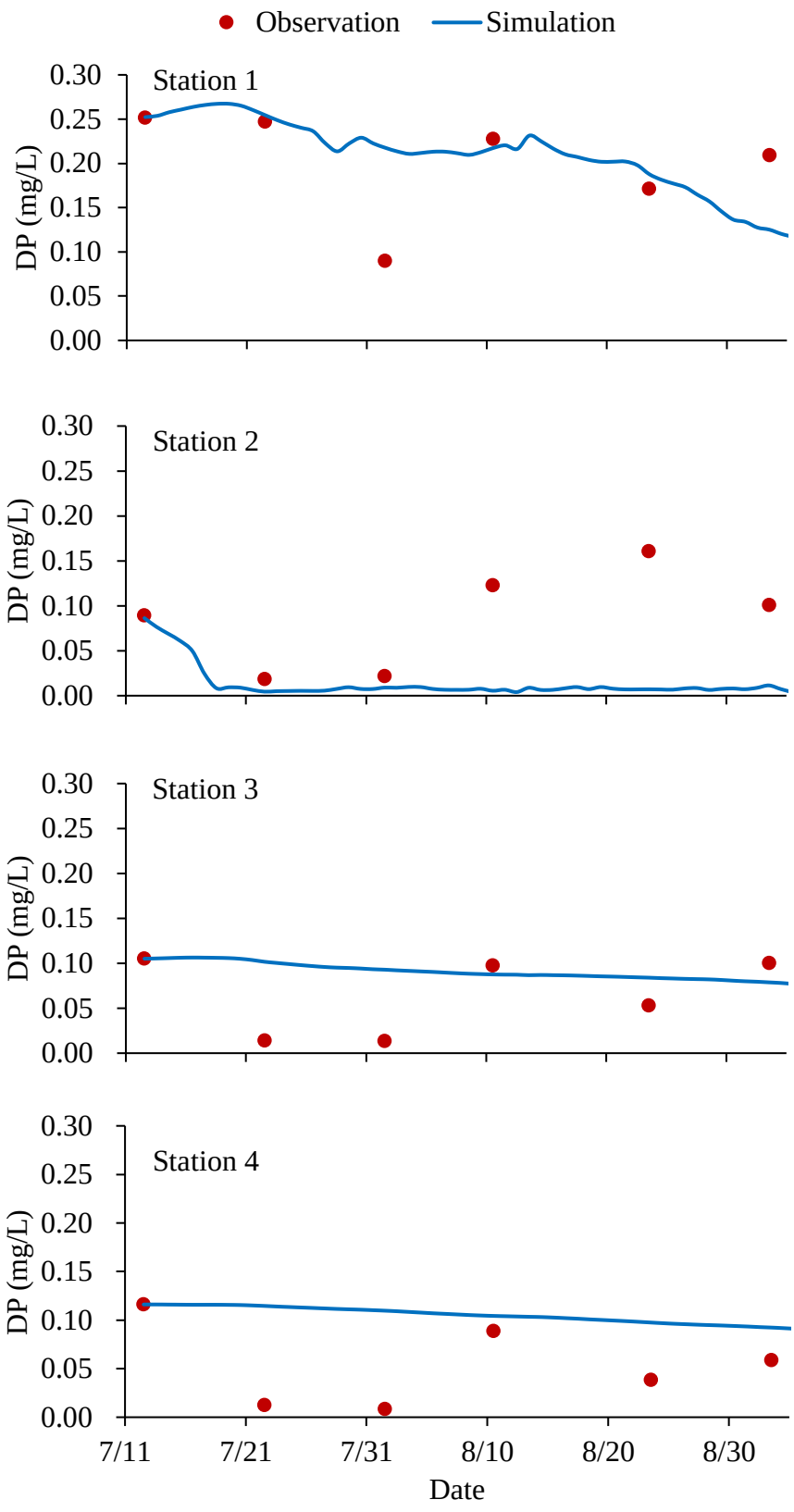

Figure 5.12 DP Concentrations during Summer 2010

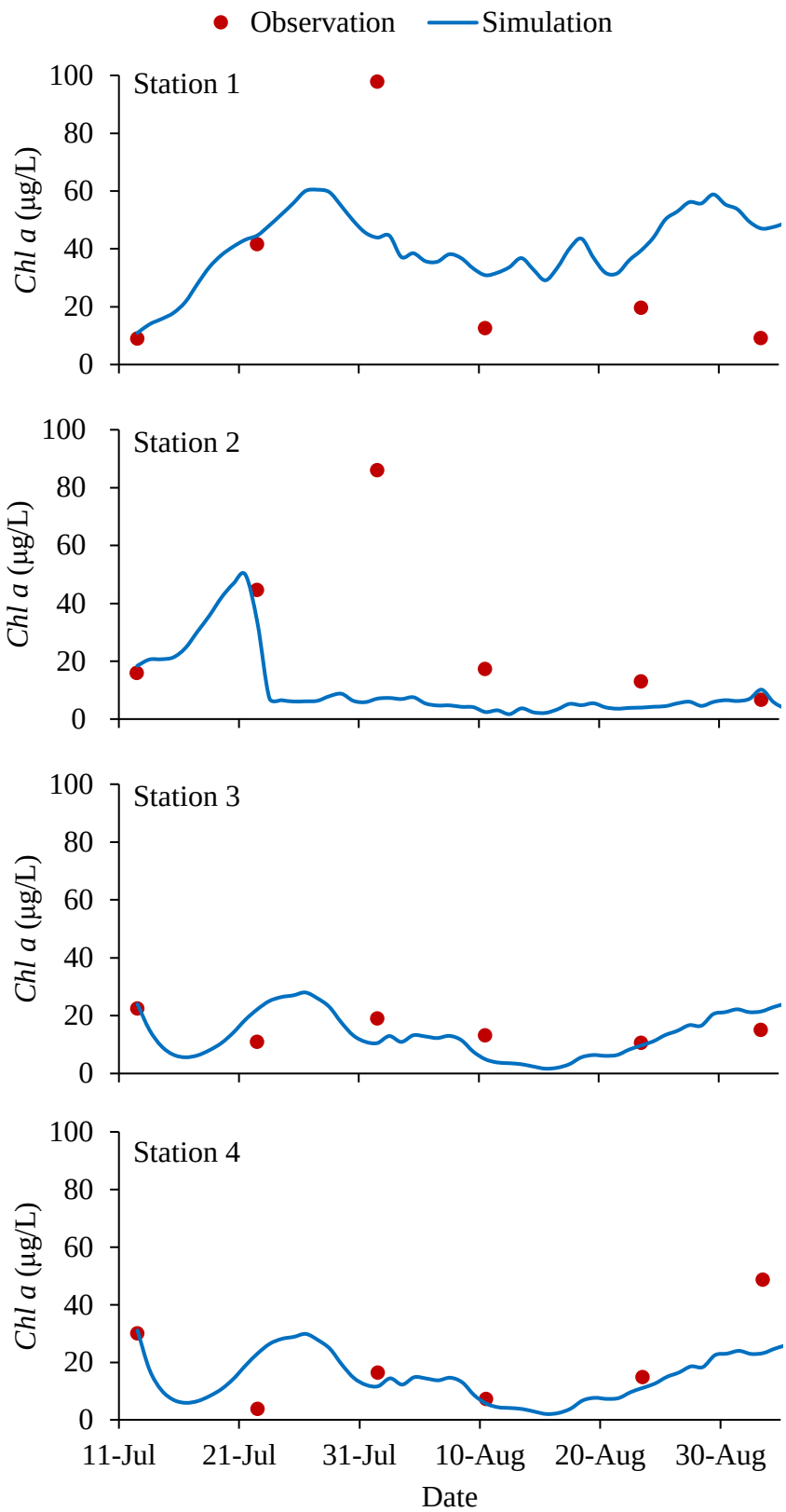

Figure 5.13 *Chl a* Concentration during Summer 2010

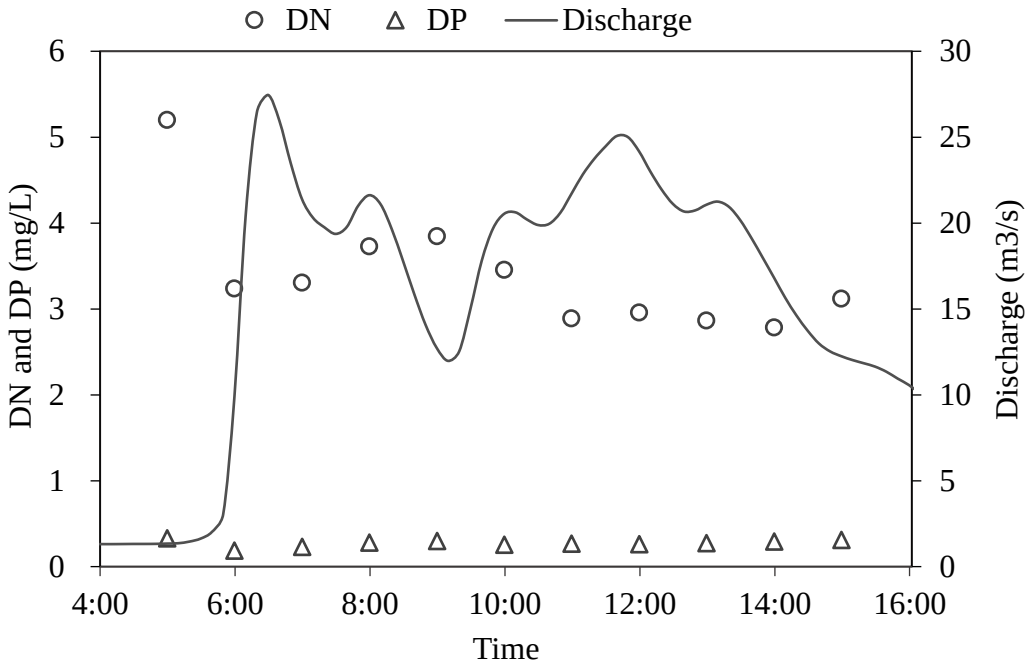

Figure 5.14 Discharge, DN, and DP Inputs on 29 July during Rainfall

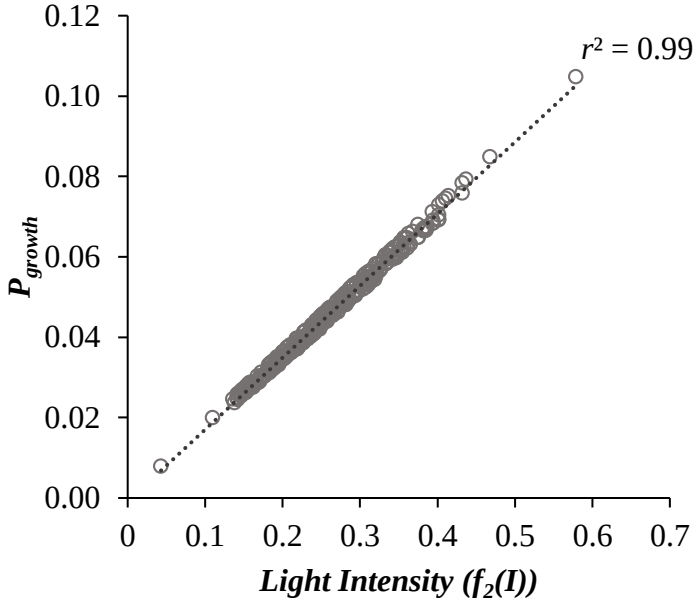

Figure 5.15 Light Intensity ($f_2(I)$) and Phytoplankton Production (P_{growth}) Relation

irradiance and deviation from optimum water temperature for phytoplankton production, as shown in equation (3). Simulated water temperatures in Atsumi Bay ranged between 23.5 and 25.5 °C, within the range of ideal water temperatures for phytoplankton growth of 20–28 °C (Ji, 2008). Moreover, after fulfilling the ideal conditions for temperature and nutrient availability, phytoplankton production (P_{growth}) depended strongly on the irradiance function $f_2(I)$ as depicted in figure 5.12.

5.4.3 Water Quality Change Pre- and Post-Rainfall

In our observations of summer 2010, we found the highest phytoplankton biomass (*Chl a*) occurred on 1 August with a peak value of 97.9 μg L^{-1}. This was associated with 42 mm of precipitation and high freshwater inputs on 29 July. On the basis of this finding, we compared the conditions pre-, during, and post-rainfall associated with the high rainfall on 29 July. For pre- and post-rainfall conditions we used data from 22 July and 1 August, respectively. These two days were appropriate for this comparison because they had similar conditions such as no precipitation, similar discharge rates (1.3–1.6 m^3 s^{-1}), low nutrient concentrations, and tidal elevations of 0.5–2.4 m.

Both the simulation and observation data for the pre-rainfall period of 22–28 July show that DN and DP were relatively stable with small fluctuations on clear days with low discharge rates (Fig. 5.8 and 5.10). However, during the rain event on 29 July, when rain fell for more than 14 hours and river discharges increased, DN concentrations increased around the river mouth compared to the previous day, especially at station 1. On 29 July, solar radiation was relatively low because of cloud cover associated with a long day of precipitation. The reduced irradiance resulted in low phytoplankton production and reduced nutrient uptake by phytoplankton.

Post-rainfall, from 30 July to 1 August, observations showed gradual changes in DN and DP concentrations, followed by an increase in *Chl a* supported by favorable irradiance on clear days. The active biological processes suggested by the increase in *Chl a* post-rainfall (Lane *et al.,* 2002) illustrate the fact that post-rainfall phytoplankton growth is substantially influenced by the availability of dissolved nutrients and is promoted by adequate water

temperature and irradiance. Figures 5.16 to 5.28 shows *Chl a* different condition between pre-, during, and post-rainfall. Increase of *Chl a* more visible on post-rainfall where the concentration was higher.

Our simulation could not reach the values as high as the observation data for station 1, however, it simulated high *Chl a* concentration around river mouth and areas between station 1, 2 and 3 with some points reached values higher than 82 μg L^{-1}. Base on the current result as show in figures to 5.16 to 5.28, the increase of phytoplankton was different at every point of estuary simulation. At some points, there were high concentrations of phytoplankton distributed around station 1 to station 3, however at other points concentration was relatively lower. The same conditions also occurred for DN and DP where the concentrations were various around estuary. Figure 5.16 – 5.28 show that mostly higher at near river mouth area where the accumulation occurred and altered the estuary water quality.

Our previous assumption about the increase of *Chl a* post-rainfall was quite acceptable, however the model also show that the increase of phytoplankton growth was occurred since 22nd July (pre-rainfall) where it reached higher concentration and maximum distribution around estuary on 27th July which is two days before rainfall. On 28th and rainfall day 29th July, the distribution seems decreasing where around those days the light intensity was also lower and effecting in less photosynthesis process for phytoplankton growth, and also phytoplankton was scattered to seaward into smaller concentrations. Post-rainfall, the figures show that phytoplankton distribution was much decreasing, however at near station 1 phytoplankton still grouping into higher concentration level where we assume that phytoplankton production continue around estuary particularly at this point.

Moreover, river DN and DP inputs relatively fluctuated depends on discharge condition. Distribution of DN and DP seems to be gradually changed between river mouth area into station 3 and seaward. The farther area from river mouth, the smaller concentration contained in water bodies. At the area where *Chl a* higher, DN and DP values tend to be lower which depicted that DN and DP mostly uptake by phytoplankton to grow. Beside decrease in some part of estuary, the distribution from river to whole estuary continue where the simulation result show stable concentration of DN and DP are available in water bodies.

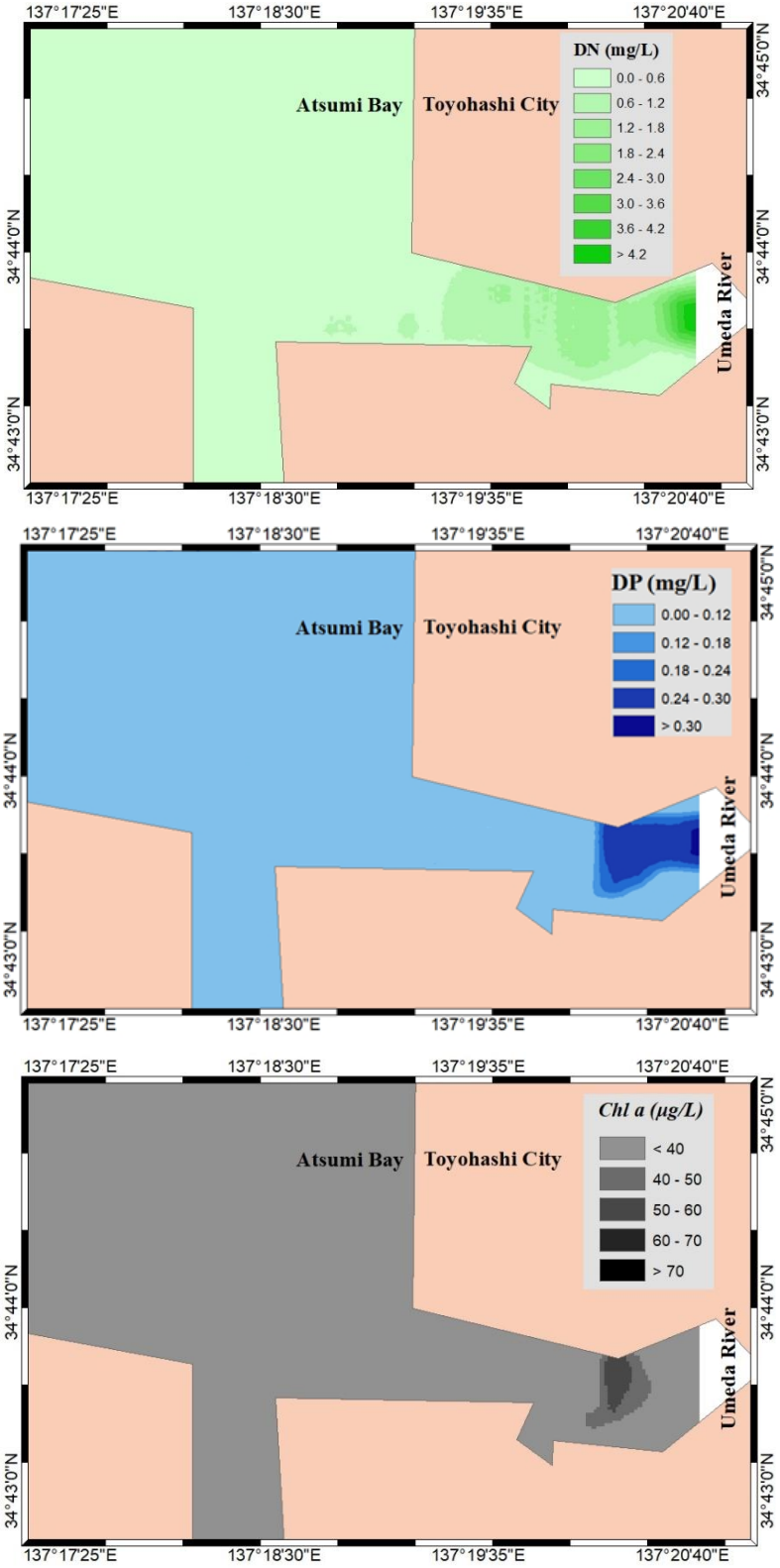

Figure 5.16 DN, DP, and *Chl a* Concentration on 22 July

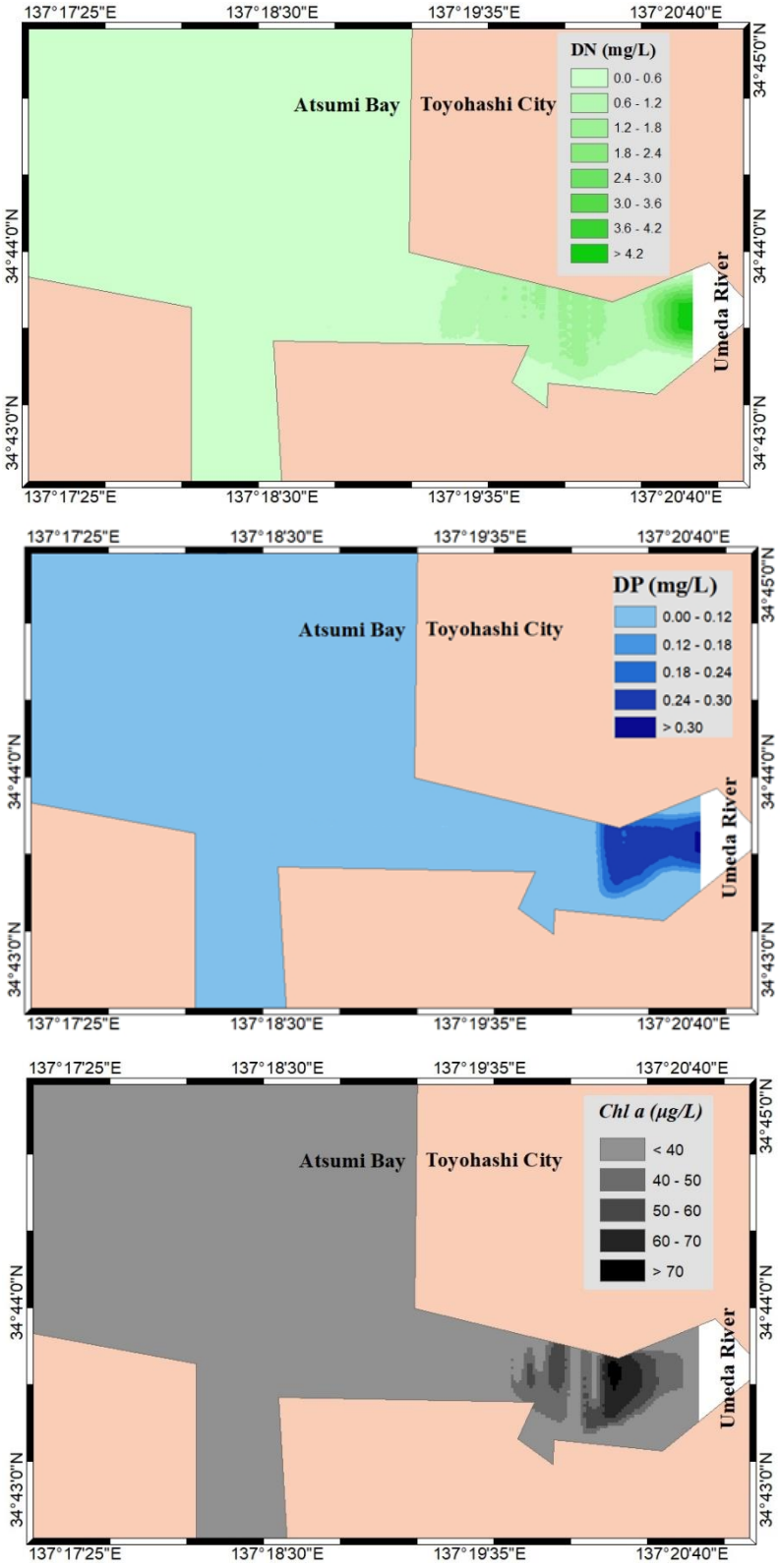

Figure 5.17 DN, DP, and *Chl a* Concentration on 23 July

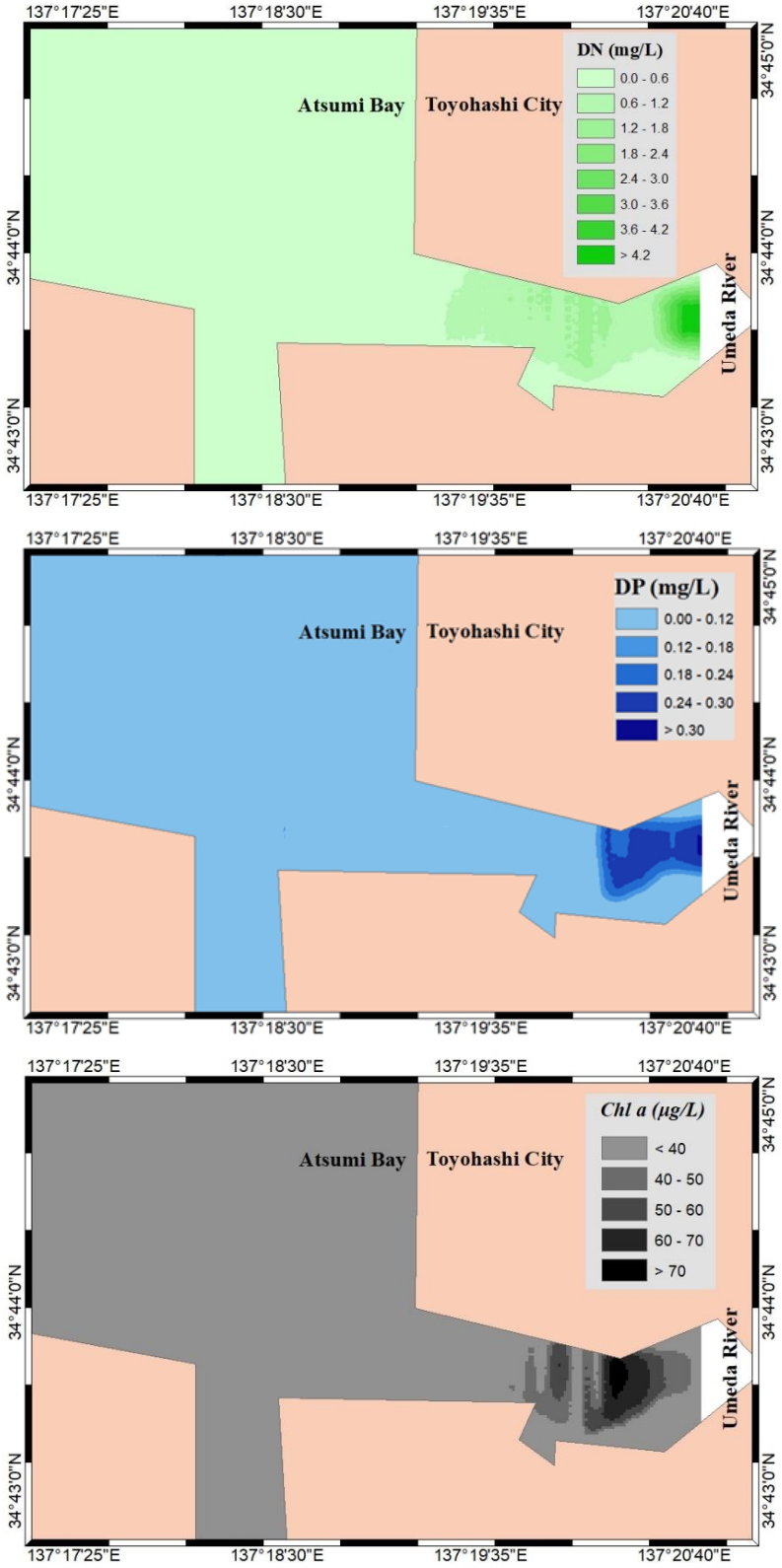

Figure 5.18 DN, DP, and *Chl a* Concentration on 24 July

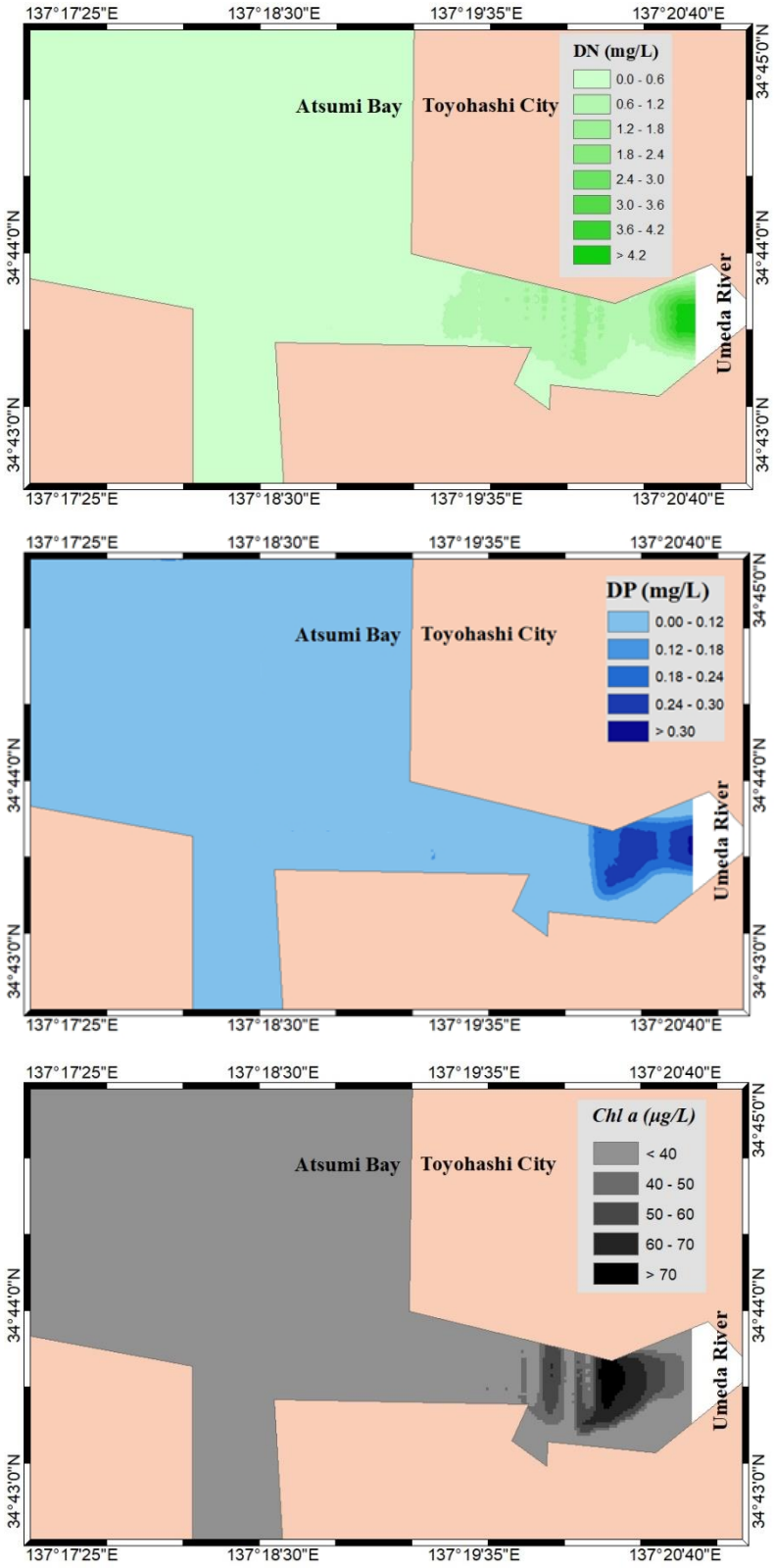

Figure 5.19 DN, DP, and *Chl a* Concentration on 25 July

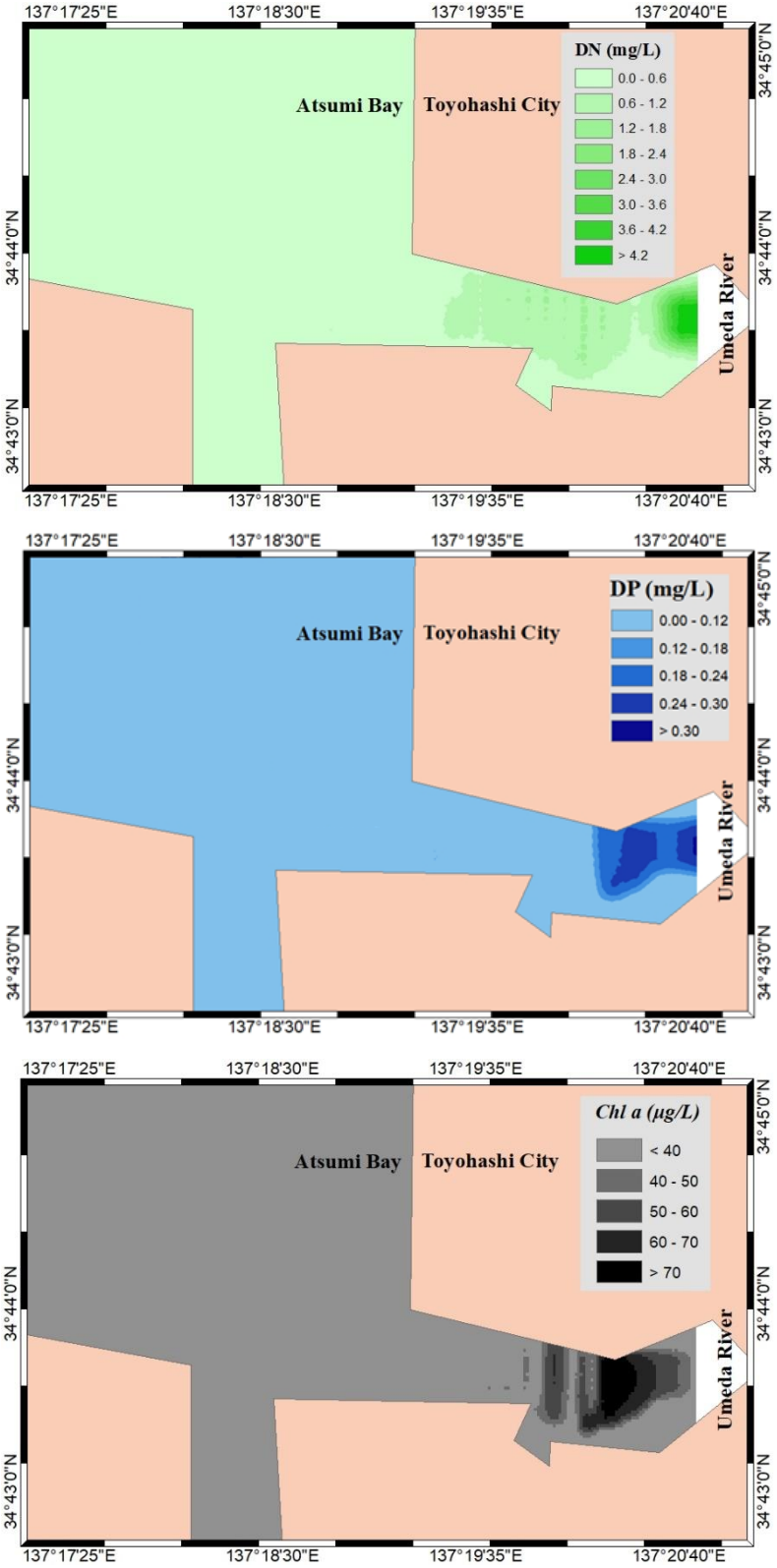

Figure 5.20 DN, DP, and *Chl a* Concentration on 26 July

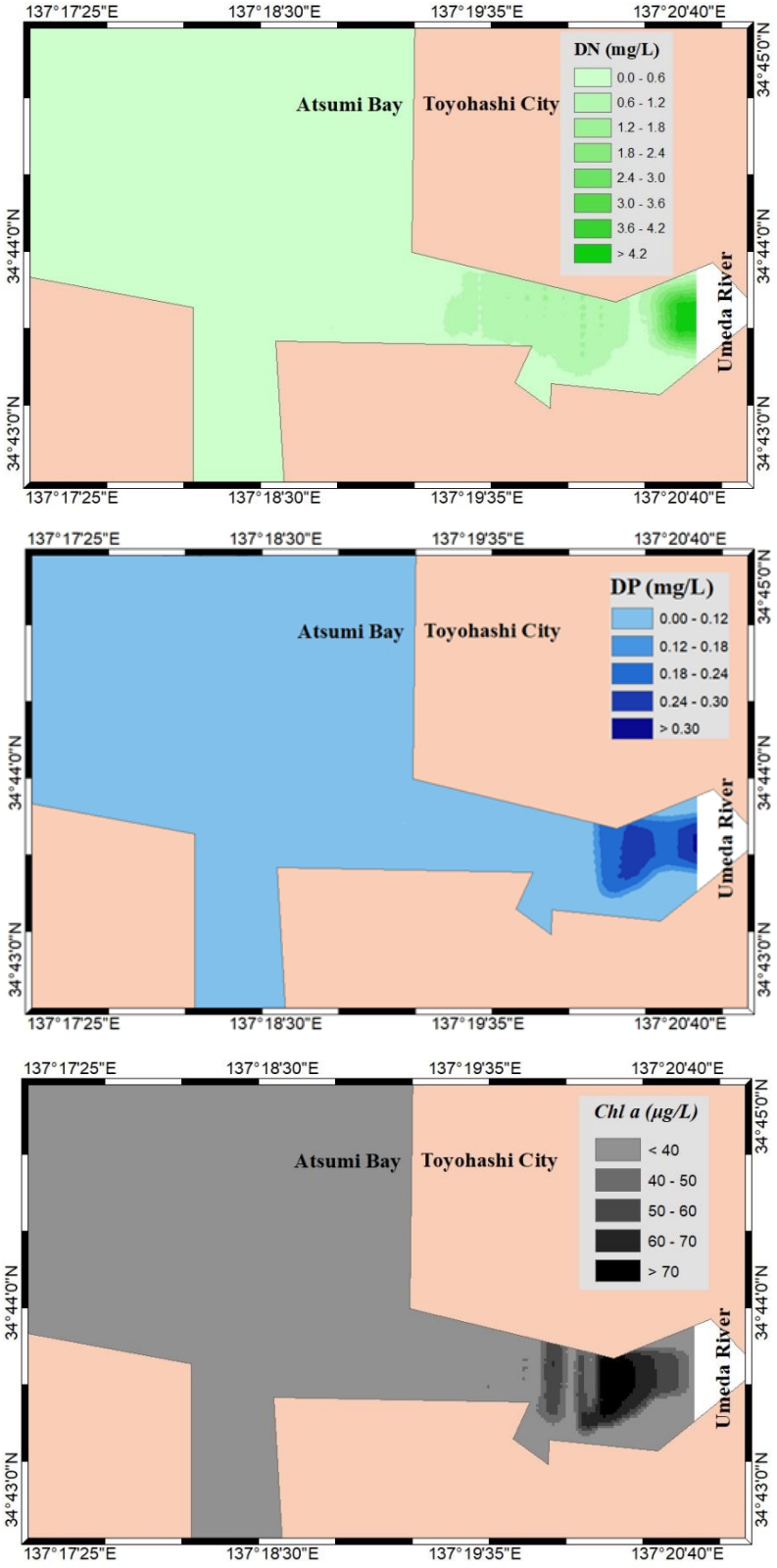

Figure 5.21 DN, DP, and *Chl a* Concentration on 27 July

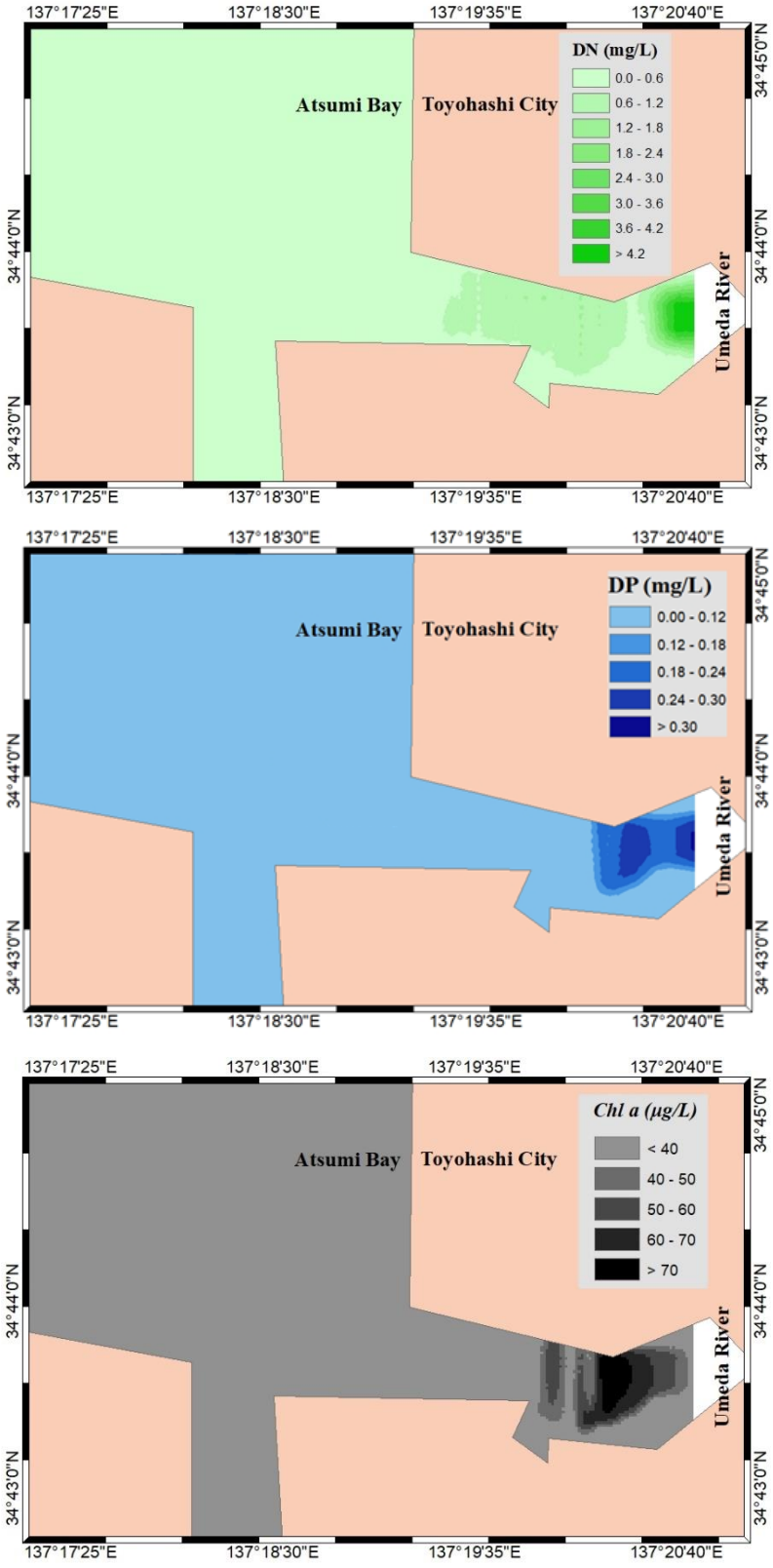

Figure 5.22 DN, DP, and *Chl a* Concentration on 28 July

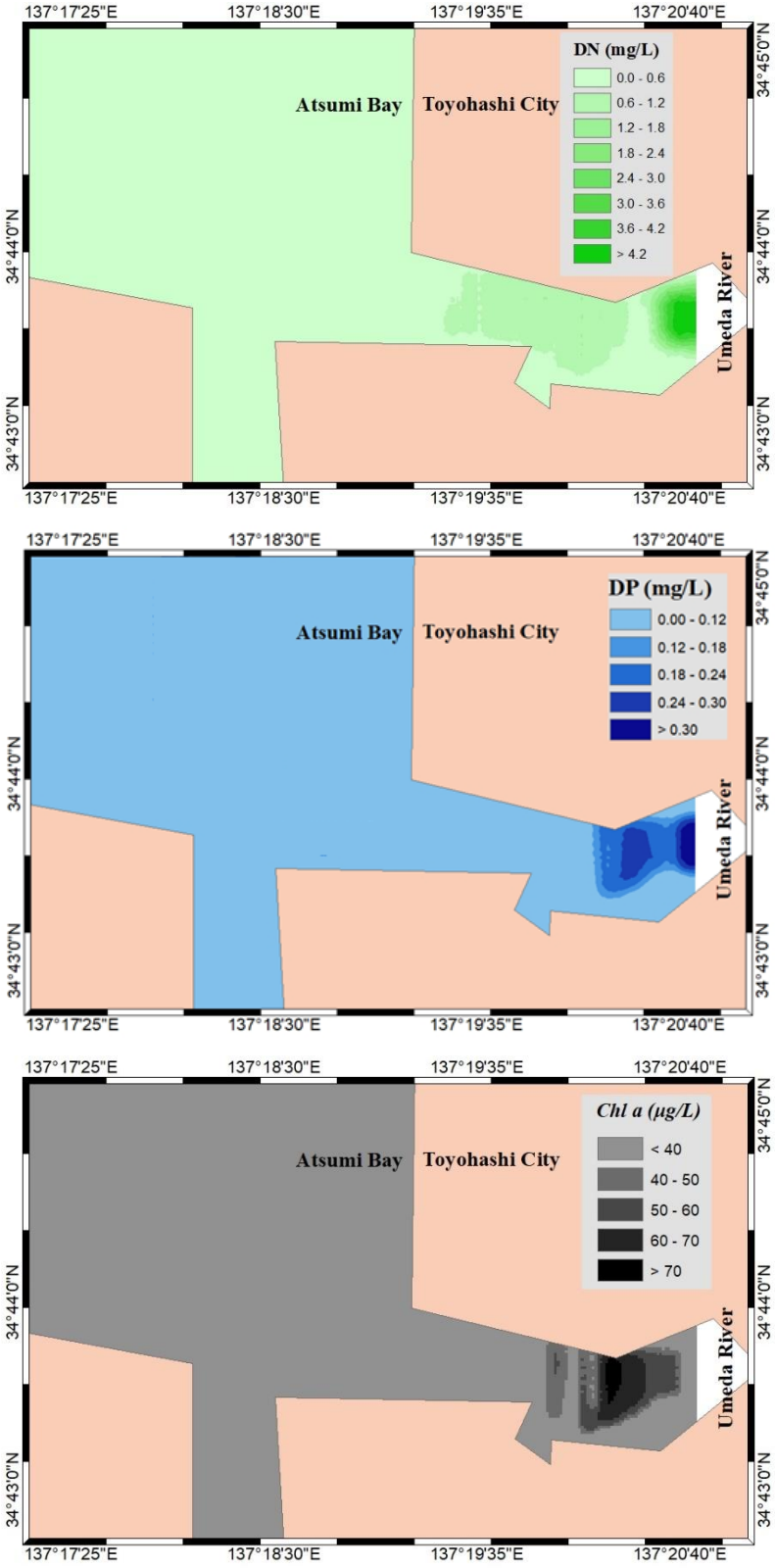

Figure 5.23 DN, DP, and *Chl a* Concentration on 29 July

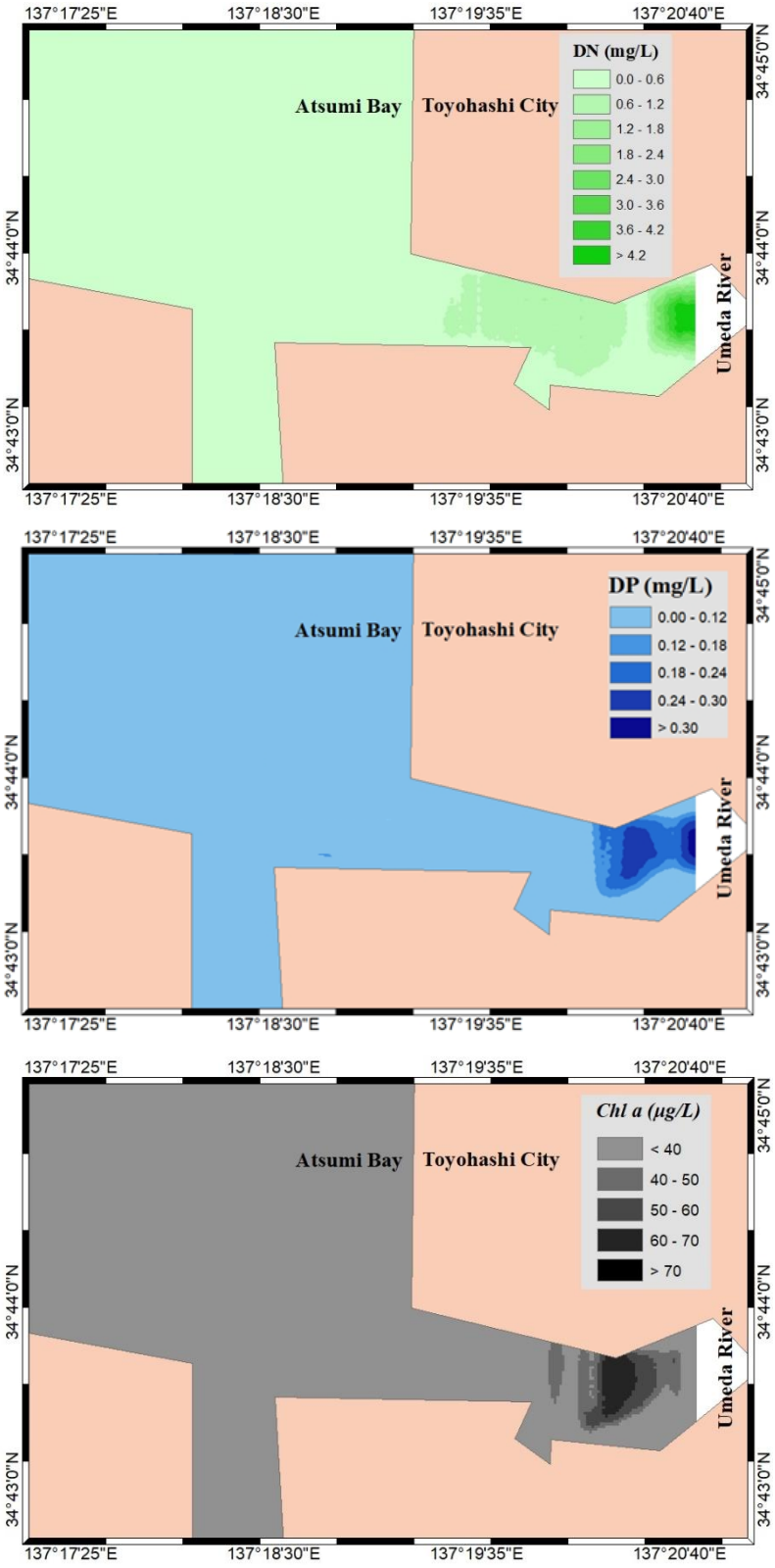

Figure 5.24 DN, DP, and *Chl a* Concentration on 30 July

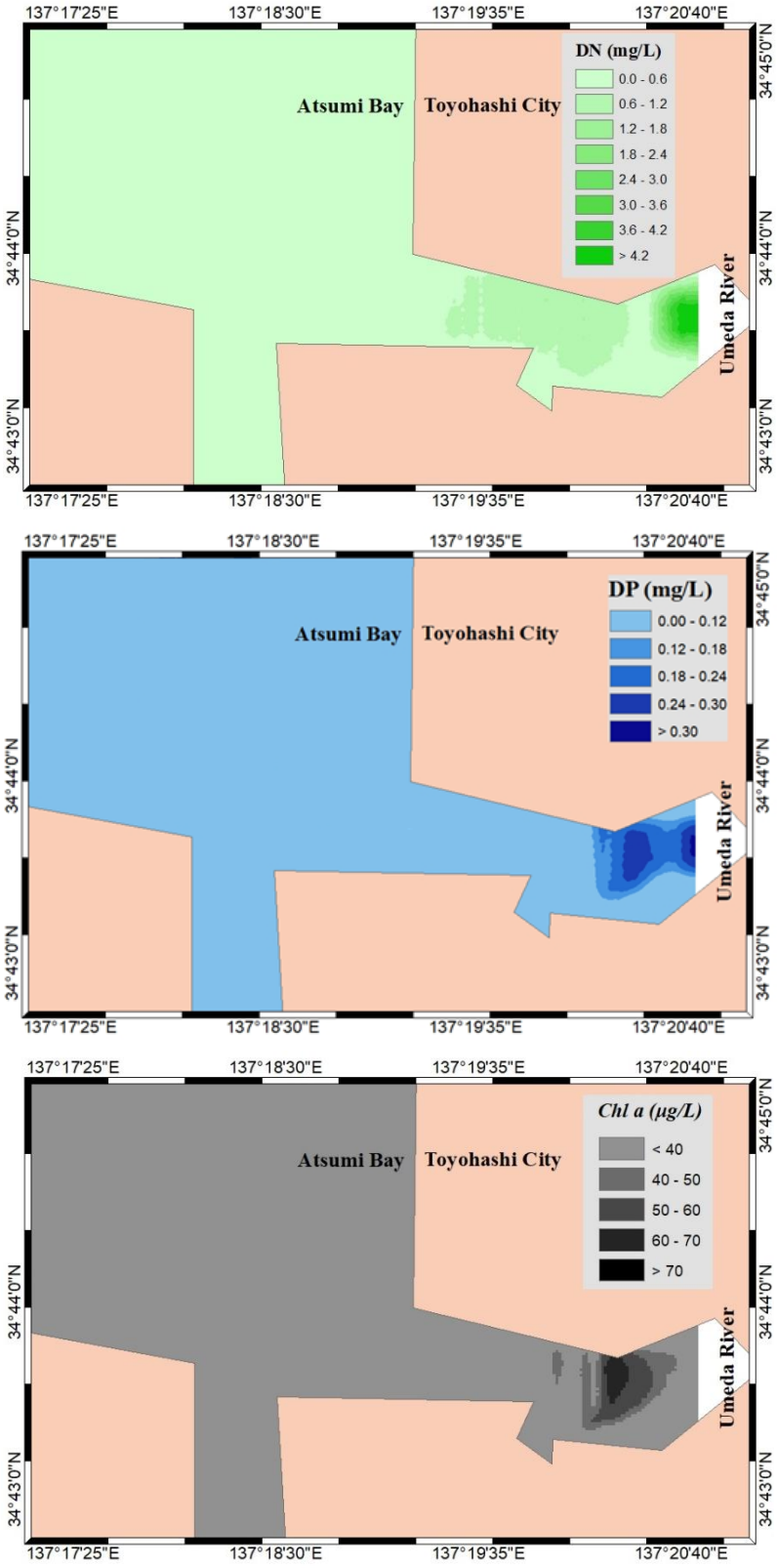

Figure 5.25 DN, DP, and *Chl a* Concentration on 31 July

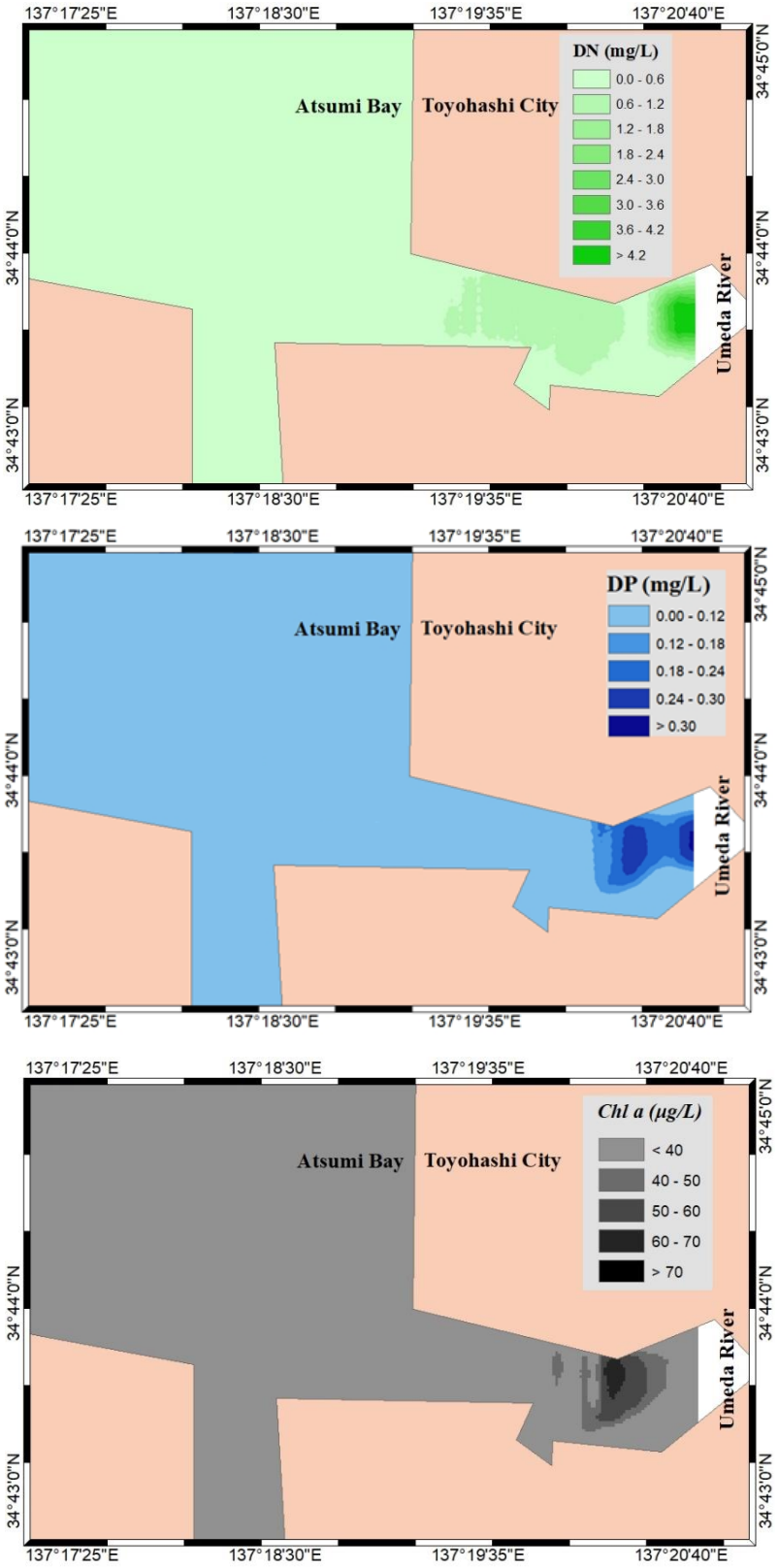

Figure 5.26 DN, DP, and *Chl a* Concentration on 1 August

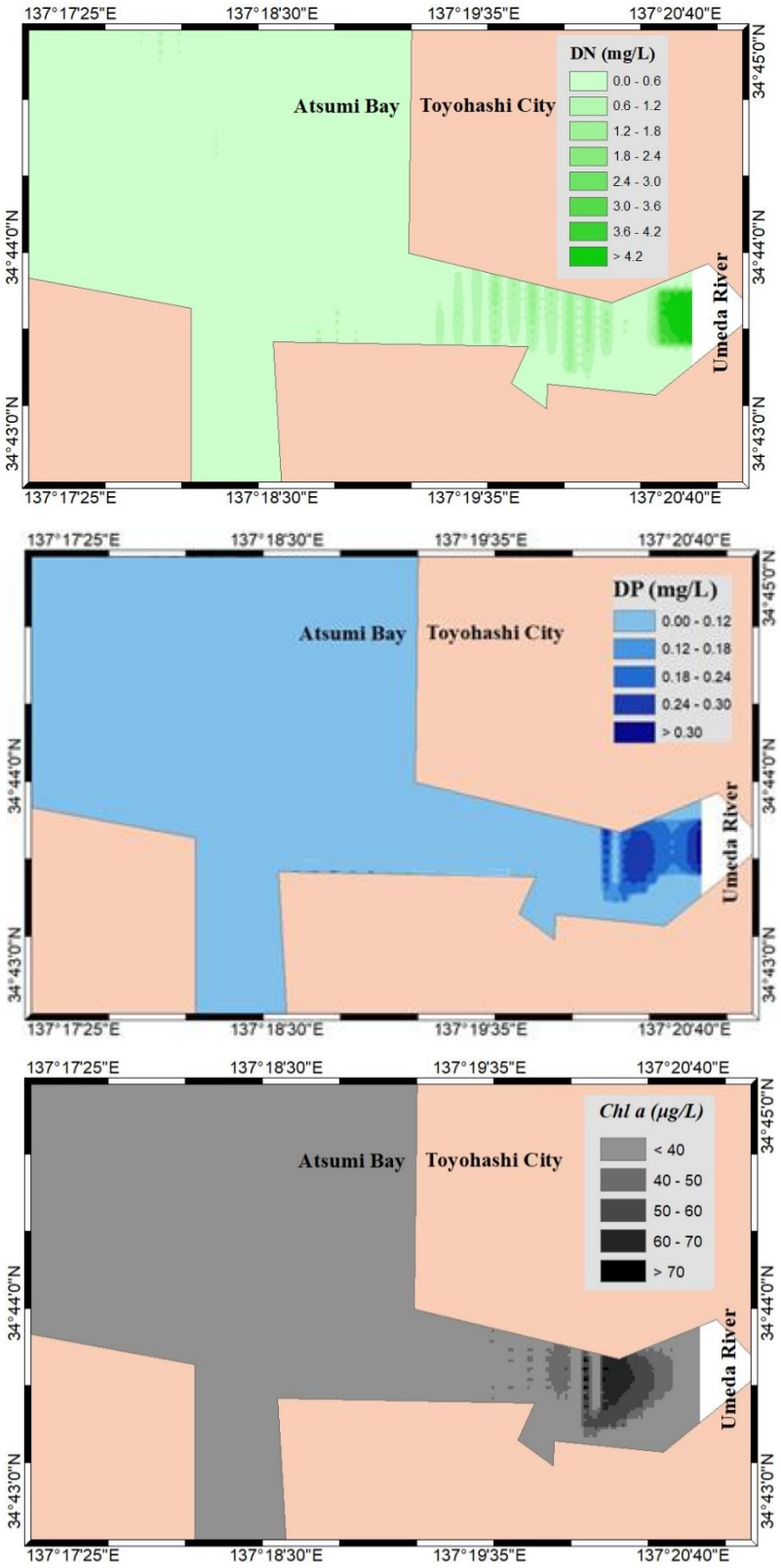

Figure 5.27 DN, DP, and *Chl a* Concentration on 2 August

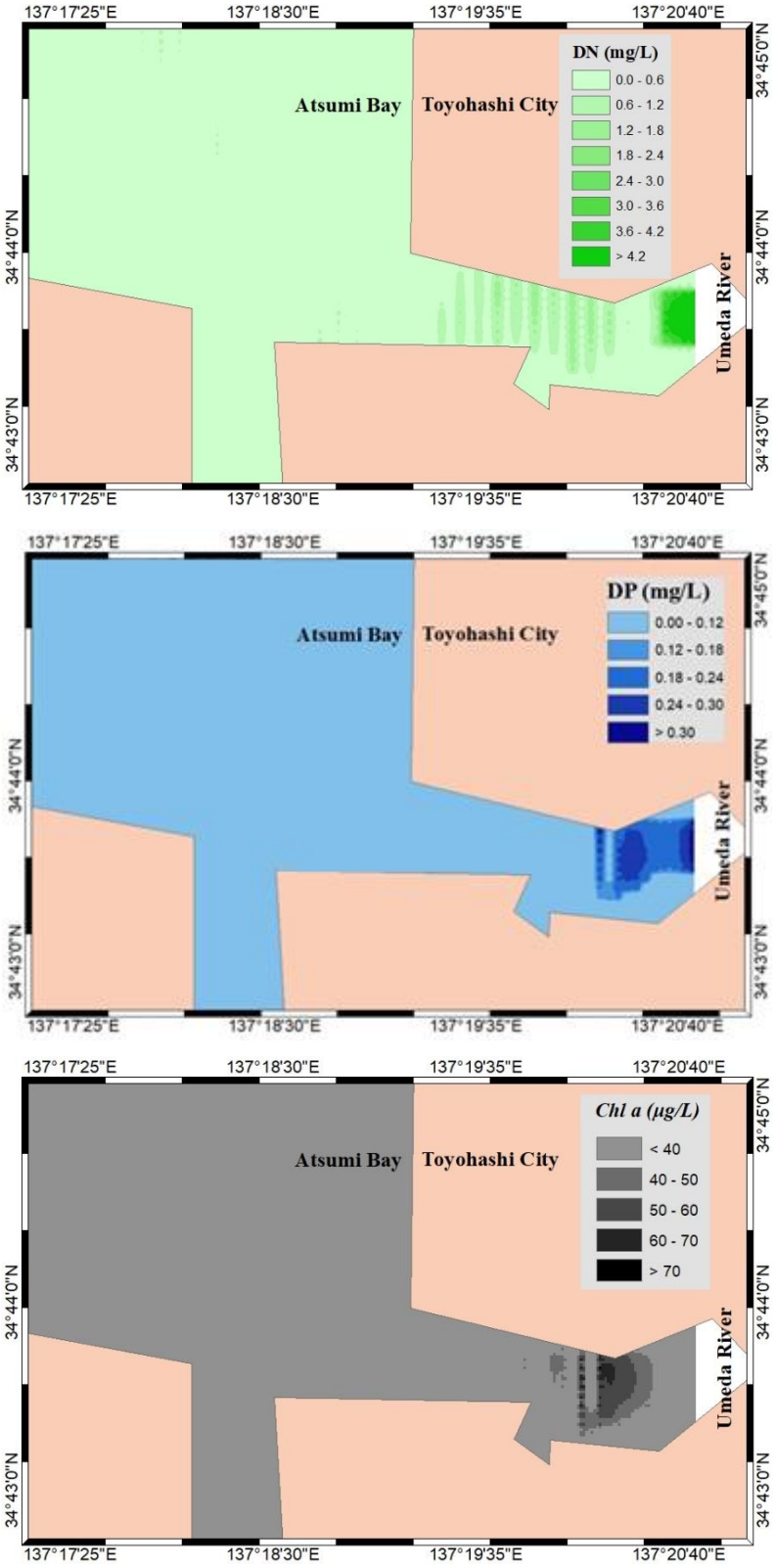

Figure 5.28 DN, DP, and *Chl a* Concentration on 3 August

5.4.4 Summary of Depth-Averaged Two-Dimensional Model

The depth-averaged two-dimensional hydrodynamics and ecological model have been developped. The results are showing that both model have good performances as shown from corelation between simulation results and observation. In hydrodyanmic model, water level observation of tidal station data and water level simulation have very well corellations with r^2 is 0.99. It is indicated that the hydrodynamic model have good performance and the results can represent the condition of Atsumi Bay area. In addition, hydrodynamic results can be used for ecological simulation parameters. In ecological model, both observation data and simulation results show good corelations. The results are indicating that nutrient concentrations in estuary generally controlled by inputs from the river. Furthermore, between pre- and post-rainfall, phytoplankton continue growing by utilizing enrichment of nutrients with support from water temperature and solar radiation to grow and effect alteration of water quality around estuary.

5.5 Conclusion

The simulation results, especially the depth-averaged two-dimensional model, are indicating that nutrients concentrations in estuary are controlled by inputs from the river. On the fine day, estuarine nutrients inputs typically low with small discharges entering estuary. Oppositely, high freshwater discharges with reached nutrients entering estuary during rainfall mostly altered nutrients concentrations. Eventually, enrichment of nutrients and support from water temperature and solar radiation are later influencing the phytoplankton growth around the estuary. Curently, the model only able to figure DN and DP dynamic in Atsumi bay. From the simulation results, freshwater inputs during rainfall had changed post rainfall DN and DP in the Umeda river transect of Atsumi bay. Post rainfall, decrease of dissolved nutrients is from the effects of freshwater dilution and phytoplankton uptake. Moreover, the influence of river inputs was dominant at river mouth station 1 rather than at other the stations. The further the station was from the river mouth, the lower the influence which depicts the large proportion differences between dissolved nutrients concentrations at river mouth station 1 and the open sea station 4.

REFERENCES

Angstrom, A. 1924. "Solar and terrestrial radiation. Report to the international commission for solar research on actinometric investigations of solar and atmospheric radiation." *Quarterly Journal of Royal Meteorological Society* 50: 121-125. doi:10.1002/qj.49705021008.

Bodergat, A-M., Rio, M., Ikeya, N., Tide versus eutrophication. Impact on ostracods populations structure of Mikawa Bay (Japan). *Rev. Micropaleontol.*, 40(1), 3-13, 1997.

Cloern, J.E. 2001. "Our evolving conceptual model of the coastal eutrophication problem." *Marine Ecology Progress Series* 210: 223-253.

Glibert, P. M. 2017. "Eutrophication, harmful algae and biodiversity — Challenging paradigms in a world of complex nutrient changes." *Marine Pollution Bulletin.* doi:doi.org/10.1016/j.marpolbul.2017.04.027.

Inoue, T, and S Esbise. 1991. "Runoff characteristicof COD, BOD, C, N and P loadings from river to enclosed coastal seas." *Marine Pollution Bulletin* 23: 11-14.

Ji, Z-G. 2008. *Hydrodynamics and Water Quality: Modeling Rivers, Lakes, and Estuaries.* Hoboken, New Jersey: John Wiley & Sons, Inc. doi:10.1002/9780470241066.

Kasih, G. A. A., and T. Kitada. 2004. "Analysis Of Factors Regulating Algal Bloom In Mikawa Bay Using Eutrophication Model." *Environmental Engineering Research* 41: 613-624.

Kasih, G.A.A., and T Kitada. 2008. "Modeling of the role of tideland in eutrophication reduction in Mikawa Bay, Japan." *Proceedings of the Symposium on Global Environment* 16: 41-50.

Lane, R. R., J.W. Day, B. Marx, E. Reves, and G.P. Kemp. 2002. "Seasonal and spatial water quality changes in the outflow plume of the Atchafalaya River, Louisiana, USA." *Estuaries* 25(1): 30-42. doi:https://doi.org/10.1007/BF02696047.

Matsukawa, Y.,, and T. Suzuki. 1985. "Box model analysis of hydrography and behaviour of nitrogen and phosphorus in a eutrophic estuary." *Journal of the Oceanographical Society of Japan* 41 (6): 407–426. doi:10.1007/BF02109035.

Nakane, T., K. Nakaka, H. Bouman, and T. Plat. 2006. "Environmental control of short-term variation in the plankton community of inner Tokyo Bay, Japan." *Estuarine, Coastal*

and Shelf Science 78 (4): 796-810. doi:doi.org/10.1016/j.ecss.2008.02.023.

Nakanishi, H., M. Ukita, M. Sekine, M. Fukagaw, and S. Murakami. 1990. "Eutrophication Control in Seto Inland Sea." *Marine Coastal Eutrophication* 1239-1256. doi:10.1016/B978-0-444-89990-3.50105-X.

Sakamoto, M., and T. Tanaka. 1989. "Phosphorus dynamics associated with phytoplankton blooms in eutrophic Mikawa Bay, Japan." *Marine Biology* 101 (2): 265-271.

Sharpley, A. N. 2013. "Agriculture, Nutrient Management, and Water Quality." *Encyclopedia of Biodiversity (Second Edition)* 95-110. doi:10.1016/B978-0-12-384719-5.00361-0.

Suzuki, C. 2016. "Assessing change of environmental dynamics by legislation in Japan, using red tide occurrence in Ise Bay as an indicator." *Marine Pollution Bulletin* 102 (2): 283-288.

Suzuki, T. 2004. "Large-scale restoration of tidal flats and shallows to suppress the development of oxygen deficient water masses in Mikawa Bay." *Bulletin of Fisheries Research Agency* Supplement No. 1: 111-121.

Chapter VI

General Conclusions

1. On summer 2010 observation, freshwater inputs during rainfall had changed post rainfall salinity stratification in the Umeda river transect of Atsumi bay. Post rainfall, an increase of nutrients and a decline in salinity after rainfall proved that a large amount of freshwater, mixed with nutrients, affected water quality conditions in the estuary. The decrease of dissolved nutrients is from the effects of freshwater dilution and phytoplankton uptake which verified by the increase of *Chl a*, PN, PP, and decrease of DN and DP. Moreover, the influence of freshwater was dominant at river mouth station 1 rather than at other the stations. The further the station was from the river mouth, the lower the influence which depicts the large proportion differences between the *Chl a*, dissolved nutrients, and particulate nutrients concentrations at river mouth station 1 and the open sea station 4. In addition, the surface layer was supplied to more than the bottom layer, because the inputs were more influencing horizontal circulation than vertical circulation. It resulted in a small alteration of nutrients and *Chl a* concentration compared to the surface layer.

2. In current study, depth-averaged two-dimensional has been developped. The results show that the model have good performance on DN, DP, and *Chl a* simulation where between simulation results and observation data have a good corelation..

3. As well as in the observation data, the simulation results also indicated that nutrients concentrations in estuary are controlled by inputs from the river. On the fine day, estuarine nutrients inputs typically low with small discharges entering estuary. Oppositely, high freshwater discharges with reached nutrients entering estuary during rainfall mostly altered nutrients concentrations. Eventually, enrichment of nutrients and support from water temperature and solar radiation are later influencing the phytoplankton growth around the estuary.

4. Curently, the model only able to figure DN and DP dynamic in Atsumi bay. From the observation data and simulation results, it show that freshwater inputs during rainfall had changed post-rainfall DN and DP in the Umeda river transect of Atsumi bay. Post-rainfall, decrease of dissolved nutrients is from the effects of freshwater dilution and phytoplankton uptake. Moreover, the influence of river inputs was dominant at river mouth station 1 rather than at other the stations. The concentrations gradually decrease from river mouth to seaward where the farther location from river mouth is getting lower influence of river inputs.